

Granular electronic systems

I. S. Beloborodov, A. V. Lopatin, and V. M. Vinokur

Materials Science Division, Argonne National Laboratory, Argonne, Illinois 60439, USA

K. B. Efetov

Theoretische Physik III, Ruhr-Universität Bochum, D-44780 Bochum, Germany

and L. D. Landau Institute for Theoretical Physics, 117940 Moscow, Russia

(Published 2 April 2007)

Granular metals are arrays of metallic particles of a size ranging usually from a few to hundreds of nanometers embedded into an insulating matrix. Metallic granules are often viewed as artificial atoms. Accordingly, granular arrays can be treated as artificial solids with programmable electronic properties. The ease of adjusting electronic properties of granular metals assures them an important role for nanotechnological applications and makes them most suitable for fundamental studies of disordered solids. This review discusses recent theoretical advances in the study of granular metals, emphasizing the interplay of disorder, quantum effects, fluctuations, and effects of confinement. These key elements are quantified by the tunneling conductance between granules g , the charging energy of a single granule E_c , the mean level spacing within a granule δ , and the mean electronic lifetime within the granule $\hbar/g\delta$. By tuning the coupling between granules the system can be made either a good metal for $g > g_c = (1/2\pi d)\ln(E_c/\delta)$ (d is the system dimensionality), or an insulator for $g < g_c$. The metallic phase in its turn is governed by the characteristic energy $\Gamma = g\delta$: at high temperatures $T > \Gamma$ the resistivity exhibits universal logarithmic temperature behavior specific to granular materials, while at $T < \Gamma$ the transport properties are those generic for all disordered metals. In the insulator phase the transport exhibits a variety of activation behaviors including the long-puzzling $\sigma \sim \exp[-(T_0/T)^{1/2}]$ hopping conductivity. Superconductivity adds to the richness of the observed phases via one more energy parameter Δ . Using a wide range of recently developed theoretical approaches, it is possible to obtain a detailed understanding of the electronic transport and thermodynamic properties of granular materials, as is required for their applications.

DOI: [10.1103/RevModPhys.79.469](https://doi.org/10.1103/RevModPhys.79.469)

PACS number(s): 73.23.Hk, 71.30.+h, 73.22.-f

CONTENTS

I. Introduction	470	3. Mott gap at large tunneling conductances	491
A. Why are granular electronic systems interesting?	470	4. Metal-insulator transition in periodic granular arrays	491
B. Physical quantities characterizing granular materials	472	G. Hopping conductivity in granular materials	492
II. Normal Granule Arrays	473	1. Density of states	492
A. Transport properties	473	2. Hopping via elastic co-tunneling	493
1. Classical conductivity	474	3. Hopping via inelastic co-tunneling	494
2. Metallic regime	474	III. Arrays Composed of Superconducting Grains	495
3. Insulating regime	477	A. General properties of granular superconductors	495
B. Model and main theoretical tools	478	1. Single grain	495
1. Hamiltonian	479	2. Macroscopic superconductivity	496
2. Diagrammatic technique for granular metals	481	3. Granular superconductor in a magnetic field	499
3. Coulomb interaction and gauge transformation	482	4. Transport properties of granular superconductors	499
4. Ambegaokar-Eckern-Schön functional	483	B. Phase diagram of granular superconductors	501
C. Metallic properties of granular arrays at not very low temperatures	484	1. Phase functional for granular superconductors	501
1. Perturbation theory	484	2. Mean-field approximation	502
2. Renormalization group	485	C. Upper critical field of a granular superconductor	503
D. Metallic properties of granular arrays at low temperatures	486	1. Critical field of a single grain	503
E. Universal description of granular materials	488	2. Critical magnetic field of a granular sample	504
F. Insulating properties of granular metals: Periodic model	489	D. Suppression of the superconducting critical temperature	505
1. Activation conductivity behavior	490	E. Magnetoresistance of granular superconductors	507
2. Mott gap at small tunneling conductances	490	IV. Discussion of the Results	510
		A. Quantitative comparison with experiments	510
		1. Logarithmic temperature dependence of the conductivity	510

2. Hopping conductivity	511
3. Negative magnetoresistance	511
B. Outlook	512
Acknowledgments	513
Appendix A: Calculation of the Tunneling Probability P_{el} in the Elastic Regime, Eq. (2.105)	513
Appendix B: Calculation of the Tunneling Probability P_{in} in the Inelastic Regime, Eq. (2.114)	515
References	516

I. INTRODUCTION

A. Why are granular electronic systems interesting?

Granular conductors form a new class of artificial materials with tunable electronic properties controlled at the nanoscale and composed of close-packed granules varying in size from a few to hundreds of nanometers (often referred to as *nanocrystals*). The granules are large enough to possess a distinct electronic structure, but sufficiently small to be mesoscopic in nature and exhibit effects of quantized electronic levels of confined electrons. Granular conductors combine the unique properties of individual and collective properties of coupled nanocrystals opening a new route for potential novel electronic, optical, and optoelectronic applications. Applications range from light-emitting devices to photovoltaic cells and biosensors. The intense interest in them is motivated not only by their important technological promise but by the appeal of dealing with an experimentally accessible model system that is governed by tunable cooperative effects of disorder, electron correlations, and quantum phenomena (Murray *et al.*, 1993; Gaponenko, 1998; Mowbray and Skolnick, 2005).

Among traditional methods of preparation of such materials, the most common are thermal evaporation and sputtering techniques. During those processes metallic and insulating components are simultaneously evaporated or sputtered onto a substrate. Diffusion of the metallic component leads to the formation of small metallic grains, usually 3–50 nm in diameter (see Fig. 1). Variations of grain size within a sample produced by these methods can be kept as low as about $\sim 10\%$ (Gerber *et al.*, 1997). Depending on the materials used for the preparation, one can obtain magnetic systems, superconductors, insulators, etc.

Recent years have seen remarkable progress in the design of granular conductors with controllable structure parameters. Granules can be capped with organic

(ligands) or inorganic molecules which connect and regulate the coupling between them. By altering the size and shape of granules one can regulate quantum confinement effects. In particular, by tuning the microscopic parameters, one can create the granular materials varying from relatively good metals to pronounced insulators as a function of the strength of electron tunneling couplings between conducting grains. This makes granular conductors a perfect exemplary system for studying the metal-insulator transition and related phenomena.

One emerging technique to create granular systems is through self-assembling colloidal nanocrystals (Collier *et al.*, 1998; Murray *et al.*, 2000). For instance, Lin *et al.* (2001) described almost perfectly periodic two-dimensional arrays of monodisperse gold nanoparticles (with grain size variations within $\sim 5\%$), covered by ligand molecules that play the role of an insulating layer. Such samples are produced via self-assembling of gold nanoparticles at the liquid-air interface during the evaporation of a colloidal droplet (Narayanan *et al.*, 2004). By changing the experimental conditions, multilayers of nanocrystals can also be created (see Figs. 2 and 3) (Parthasarathy *et al.*, 2001, 2004; Tran *et al.*, 2005). Other important examples include Langmuir films of colloidal Ag (Collier *et al.*, 1997; Du *et al.*, 2002) and arrays of semiconductor quantum dots (Murray *et al.*, 1993; Du *et al.*, 2002; Wehrenberg *et al.*, 2002; Yu *et al.*, 2004).

Of the range of techniques developed for the fabrication of semiconductor quantum dot arrays, the most successful appears to be the self-assembled technique of epitaxial growth of two semiconductors having significantly different lattice constants. For the prototype system of InAs on GaAs, where the lattice mismatch is 7%, InAs initially deposited on GaAs grows as a strained two-dimensional layer (referred to as the wetting layer) (Mowbray and Skolnick, 2005). These materials and $\text{In}_2\text{O}_3:\text{Sn}$ [known as indium tin oxide (ITO)] are the most widely studied systems. They exhibit a high visible transparency and a good electrical conductance. They are used as electrodes in light-emitting diodes (Kim *et al.*, 1998; Zhu *et al.*, 2000), solar cells (Gordon, 2000), smart windows, and flat panel displays.

All these experimental achievements and technological prospects call for a comprehensive theory able to provide a quantitative description of the transport and thermodynamic properties of granular conductors, which can therefore serve as a basis for the clever design

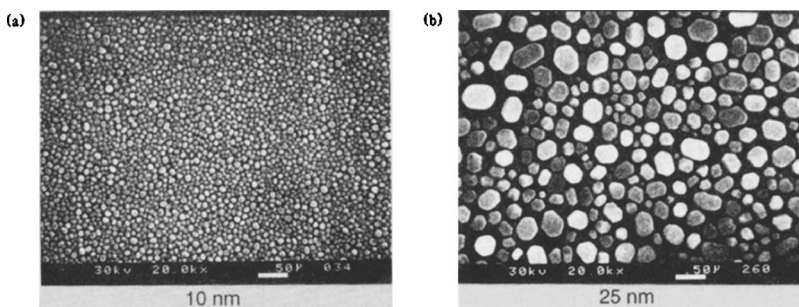


FIG. 1. Scanning electron microscope photographs of indium evaporated onto SiO_2 at room temperature. From Yu *et al.*, 1991.

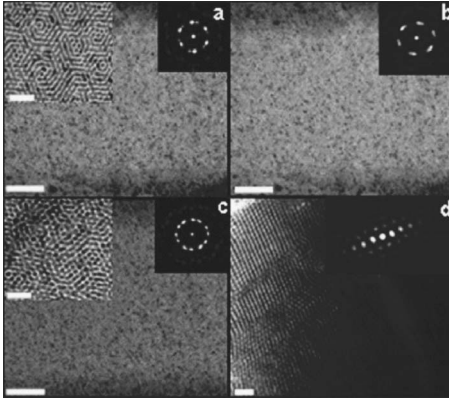


FIG. 2. Transmission electron micrographs showing periodic granular (a) bilayers, (b) trilayers, (c) tetralayers, and (d) thick films. The insets on the left sides of panels (a) and (c) are the zoomed-in images. The scale bars correspond to (a)–(c) 200 nm and (d) 40 nm. From [Tran *et al.*, 2005](#).

of devices for the new generation of nanoelectronics.

It has been realized for quite some time that granular-ity can produce new physics, even further extending further the already rich list of remarkable effects exhibited by disordered systems. One of the early observations was the stretched-exponential temperature behavior of the conductivity in strongly disordered films and arrays of metallic granules in the insulating regime [see [Abeles *et al.* \(1975\)](#) for a review]:

$$\sigma(T) \sim \exp(-\sqrt{T_0/T}), \quad (1.1)$$

with T_0 being a material-dependent constant. This behavior resembles the Mott-Efros-Shklovskii variable-range hopping conductivity in semiconductors ([Efros and Shklovskii, 1975](#); [Shklovskii and Efros, 1988](#)) and appears to be generic for both metallic and semiconducting granular arrays—either irregular ([Abeles *et al.*, 1975](#)) or strictly periodic ([Yu *et al.*, 2004](#); [Romero and Drndic, 2005](#); [Tran *et al.*, 2005](#)). Several explanations have been advanced for this striking behavior, but real understanding was achieved only recently ([Zhang and Shklovskii, 2004](#); [Beloborodov *et al.*, 2005](#); [Feigel'man and Ioselevich, 2005](#); [Tran *et al.*, 2005](#)).

A recent incitement to intense study of the physics of granular materials was given by [Simon *et al.* \(1987\)](#) and [Gerber *et al.* \(1997\)](#), where a logarithmic dependence of the conductivity $\sigma(T)$,

$$\sigma(T) = a + b \ln T, \quad (1.2)$$

with a and b material-dependent constants, was observed in the metallic conductivity domain. This logarithmic behavior has been observed in both two- and three-dimensional samples thus ruling out the tempting explanation in terms of weak localization ([Abrahams *et al.*, 1979](#); [Gorkov *et al.*, 1979](#)) or interaction corrections ([Altshuler *et al.*, 1980](#); [Lee and Ramakrishnan, 1985](#); [Belitz and Kirkpatrick, 1994](#)), which result in logarithmic behavior in two dimensions only. New models were developed to understand these results ([Efetov and Tschersich, 2002, 2003](#); [Beloborodov *et al.*, 2003, 2004](#)) and

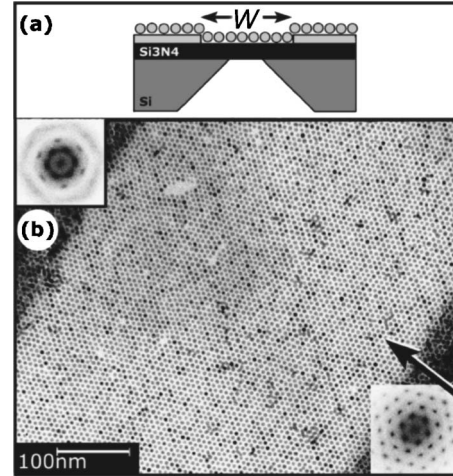


FIG. 3. Transmission electron micrograph image of nanocrystals (a) monolayer and in-plane electrodes, (b) highly ordered superlattice between electrodes visible at the upper left and lower right. Adapted from [Parthasarathy *et al.*, 2001](#).

evolved into a new direction of research that will be one of the major topics of our review.

The feature of granular materials that plays a fundamental role, especially at low temperatures, is the pronounced discreteness of the electronic levels due to electron confinement within a single grain. The mesoscopic scale of the grains causes the level statistics and all related effects ([Halperin, 1986](#); [Nagaev *et al.*, 1992](#)). The mean level spacing δ in a single grain is inversely proportional to the volume of the grain,

$$\delta = (\nu V)^{-1}, \quad (1.3)$$

where V is the volume of the grain and ν is the density of states at the Fermi energy. For metal particles of the size of several nanometers, the parameter δ is typically of the order of several kelvin. For example, for an aluminum particle with radius $R=5$ nm one has $\delta \sim 1$ K. However, we concentrate on the temperature range $T > \delta$ where quantum size effects are not important. In fact both types of conductivity behavior, Eqs. (1.1) and (1.2), have been observed at temperatures $T > \delta$.

Superconductivity brings yet more diversity to the interesting effects in granular materials ([Shapira and Deutscher, 1983](#); [Jaeger *et al.*, 1989](#); [Gerber *et al.*, 1997](#); [Hadacek *et al.*, 2004](#)). One of them is a counterintuitive suppression of the conductivity due to superconducting fluctuations.

In this review we summarize the recent theoretical progress in understanding the phenomena observed in granular metals and superconductors. These are effects that do not demand ultralow temperatures (and thus very sophisticated experimental setups) and are thus promising from the standpoint of possible applications. The physics of these phenomena is not particularly material specific and our consideration will be based on correspondingly general models of granular systems.

B. Physical quantities characterizing granular materials

This review deals with systems that we call granular metals, which are well modeled by an array of mesoscopically different metallic particles identical in size and shape, with the intergranular electron coupling being described via the tunneling matrix. The grain arrangements may be either periodic or irregular.

The effect of irregularities in the grain positions and in the strengths of the tunneling coupling on the physical properties of granular systems is different for metallic and insulating samples. If the coupling between the grains is sufficiently strong and the system is well conducting, the irregularities are not very important. In contrast, irregularities become crucial in the limit of low coupling where the system is an insulator. As a matter of practice, recent advances in fabrication techniques now permit very regular arrays with fluctuations in the granule size within 5% precision (Yu *et al.*, 2004; Tran *et al.*, 2005). As regular arrays promise many technological applications further progress in making perfect systems is expected.

At the same time, disorder related to internal defects inside and/or on the surface of the individual granules and to charged impurities in the insulating substrate or matrix is unavoidable. Even in metallic grains with mean free paths exceeding their size, electrons that move ballistically within the granules still scatter at the grain-boundary irregularities; the electron motion becomes chaotic with the resulting effect equivalent to the action of intragranular disorder [see, e.g., Efetov (1997)]. This surface chaotization would be absent in atomically perfect spherical (or, say, cubical) granules. In such ideal granules the additional degeneracies of the energy levels would lead to singularities in physical quantities. However, the slightest deviations (even of the order of 1 Å or the order of the electron wavelength) of the shape of the grains from ideal spheres or cubes will lift the accidental degeneracy of the levels (this would be equivalent to adding internal disorder). Thus one can justly assume that the grains are always microscopically irregular. Moreover, the coupling between grains is the source of additional irregularities. We thus can adopt a model with diffusive electron motion within each grain without any loss of generality. In this model the use of Eq. (1.3) for the mean level spacing δ is fully justified.

The key parameter that determines most of the physical properties of the granular array is the average tunneling conductance G between neighboring grains. It is convenient to introduce the dimensionless conductance g (corresponding to one spin component) measured in units of the quantum conductance e^2/h : $g = G/(2e^2/h)$. As we will see below, samples with $g \geq 1$ exhibit metallic transport properties, while those with $g \lesssim 1$ show insulating behavior.

One of the most important energy parameters of the granular system is the single-grain Coulomb charging energy E_c . This energy is equal to the change in energy of the grain when adding or removing one electron, and it plays a crucial role in the transport properties in the

insulating regime when electrons are localized in the grains, such that the charge of each grain is quantized. The physics of the insulating state is closely related to the well-known phenomenon of the Coulomb blockade of a single grain connected to a metallic reservoir.

The behavior of a single grain in contact with a reservoir has been discussed in many articles and reviews [see, e.g., Averin and Likharev (1991), Averin and Nazarov (1992), and Aleiner *et al.* (2002)]. The main features of the Coulomb blockade can be summarized as follows: (i) If the grain is weakly coupled to the metallic contact $g \ll 1$, the charge on the grain is almost quantized; this is the regime of the so-called Coulomb blockade. (ii) In the opposite limit $g \gg 1$, the effects of the charge quantization are negligible and electrons are freely exchanged between the granule and reservoir.

Although the systems we consider are arrays of interconnected granules rather than a single grain coupled to a bulk metal, a somewhat similar behavior is expected. In the regime of strong coupling between grains $g \gg 1$, electrons propagate easily through the granular sample and the Coulomb interaction is screened. In the opposite limit of low coupling $g \ll 1$, the charge on each grain becomes quantized as in standard Coulomb blockade behavior. In this case an electron has to overcome an electrostatic barrier of the order E_c in order to hop onto a neighboring granule. This impedes the transport at temperatures T lower than E_c .

Throughout this review we always assume that the mean level spacing δ from Eq. (1.3) is the smallest energy scale. In particular, in all cases we assume that the condition $E_c \gg \delta$ is satisfied. This is the most realistic condition when dealing with metallic particles of a nanometer size scale (given that the charging energy E_c is inversely proportional to the radius a of the grains, whereas the mean level spacing δ is inversely proportional to the volume V) and also taking into account the high density of energy states in metals. Note that this may not be the case in arrays of semiconductor dots, where E_c and δ may appear of the same order, but this goes beyond the scope of our review.

Another important thing to remember is that the intergranular (tunneling) conductance g is much smaller than the intragrain conductance g_0 by the very meaning of the notion of a “granular system”:

$$g \ll g_0. \quad (1.4)$$

The intragrain conductance g_0 is caused by scattering on impurities or on the boundaries of the grains and the inequality (1.4) means that the grains are not very dirty. The case $g \sim g_0$ can be viewed as a homogeneously disordered system and we dwell on this limit here. The single-grain conductance g_0 can be most easily defined as the physical conductance of a granule with cubic geometry measured in units of the quantum conductance e^2/h . In mesoscopic physics it is customary, however, to relate the single-grain conductance g_0 to the single-grain Thouless energy E_{Th} as $g_0 = E_{Th}/\delta$, where the energy E_{Th} is defined as

$$E_{\text{Th}} = D_0/a^2, \quad (1.5)$$

and $D_0 = v_F^2 \tau / d$ is the classical diffusion coefficient. Other parameters are v_F , the Fermi velocity, τ , the elastic scattering time within the grains, and d , the dimensionality of the grain. The length a in Eq. (1.5) is the linear size (radius) of the grain. If the grains are not very dirty, such that electrons move inside the grains ballistically, the mean free path $l = v_F \tau$ should be replaced by the size of the grains $2a$. The Thouless energy E_{Th} , Eq. (1.5), is proportional to the inverse time that it takes for an electron to traverse the grain. The energy E_{Th} exceeds the mean level spacing δ , Eq. (1.3), and therefore the intragrain conductance g_0 is always large $g_0 \gg 1$, whereas the intergranular conductance g can be either larger or smaller than unity.

The above parameters make up a full set of variables describing the properties of normal granular metals. If the constituent particles are made of a superconductor material, a wealth of new interesting phenomena arises. The behavior of such a system can be quantified by adding one more energy parameter, the superconducting gap Δ of the material of a single granule. Now, if the intergrain coupling is sufficiently strong, the system can turn into a superconductor at sufficiently low temperatures. The properties of such a superconductor are not very different from those of bulk superconductors.

On the contrary, in the opposite limit of weak coupling between the granules, an array of superconducting grains can transform into an insulator at $T=0$. In this regime Cooper pairs are locally formed in each grain but remain localized inside the grains due to the strong on-site Coulomb repulsion leading to the Coulomb blockade. Because of localization, the number of Cooper pairs in each grain is fixed and, according to the uncertainty principle, this leads to strong phase fluctuations. Thus the system does not develop global coherence, and global macroscopic superconductivity is suppressed. One can describe this effect using the model of superconductor grains coupled via Josephson junctions. Such a system is characterized by three energy parameters: the superconductor gap Δ , characterizing a single grain, the Josephson coupling J , and the grain charging Coulomb energy E_c . Strong Josephson coupling $J \gg E_c$ suppresses the phase fluctuations leading to the globally coherent superconducting state at sufficiently low temperatures. If $J \ll E_c$, the Coulomb blockade prevails, the Cooper pairs become localized at $T \rightarrow 0$, and the system falls into an insulating state.

Note that even in the insulating state the superconducting gap Δ still exists in each grain and its value is close to the gap magnitude in the bulk, provided $\Delta \gg \delta$. If the latter inequality is not satisfied, the superconducting gap in the grains is suppressed or can even be fully destroyed (Anderson, 1959, 1964). There are interesting effects in this regime but we do not consider them here because the relevant region of the parameters corresponds to either too small grains or too weak superconductors.

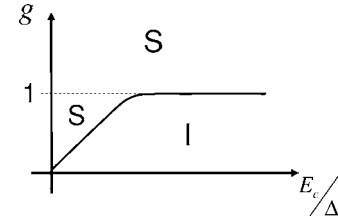


FIG. 4. Schematic phase diagram for granular superconductors at temperature $T=0$. Symbols S and I stand for superconducting and insulating phases, respectively.

At low temperatures, the Josephson coupling J is expressed via the tunneling conductance g as $J = \pi g \Delta / 2$ (Ambegaokar and Baratoff, 1963) and, at first glance, one might conclude that the transition between the insulating and superconducting states should have happened at $g \sim E_c / \Delta$. However, this simple estimate holds only in the weak-coupling regime $g < 1$, which assumes $E_c < \Delta$. At stronger coupling, the Coulomb energy E_c is renormalized down to the value $E_c \rightarrow \tilde{E} \sim \Delta / g$ (Larkin and Ovchinnikov, 1983; Chakravarty *et al.*, 1987) due to electron tunneling between neighboring grains. Therefore in the limit of strong coupling $g \gg 1$ the effective Coulomb energy \tilde{E} is always smaller than the Josephson coupling $\tilde{E} < J$, implying a superconducting ground state. Shown in Fig. 4 is the schematic phase diagram summarizing the above considerations (Chakravarty *et al.*, 1987). For many superconducting granular samples available experimentally the ratio E_c / Δ is large. In this case, as one can see from the phase diagram in Fig. 4, the transition between the superconducting and insulating phases at $T \rightarrow 0$ occurs at $g \sim 1$ (Orr *et al.*, 1986; Chakravarty *et al.*, 1987).

To conclude our brief introduction to granular superconductors, we note that, for most of the experimentally available samples, the grains are much smaller than the bulk superconducting coherence length of the granule material,

$$a \ll \xi_0. \quad (1.6)$$

This allows one to neglect variations of the superconducting order parameter Δ inside the grains and treat a single grain as a zero-dimensional object. As the condition (1.6) is at this point the most common experimental situation, we further concentrate mainly on this regime.

As we now see, depending on the parameters of the system, many different physical situations appear, and the phase diagram of a granular material is quite rich. In Secs. II and III we focus on systems consisting of normal and superconducting grains, respectively.

II. NORMAL GRANULE ARRAYS

A. Transport properties

We start our discussion with the properties of granular systems consisting of normal grains by presenting the main results and their qualitative explanations. This may

help the reader to understand the basic physics of the system and to learn important formulas suitable for a direct comparison with experiments without going into the technical detail of theoretical models, which will be presented in subsequent parts of each section.

1. Classical conductivity

The key parameter that determines the transport properties of granular materials is the tunneling conductance g . In the strong-coupling regime $g \gg 1$ a granular array has metallic properties, while in the opposite case $g \ll 1$ the array is an insulator. The insulating state appears as a result of the strong Coulomb correlations that block electron transport at low temperatures. Generally speaking, apart from the Coulomb interaction effects one also has to consider the effects of quantum interference that may play an important role in low-conducting samples. In homogeneously disordered systems interference effects play an important role, leading to the localization of electron states in the absence of interaction (Anderson, 1958).

In the metallic regime and at high enough temperatures, both Coulomb correlation and interference effects are weak. In this case the global sample conductivity σ_0 is given by the classical Drude formula; in particular, for a periodic cubic granular array

$$\sigma_0 = 2e^2 g a^{2-d}, \quad (2.1)$$

where a is the size of the grains and d is the dimensionality of the sample. Equation (2.1) has a straightforward meaning: in order to obtain the physical conductance of the contact, one should multiply its dimensionless conductance g by $2e^2$ (the factor 2 is due to spin and $\hbar = 1$) and, then, multiplying the result by a^{2-d} , one arrives at the conductivity per unit volume.

Although Eq. (2.1) is written for a periodic array, the electron system is not translationally invariant, otherwise the sample conductivity would be infinite. Equation (2.1) is valid for grains with internal disorder, such that the electron motion inside the grains is chaotic. When the electron hops from grain to grain, its momentum is not conserved and this leads to the finite conductivity σ_0 , Eq. (2.1). The conductance of the contact g depends on the microscopic properties of the contact, and we consider it in most cases as a phenomenological dimensionless parameter controlling the behavior of the system. Note that the model of a periodic array assumes no variation in tunneling conductances.

Upon decreasing the temperature Coulomb interactions become relevant and Eq. (2.1) no longer holds. Below we discuss Coulomb effects in more detail and find that their manifestation in granular systems may differ noticeably from that in “homogeneously disordered” metals.

2. Metallic regime

In the metallic regime electrons tunnel easily from granule to granule. The time τ_0 that the electron spends inside a grain plays an important role in the metallic

regime: the corresponding characteristic energy $\Gamma = \tau_0^{-1}$ is related to the tunneling conductance and the mean energy-level spacing as

$$\Gamma = g \delta. \quad (2.2)$$

The energy Γ can also be interpreted as the width of the smearing of the energy levels in the grains. In the limit of large conductances $g \gg 1$ this width exceeds the energy spacing δ and the discreteness of the levels within a single grain ceases to be relevant.

Since the electron motion on scales well exceeding the granule size is always diffusive (even in the case of the ballistic electron motion inside each grain), the electron motion on the time scales larger than Γ^{-1} can be described by the effective diffusion coefficient D_{eff} related to Γ as

$$D_{\text{eff}} = \Gamma a^2. \quad (2.3)$$

Then the Einstein relation gives the conductivity of the granular sample as

$$\sigma_0 = 2e^2 \nu D_{\text{eff}}. \quad (2.4)$$

For periodic arrays Eq. (2.4) is equivalent to Eq. (2.1), which can be seen from Eqs. (1.3), (2.2), and (2.3). At the same time Eq. (2.4) is more general than Eq. (2.1) since with the properly defined diffusion constant D_{eff} it applies to arrays with arbitrary grain arrangement as well.

The energy scale Γ plays a very important role; many physical quantities have qualitatively different behavior depending on whether they are dominated by energies higher or lower than Γ .

From the experience with homogeneously disordered metals one can envision two major causes that may alter the classical conductivity σ_0 in Eq. (2.1): (i) electron-electron interactions (Altshuler and Aronov, 1985; Lee and Ramakrishnan, 1985) and (ii) quantum interference effects (Abrahams *et al.*, 1979; Gorkov *et al.*, 1979). Accordingly, constructing the theory of granular conductors with reference to the highly advanced theory of disordered metals, one can expect two corresponding distinct corrections to σ_0 . Since in the metallic domain electrons effectively screen out the on-site Coulomb interactions, the bare magnitudes of which are high because of the small sizes of the grains, the notion of interaction corrections to the conductivity is well justified.

To gain a qualitative understanding of interaction effects, we introduce the characteristic interaction temporal scale $\tau_T \sim \hbar / T$ and the corresponding spatial scale $L_T \sim \sqrt{D_{\text{eff}} / T}$ associated with this time. One expects that the behavior of the interaction correction is different on distances exceeding the granule size $L_T > a$ and within the granule $L_T < a$. Using Eq. (2.3) to find the effective diffusion coefficient D_{eff} , one immediately sees that these conditions imply the existence of two distinct temperature regions $T > \Gamma$ and $T < \Gamma$ with respect to interaction contributions. Accordingly, the correction to the conductivity due to Coulomb interaction can be written as a sum of contributions coming from high, $\varepsilon > \Gamma$, and low, $\varepsilon < \Gamma$, energies. This separation of contribution

naturally follows from the diagrammatic approach where the two contributions in question are represented by two distinct sets of diagrams. Deferring the details for later, the result is as follows: denoting the corrections coming from the high and low energies with respect to Γ as $\delta\sigma_1$ and $\delta\sigma_2$, respectively, we write

$$\sigma = \sigma_0 + \delta\sigma_1 + \delta\sigma_2 \quad (2.5)$$

with

$$\frac{\delta\sigma_1}{\sigma_0} = -\frac{1}{2\pi dg} \ln \left[\frac{gE_c}{\max(T, \Gamma)} \right] \quad (2.6)$$

(Efetov and Tschersich, 2002, 2003) and

$$\frac{\delta\sigma_2}{\sigma_0} = \begin{cases} \frac{\alpha}{12\pi^2 g} \sqrt{\frac{T}{\Gamma}}, & d=3 \\ -\frac{1}{4\pi^2 g} \ln \frac{\Gamma}{T}, & d=2 \\ -\frac{\beta}{4\pi g} \sqrt{\frac{\Gamma}{T}}, & d=1, \end{cases} \quad (2.7)$$

where $\alpha \approx 1.83$ and $\beta \approx 3.13$ are numerical constants (Beloborodov *et al.*, 2003). The high-energy contribution $\delta\sigma_1$ in Eq. (2.5) contains the dimensionality of the array d merely as a coefficient and is, in this sense, universal. On the contrary, the low-energy contribution $\delta\sigma_2$ in Eq. (2.5) has a different functional form for different array dimensionalities. [Note that for the three-dimensional correction we have kept the temperature-dependent part only.]

At high temperatures $T > \Gamma$ the correction $\delta\sigma_1$, Eq. (2.5), grows logarithmically with decreasing temperature. Upon further lowering the temperature this correction saturates at $T \approx \Gamma$ and remains constant at $T < \Gamma$. Then the correction $\delta\sigma_2$ in Eq. (2.7) from the low-energy scales, $\varepsilon \leq \Gamma$, where coherent electron motion on scales larger than the grain size a dominates the physics, and which is similar to that derived for homogeneous disordered metals (Altshuler and Aronov, 1985), comes into play. In the low-temperature regime it is this term that entirely determines the temperature dependence of the conductivity. At the same time, the contribution $\delta\sigma_1$, although temperature independent, still exists in this regime and can even be larger in magnitude than $\delta\sigma_2$. Equation (2.6) can be written for $T > \Gamma$ in the form Eq. (1.2) which has been observed in a number of experiments (Simon *et al.*, 1987; Fujimori *et al.*, 1994; Gerber *et al.*, 1997; Rotkina, 2005) (see, e.g., Fig. 5).

Rewriting the low-energy contribution $\delta\sigma_2$ in terms of the effective diffusion coefficient D_{eff} from Eq. (2.3) one reproduces the Altshuler-Aronov corrections (Altshuler and Aronov, 1985). This reflects the universal character of large-scale behavior for a disordered system, and we show rigorously in Sec. II.D that indeed the granular metal model can be reduced to an effective disordered medium on distances much larger than a single-grain size (i.e., coming from the low-energy, $T < \Gamma$, excitations). The contribution $\delta\sigma_1$, which is dominated by the

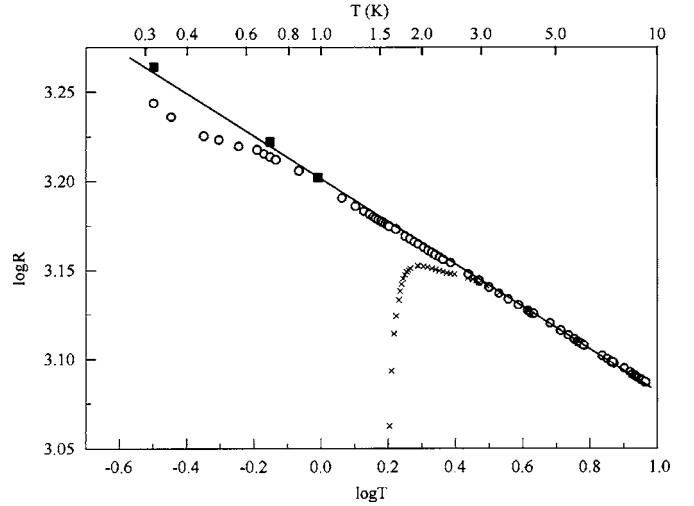


FIG. 5. Resistance of 3D granular Al-Ge sample as a function of temperature on a log-log scale, as measured at (zero) (\times) and 100 kOe field (open circles). Sample room-temperature resistance is 500 Ω . From Gerber *et al.*, 1997.

energies $\varepsilon > \Gamma$, is the consequence of and specific to the granularity—and does not exist in homogeneously disordered metals.

Now we turn to quantum interference (weak-localization) effects that exist also in systems without any electron-electron interaction. In the metallic regime, where perturbation theory holds with respect to the inverse tunneling conductance $1/g$, the interaction and weak-localization corrections can be considered independently in leading order.

The weak-localization correction is of a purely quantum origin: it stems from the quantum interference of electrons moving along self-intersecting trajectories and is proportional to the return probability of an electron diffusing in a disordered medium. In one- or two-dimensional conductors the probability of returning infinitely many times is unity and the returning trajectories can be infinitely long. Thus fully coherent electron propagation would lead to a divergent weak-localization correction. The finite phase relaxation (dephasing) time prevents long trajectories and limits the correction. Adapting here the concept of the effective disordered medium we can assume that the results of Altshuler and Aronov (1985) for homogeneously disordered metals apply to granular metals with the proper renormalization of the diffusion constant. We introduce the effective dephasing length $L_\phi = \sqrt{D_{\text{eff}} \tau_\phi} \sim a \sqrt{\Gamma \tau_\phi}$, where τ_ϕ is the dephasing time, which determines the scale for the interference effects. At low temperatures the dephasing time τ_ϕ is large and the decoherence length L_ϕ can exceed the size a of a single grain, $L_\phi > a$. In this regime the relevant electron trajectories pass through many granules and quantum interference effects are similar to those in homogeneously disordered metals and contribute essentially to the conductivity. With increasing temperature the decoherence length L_ϕ decreases and as soon as it drops to the grain size, $L_\phi \sim a$, the trajectories

contributing to weak localization traverse to only one neighbor and the weak-localization correction is suppressed. Using Eq. (2.3) we write the last condition separating the domains of “relevance” and “irrelevance” of weak-localization effects as $\tau_\phi \sim \Gamma^{-1}$. For $\tau_\phi > \Gamma^{-1}$ (or $L_\phi > a$) the quantum interference effects are important, while for $\tau_\phi < \Gamma^{-1}$ (or $L_\phi < a$) the corresponding correction drops rapidly with temperature.

The final result for the quantum interference corrections reads (Beloborodov *et al.*, 2004b; Biagini, Canera, *et al.*, 2005)

$$\frac{\delta\sigma_{\text{WL}}}{\sigma_0} = -\frac{1}{4\pi^2 g} \ln(\tau_\phi \Gamma) \quad (2.8)$$

for granular films and

$$\frac{\delta\sigma_{\text{WL}}}{\sigma_0} = -\frac{1}{2\pi g} (\tau_\phi \Gamma)^{1/2} \quad (2.9)$$

for granular wires. In both equations τ_ϕ is the dephasing time. Within this time the wave function retains its coherence. The most common mechanism of dephasing, the electron-electron interactions, gives for the dephasing time (Altshuler *et al.*, 1982)

$$\tau_\phi^{-1} = \begin{cases} \frac{T}{g}, & d=2 \\ \left(\frac{T^2 \delta}{g}\right)^{1/3}, & d=1. \end{cases} \quad (2.10)$$

In this case the condition $\Gamma \approx \tau_\phi^{-1}$ defines (in the 2D case) yet another characteristic energy scale $T^* = g^2 \delta$, which marks the interval of relevance of weak-localization effects.

The quantum interference correction $\delta\sigma_{\text{WL}}$ is suppressed by applying even a relatively weak magnetic field; the dependence upon the magnetic field can serve as a test for identifying weak-localization effects. At sufficient fields, the main temperature dependence of the conductivity will thus come from electron-electron interaction effects, Eqs. (2.6) and (2.7).

Both electron-electron interactions and quantum interference effects decrease the conductivity of a granular system at low temperatures, as in homogeneously disordered systems. The important feature is that the granularity restrains screening, thus enhancing the role of Coulomb interaction: this is reflected by the contribution $\delta\sigma_1$ to the conductivity which is specific to granular conductors but absent in homogeneously disordered metals. As a result, in 3D (and, to some extent, in 2D; see below) granular systems the Coulomb interactions can become the main driving force of a metal-insulator transition.

This question is worth a more detailed discussion. The granular contribution $\delta\sigma_1$ comes from short distances and is actually the renormalization of the tunneling conductance between the grains:

$$g \rightarrow \tilde{g} = g - \frac{1}{2\pi d} \ln \left[\frac{gE_c}{\max(T, \Gamma)} \right]. \quad (2.11)$$

Using renormalization-group methods one can show that Eq. (2.11) represents the solution of the renormalization-group equation for the effective conductance \tilde{g} rather than a merely perturbative correction. As such, it holds not only when the second term on the right-hand side of Eq. (2.11) is much smaller than the first one but in a broader temperature region—as long as the renormalized conductance is large, $\tilde{g} > 1$. It is important that the logarithm in Eq. (2.11) saturates at temperatures of the order of Γ . Then one sees from Eq. (2.11) that the renormalized conductance \tilde{g} may remain large in the limit $T \rightarrow 0$ only provided the original (bare) conductance g is larger than its critical value

$$g_c = (1/2\pi d) \ln(E_c / \delta). \quad (2.12)$$

If $g < g_c$, the effective conductance \tilde{g} renormalizes down to zero at finite temperature. Of course, as soon as \tilde{g} becomes of the order of unity, Eq. (2.11) is no longer valid, but it is generally accepted—in the spirit of the renormalization-group approach—that conductance flow to low values signals electron localization [a recent exact solution for a model equivalent to a single grain connected to a metallic contact lends confidence to this conclusion (Lukyanov and Zamolodchikov, 2004)]. The result (2.12) can also be obtained by analyzing the stability of the insulating state, as discussed below.

The physical meaning of the critical conductance g_c is most transparent for a 3D system: in this case, there are no infrared divergencies and both the localization and Altshuler-Aronov corrections are unimportant even in the limit $T \rightarrow 0$. This implies that as long as $g > g_c$ the granular conductor remains metallic.

At $g < g_c$ the conductance renormalizes to low values at temperatures exceeding Γ , thus signaling the development of the Coulomb blockade. Upon further temperature decrease the system resistance begins to grow exponentially at a certain characteristic temperature T_{ch} , indicating the onset of insulating behavior. The temperature T_{ch} tends to zero in the limit $g \rightarrow g_c$. Thus in three dimensions the value g_c marks the boundary between the insulating and metallic states at $T \rightarrow 0$.

The interpretation of the critical value g_c is less straightforward in the case of granular films, since at $g > g_c$ the low-temperature conductivity corrections due to interaction and localization effects diverge logarithmically. This means apparently that the system becomes an insulator without a sharp transition. Yet the notion of g_c still makes sense as a marker distinguishing between systems that are strong Coulomb insulators at low temperatures ($g < g_c$) and those that are weak insulators ($g > g_c$).

The above results have been obtained within the model of a periodic granular array (cubic lattice), neglecting dispersion of the tunneling conductance. In reality, typical granular samples are disordered. It is then important to understand what effect the irregularities in

the granules' arrangement may have. It is plausible that the universal regime of low energies is hardly affected by the irregularities since all physical characteristics in this regime can be expressed through the effective diffusion coefficient of the medium. At the same time, the physical results that are controlled by the local physics, in particular, the critical value g_c , are sensitive to the grain arrangements. In some cases the irregularities can be incorporated at almost no expense. For example, breaking some finite fraction of junctions between the granules merely changes the average coordination number z , which appears as the $1/2d$ factor in Eqs. (2.11) and (2.12) for the critical conductance. This means that the dispersion in tunneling conductance is not expected to change noticeably, for example, the position of the metal-insulator transition (which may acquire a percolation character), and can be taken into account by replacing $2d$ in Eqs. (2.11) and (2.12) with the effective coordination number $z_{\text{eff}} < z$.

In general, proper treatment of disorder in the grain arrangement may appear more tedious. Yet we do not expect that it can change the physics of the metallic state qualitatively. Irregularities of grain displacements and of other quantities characterizing the system play a much more important role in the insulating regime, which we briefly review in the following section.

3. Insulating regime

We begin with a periodic granular array which, in the regime of weak coupling between the grains, is an exemplary Mott insulator at low temperatures. The electron transport is mediated by electron hopping from grain to grain. However, leaving a neutral grain and entering its neighbor involves a considerable electrostatic energy cost, and electron transport is blocked at low temperatures by the Coulomb gap in the electron excitation spectrum Δ_M . At very small tunneling conductances this gap is simply the Coulomb charging energy of the grain, $\Delta_M = E_c$. Virtual electron tunneling to neighboring grains leads to a reduction of the Mott gap Δ_M and, in the limit of noticeable tunneling, the gap decays exponentially in g (Beloborodov, Lopatin, and Vinokur, 2005) until it reaches the inverse escape rate from a single grain Γ . At $\Delta_M \sim \Gamma$ the system falls into the regime of weak Coulomb correlations and the insulator-metal transition occurs in three dimensions. Using $\Delta_M \sim \Gamma$ to estimate the transition point, one arrives within logarithmic accuracy at the same result for the critical conductance g_c as that derived from renormalization-group considerations (see for details Sec. II.F).

The presence of the hard gap in the excitation spectrum leads to an activation dependence (Arrhenius law) of the conductivity on temperature:

$$\sigma \sim e^{-\Delta_M/T}, \quad T \ll \Delta_M. \quad (2.13)$$

Indeed, the finite-temperature conductivity is due to electrons and holes that are present in the system as real excitations. Their density is given by the Gibbs distribu-

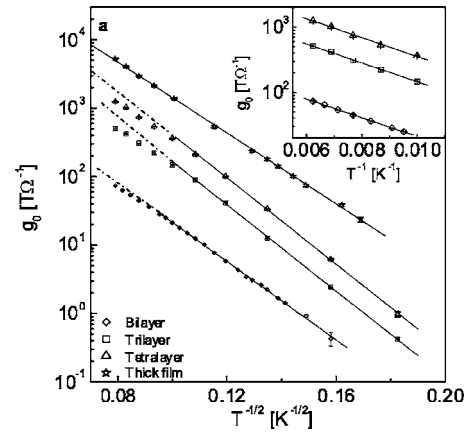


FIG. 6. Conductance g_0 vs inverse temperature $T^{-1/2}$ for periodic granular multilayer and thick film shown in Fig. 2. Inset: for the high-temperature range g_0 has been replotted as a function of T^{-1} , indicating Arrhenius behavior from 100 to 160 K. From Tran *et al.*, 2005.

tion, which results in an exponential dependence of the conductivity, Eq. (2.13).

However, the activation behavior is usually not observed in real granular samples at low temperatures. Instead, the experimentally observed resistivity follows the law Eq. (1.1), which resembles the Efros-Shklovskii law derived for doped semiconductors. The fact that the observed conductivity behavior cannot be explained in terms of the periodic model suggests that disorder plays a crucial role in the low-temperature conductivity in the insulating state.

The stretched-exponential Shklovskii-Efros-like conductivity behavior in granular conductors remained a challenging puzzle for a long time. Several explanations were advanced; in particular, it was proposed (Abeles *et al.*, 1975) that random variations of the capacitance resulting from the grain-size dispersion could provide the dependence of Eq. (1.1). However, capacitance disorder can never lift the Coulomb blockade in a single grain completely and therefore cannot give rise to a finite density of states at the Fermi level (Pollak and Adkins, 1992; Zhang and Shklovskii, 2004). Furthermore, the stretched-exponential dependence, Eq. (1.1), was observed in periodic arrays of quantum dots (Yakimov *et al.*, 2003) and artificially manufactured metallic periodic granular systems (Tran *et al.*, 2005) (see Fig. 6), where the size of the granules and the periodicity in the dot arrangement were controlled within a few percent accuracy. Neither of those systems possesses any noticeable capacitance disorder, yet the dependence (1.1) is observed. This indicates that electrostatic disorder unrelated to grain-size variations but caused most probably by charged defects in the insulating matrix or substrate is responsible for lifting the Coulomb blockade and for the finite density of states near the Fermi level resulting in the dependence (1.1).

There is, however, another ingredient necessary for the variable-range-hopping (VRH) type of conductivity to occur (apart from a finite density of states at energies

close to the Fermi level): a finite, although decaying exponentially with distance, probability for tunneling to spatially remote—and not only to adjacent—states close to the Fermi level. Accordingly, the problem of the hopping transport in granular conductors is twofold and a model should contain (i) an explanation of the origin of the finite density of states near the Fermi level and the role of the Coulomb correlations in forming this density of states, and (ii) quantitative description of the mechanism of tunneling over long distances through a dense array of metallic grains.

The behavior of the density of states, as mentioned above, can be caused by an on-site random potential, which in turn is induced by carrier traps in the insulating matrix in granular conductors. Traps with energies lower than the Fermi level are charged and induce a potential of the order of $e^2/\kappa r$ on the closest granule, where κ is the dielectric constant of the insulator and r is the distance from the granule to the trap. This is similar to Coulomb blockade energies due to charged metallic granules during the transport process. Such a mechanism was considered by [Zhang and Shklovskii \(2004\)](#). In 2D granular arrays and/or arrays of quantum dots, one can expect that the induced random potential originates also from imperfections and charged defects in the substrate.

We model the electrostatic disorder via the random potential V_i , where i is the grain index. Such a potential gives rise to a flat bare density of states at the Fermi level. In complete analogy with semiconductors, the bare density of states should be suppressed by the long-range Coulomb interaction ([Efros and Shklovskii, 1975](#); [Shklovskii and Efros, 1988](#)).

Next we consider electron hopping over distances well exceeding the average granule size in a dense granular array. This process can be realized as tunneling via virtual electron levels in a sequence of grains. Virtual electron tunneling through a single granule or a quantum dot (the so-called co-tunneling) was first considered by [Averin and Nazarov \(1990\)](#), where two different mechanisms for charge transport through a single quantum dot in the Coulomb blockade regime were identified; namely, there are elastic and inelastic co-tunneling mechanisms. In the course of elastic co-tunneling the charge is transferred via the tunneling of an electron through an intermediate virtual state in the dot such that the electron leaves the dot with the same energy as it came in with. In the latter mechanism (inelastic co-tunneling) an electron that comes out of the dot has a different energy from that of the incoming one. After inelastic co-tunneling the electron leaves behind in the granule electron-hole excitations absorbing the incoming and outgoing energy differences. Note that both these processes are realized via classically inaccessible intermediate states, i.e., both mechanisms occur in the form of charge transfer via a virtual state. The inelastic co-tunneling dominates at temperatures larger than $T_1 \sim \sqrt{E_c \delta}$ ([Averin and Nazarov, 1990](#)).

These two co-tunneling mechanisms can be generalized to the case of multiple co-tunneling through several

grains. The tunneling probability should fall off exponentially with the distance (or the number N of granules left behind) ([Beloborodov, Lopatin, and Vinokur, 2005](#); [Feigel'man and Ioselevich, 2005](#); [Tran *et al.*, 2005](#)), which is equivalent to the exponentially decaying probability of tunneling between states near the Fermi surface in the theory of Mott, Efros, and Shklovskii ([Efros and Shklovskii, 1975](#); [Shklovskii and Efros, 1988](#)).

Thus hopping processes in amorphous semiconductors and granular materials are alike—up to the specific expressions for the localization lengths—and by minimizing the hopping probability in the same manner as in the classic Efros-Shklovskii work, one ends up with the hopping conductivity σ in the form

$$\sigma \sim \exp[-(T_0/T)^{1/2}], \quad (2.14)$$

where T_0 is a characteristic temperature depending on the particular microscopic characteristics. Explicit expressions for this temperature in different regimes are given in Sec. II.G. Equation (2.14) explains the experimentally observed conductivity behavior in poorly conducting granular materials [see Eq. (1.1)].

Our discussion of variable-range hopping via virtual electron tunneling through many grains is based on the assumption that the hopping length r^* exceeds the size of a single grain a . This length decays when the temperature increases and reaches the grain size at some characteristic temperature \tilde{T} . Then the VRH picture no longer applies; the hops occur between adjacent granules only. Once the probability of a single jump is defined, the quantum effects can be neglected and one can use a classical approach. In particular, at temperatures $T \geq \tilde{T}$ one expects the conductivity to follow the simple Arrhenius law.

The classical approach to transport in granular metals was developed by [Middleton and Wingreen \(1993\)](#) and [Jha and Middleton \(2005\)](#). One of the results of their study is the presence of a threshold voltage below which the conductivity is exactly zero at $T=0$. The existence of such a threshold voltage is a consequence of the classical approach where multiple co-tunneling processes are not taken into account.

In order to match the results of the classical and hopping theories one would have to generalize the approach of [Middleton and Wingreen \(1993\)](#) to include multiple co-tunneling processes. Development of such a theory, in our opinion, is an interesting and important task.

B. Model and main theoretical tools

From the theoretical point of view a granular conductor is an appealing exemplary system whose behavior is governed by a nontrivial interplay of electron-electron interactions, disorder, and quantum fluctuations. The powerful approaches that allowed for recent breakthroughs in our understanding of the physics of granular media are based on effective field theories; in particular, the phase action technique appeared suitable. For situations that fall outside its range of applicability, the ap-

appropriate diagrammatic techniques, generalizing those for homogeneously disordered systems, can be developed. In this section we present in detail a model for the description of granular metals and introduce both complementary methods, which serve as a foundation for the quantitative description of granular conductors.

1. Hamiltonian

We model the granular system as an array of metallic particles connected via tunneling contacts. The Hamiltonian \hat{H} describing a granular conductor has the form

$$\hat{H} = \sum_i \hat{H}_{0,i} + \hat{H}_I + \hat{H}_t, \quad (2.15)$$

where $\hat{H}_{0,i}$ stands for the Hamiltonian of noninteracting electrons in grain i , \hat{H}_I represents the interactions, and \hat{H}_t describes the electron tunneling between the grains. We now discuss each term in Eq. (2.15).

The $\hat{H}_{0,i}$ term describes the free electrons within each grain in the presence of impurities,

$$\hat{H}_{0,i} = \int \hat{\psi}_i^\dagger(\mathbf{r}) \left(-\frac{\nabla^2}{2m} + u_i(\mathbf{r}) - \mu \right) \hat{\psi}_i(\mathbf{r}) d\mathbf{r}, \quad (2.16)$$

where $\hat{\psi}_i^\dagger(\mathbf{r})$ and $\hat{\psi}_i(\mathbf{r})$ are the electron creation and annihilation operators, μ is the chemical potential, and $u_i(\mathbf{r})$ is the disorder potential responsible for the electron scattering inside the i th grain. We adopt the Gaussian distribution for $u_i(\mathbf{r})$ with pair correlations,

$$\langle u_i(\mathbf{r}) u_j(\mathbf{r}') \rangle = \frac{1}{2\pi\nu\tau_{\text{imp}}} \delta(\mathbf{r} - \mathbf{r}') \delta_{ij}. \quad (2.17)$$

Throughout, we assume that all grains are in the diffusive limit, i.e., the electron mean free path l within each grain is smaller than the grain size a . This assumption simplifies our calculations because it allows us to avoid considering the electron scattering from the grain boundaries, which becomes the main “disorder” mechanism in the case of ballistic grains. At the same time, most of the results obtained in the diffusive limit are expected to hold also for ballistic grains with an irregular surface as long as the single-grain diffusion coefficient D_0 does not enter the final result. This happens in normal grains provided all relevant energies are smaller than the Thouless energy E_{Th} of a single grain, Eq. (1.5). Actually, for typical grain sizes of the order 100 Å the mean free path l is comparable with the granule size a .

A single grain may be considered within the standard diagrammatic approach developed for disordered metals (Abrikosov *et al.*, 1965). The main building block for the diagrams is the single-electron Green’s function averaged over disorder and it can be derived using the self-consistent Born approximation (SCBA). The diagram shown in Fig. 7(a) represents the relevant contribution to the self-energy:

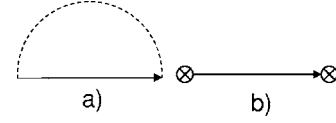


FIG. 7. Self-energy of the electron Green’s function averaged over the impurity potential inside the grains and over tunneling elements between the grains. Averaging over the impurity potential is represented by (a) the dotted line while tunneling elements are represented by (b) crossed circles.

$$G_{0\varepsilon}(\mathbf{p}) = \left(i\varepsilon - \xi(\mathbf{p}) + i \frac{\text{sgn}(\varepsilon)}{2\tau_{\text{imp}}} \right)^{-1}. \quad (2.18)$$

Another important block for the diagrammatic technique is the diffusion propagator (diffusion) which is just the impurity-averaged particle-hole propagator. In bulk disordered metals it is given by

$$D(\omega, \mathbf{q}) = \frac{1}{D_0 \mathbf{q}^2 + |\omega|}, \quad (2.19)$$

where D_0 is the classical diffusion coefficient and ω is the Matsubara frequency.

In a grain, however, the term \mathbf{q}^2 has to be replaced by the Laplace operator with the proper boundary conditions (Efetov, 1983, 1997; Aleiner *et al.*, 2002). This procedure leads to the quantization of diffusion modes and to the appearance of the lowest excitation energy of the order of D_0/a^2 with a being the grain size. This is just the Thouless energy E_{Th} that was defined in Eq. (1.5).

The Thouless energy of a nanoscale grain is large and this allows us to simplify calculations by neglecting all nonzero space harmonics in the diffusion propagator Eq. (2.19). Throughout we assume that E_{Th} is the largest energy scale associated with our system and use the zero-dimensional approximation for the diffusion propagator,

$$D(\omega) = 1/|\omega|. \quad (2.20)$$

Now we turn to the description of the electron-electron interaction, the second term \hat{H}_I in the Hamiltonian Eq. (2.15). We begin by considering interaction effects in an isolated grain and then turn to a discussion of the intergranular terms which are important because of the long-range character of the Coulomb interaction.

The most general form of the electron-electron interaction \hat{H}_I in an isolated grain is

$$\hat{H}_I^{(0)} = \frac{1}{2} \sum_{p,q,r,s} \mathcal{H}_{pqrs} \psi_{p,\alpha}^\dagger \psi_{q,\beta}^\dagger \psi_{r,\beta} \psi_{s,\alpha}, \quad (2.21)$$

where the subscripts p , q , r , and s stand for states in the grains, and α and β label electron spins.

The matrix \mathcal{H}_{pqrs} is a complicated object, but in the low-energy region of the parameters not all of the matrix elements are of the same order. In the case of disordered grains that we consider, only the elements with pair indices survive (Aleiner *et al.*, 2002); all others are small in the parameter $1/g_0$, where g_0 is the single-grain

conductance. Thus in the leading order in $1/g_0$ the in-grain interaction term is (Aleiner *et al.*, 2002)

$$H_I^{(0)} = E_c \hat{n}^2 + J_S \hat{S}^2 + \lambda \hat{T}^\dagger \hat{T}. \quad (2.22)$$

Here $\hat{n} = \int \hat{\psi}_i^\dagger(\mathbf{r}) \hat{\psi}_i(\mathbf{r}) d\mathbf{r} - N_0$ is the number of excess electrons in the grain with respect to the electron number in the charge-neutral state N_0 , \hat{S} is the total spin of the grain, and \hat{T}^\dagger, \hat{T} are the Cooper pair creation and annihilation operators: $T = \sum_p \hat{\psi}_{p,\uparrow} \hat{\psi}_{p,\downarrow}$. The interaction strengths in these three channels are controlled by the coupling constants E_c , J_S , and λ , respectively. The coupling constants in the spin and BCS channels, J_S and λ , cannot be large and are, at most, of the order of δ . At the same time the charging energy E_c is usually much larger than δ . For this reason, in the absence of the superconductivity, the most noticeable effects come from Coulomb correlations.

The above considerations of the interactions in a single grain can be easily generalized to the case of a granular array. It is clear that the bare interactions in the spin and Cooper pair channels are short range and thus they have to be diagonal in the granular indices. At the same time the Coulomb interaction is long range and its off-diagonal components cannot be neglected. Thus we arrive at the following Hamiltonian that describes the Coulomb correlations:

$$\hat{H}_c = \frac{e^2}{2} \sum_{ij} \hat{n}_i C_{ij}^{-1} \hat{n}_j, \quad (2.23)$$

where C_{ij}^{-1} is the capacitance matrix, which can be found by solving the classical electrostatic problem of metallic particles embedded into the insulating matrix. Note that, since metallic grains have infinite dielectric constant, the effective dielectric constant of the whole sample can be considerably larger than the dielectric constant of its insulating component. Thus the effective single-grain charging energy can be much less than the electrostatic energy of a single grain in a vacuum.

The Hamiltonian \hat{H}_c describing the long-range part of the Coulomb interaction, Eq. (2.23), was derived for granular superconductors in early work (Efetov, 1980). As far as normal grains are concerned, the proper derivation has been given in the review by Aleiner *et al.* (2002). The term \hat{H}_c , Eq. (2.23), commutes with the free part $\hat{H}_{0,i}$, Eq. (2.16), and therefore does not describe the dynamics in a single insulating granule. For macroscopic transport to occur the electron transfer from grain to grain has to be switched on, and we turn now to the third term \hat{H}_t in Eq. (2.15) describing electron tunneling between neighboring grains. We write this term in the form

$$\hat{H}_t = \sum_{i,j;p,q} t_{ij;pq} \hat{\psi}_{pi}^\dagger \hat{\psi}_{qj}, \quad (2.24)$$

where the summation is performed over the states p, q of each grain and over the neighboring grains i and j

(Cohen *et al.*, 1962; Ambegaokar and Baratoff, 1963; Abrikosov, 1988). It is assumed that the linear size of the intergrain contact area well exceeds atomic distances, i.e., there is a large number of conducting channels between the grains. At the same time, the magnitude of the potential barrier between the grains can be large; this can easily be achieved experimentally by the process of oxidation. Therefore the tunneling conductance g , which is roughly proportional to the area of the contact and to the square of the tunneling matrix element t_{ij} , can be set either larger or smaller than unity.

While the dependence of the tunneling elements $t_{ij;pq}$ on the state numbers p, q is not important for transport through conventional point contacts and is usually neglected (Cohen *et al.*, 1962; Ambegaokar and Baratoff, 1963; Abrikosov, 1988), it may become relevant for granular arrays. Whether the electron motion in the grains is chaotic or can be viewed as an integrable billiard controls the importance of this dependence. In order to clarify this point we write the matrix elements $t_{ij;pq}$ as

$$t_{ij;pq} = \int t_{ij}(\mathbf{s}_{ij}) \phi_p^*(\mathbf{s}_{ij}) \phi_q(\mathbf{s}_{ij}) d\mathbf{s}_{ij}, \quad (2.25)$$

where \mathbf{s}_{ij} is the coordinate on the junction between the grains i and j and $\phi_p(\mathbf{r}_i)$ are the wave functions. The integration over \mathbf{s}_{ij} in Eq. (2.25) extends over the area of the junction.

If the grains do not contain any disorder and have a perfect shape (e.g., cubes or spheres), the array is a completely periodic system and according to the Bloch theorem the total resistivity is zero. The presence of internal disorder or irregularities of the shape of the grains changes the situation, giving rise to a finite resistivity. In the latter case one may employ the random matrix theory (RMT) (Mehta, 1991; Beenakker, 1997; Alhassid, 2000) for an isolated single grain or, which is equivalent, the zero-dimensional σ model (Efetov, 1997). It is well known (Mehta, 1991) that this theory, when applied to the eigenfunctions, leads to a Gaussian distribution $W\{\phi_p(\mathbf{r})\}$ of their amplitudes,

$$W\{\phi_p(\mathbf{r})\} = \exp[-|\phi_p(\mathbf{r})|^2 V], \quad (2.26)$$

where V is the volume of the grain. Further, the Gaussian distribution of the wave function amplitudes $\phi_p(\mathbf{r}_i)$ and the fact that their correlations decay rapidly with increasing spatial distance and increasing energy-level spacing (the characteristic scales are the wavelength and the mean level spacing, respectively) lead to a Gaussian distribution of the matrix elements $t_{ij;pq}$.

These correlators can be simply transformed to

$$\begin{aligned} \langle t_{p_1 q_1} t_{p_2 q_2} \rangle &= \frac{g_{ij} \delta_i \delta_j}{2\pi} (\delta_{p_1 p_2} \delta_{q_1 q_2} + \delta_{p_1 q_2} \delta_{p_2 q_1}), \\ \langle t_{pq} \rangle &= 0, \end{aligned} \quad (2.27)$$

where δ_i is the mean level spacing in grain i . In Eq. (2.27) the matrix elements t_{pq} are taken for the same contact between the grains i and j ; otherwise the corre-

lations vanish. As we will see, the constant g_{ij} is nothing but the tunneling conductance of the contact.

Equation (2.27) is written for time-reversal-invariant systems (orthogonal ensembles). This, in particular, means that there is no magnetic field and/or no magnetic impurities present and therefore all eigenfunctions of an insulated grain can be chosen to be real. In the limit of comparatively strong magnetic fields, one arrives at the unitary ensemble and the first term in the correlation function of the matrix elements in Eq. (2.27) vanishes. However, for metallic grains of the order of 5–10 nm in size the characteristic magnetic field that requires a description in terms of the unitary ensemble is of the order of several teslas. Thus in the subsequent discussion we use Eq. (2.27), assuming that the applied magnetic fields are not that high.

To conclude this part, we have reformulated the initial theory with impurities and regular tunneling matrix elements in terms of a model with random tunneling elements. This equivalence holds for zero-dimensional grains, or for situations when all characteristic energies are smaller than the Thouless energy E_{Th} , Eq. (1.5). Working with random tunneling elements turns out to be the more convenient approach.

The model introduced in this section, Eqs. (2.15)–(2.17), (2.23), (2.24), and (2.27), describes a strongly correlated electronic disordered system which cannot be solved exactly. Below we introduce two complementary approaches to explore this problem in different regimes. One of these approaches—the diagrammatic technique—is especially useful if a perturbative expansion is possible with respect to one of the relevant parameters. The second method is based on the gauge transformation, which allows us to eliminate the explicit Coulomb interaction term in the Hamiltonian at the expense of an appearing phase field. As shown below, this approach offers a very powerful tool in its domain of applicability.

2. Diagrammatic technique for granular metals

There are two routes to construct a diagrammatic technique for granular metallic systems. First, one can work in the basis of the exact single-grain eigenfunctions and use the distribution of the tunneling elements (2.27) for the description of scattering between the different states of neighboring grains. In this case the impurities inside each grain are treated exactly, and by definition the diagrams that represent impurity scattering within each grain do not appear in this representation. The alternative approach is equivalent to the conventional cross technique: one begins with the momentum representation and then carries out the standard averaging over impurities within each grain. Tunneling between grains can then be viewed as an intergranular scattering. The corresponding matrix elements, as in the first method, can be viewed as Gaussian random variables. We prefer to follow the latter approach since it is straightforwardly related to the standard diagrammatic technique for homogeneously disordered metals, mak-

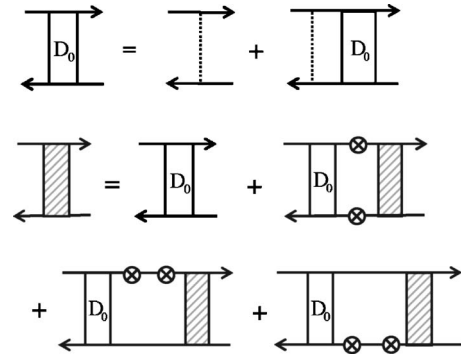


FIG. 8. Diagrams represent the Dyson equation (a) for a single-grain diffusion propagator Eq. (2.20) and (b) for the whole granular system Eq. (2.29). Dotted lines represent the impurity scattering while crossed circles stand for intergranular tunneling elements.

ing it easier to make comparisons to well-known situations in disordered metals when available.

Following Abrikosov *et al.* (1965) we construct the action expansions with respect to both types of disorder: potential disorder within each grain $u(\mathbf{r})$ and the intergranular scattering matrix elements t_{pq} . Shown in Fig. 7 are the lowest-order diagrams representing both contributions to the self-energy of the single-electron Green's function in the granular metals obtained by averaging over $u(\mathbf{r})$ and t_{pq} . The diagram (a) describes the potential scattering within a single grain, while diagram (b) represents intergranular scattering. Both processes result in a similar contribution proportional to $\text{sgn } \omega$ to the electron self-energy. This shows that on the level of the single-electron Green's function the intergranular scattering results merely in the renormalization of the relaxation time τ ,

$$\tau^{-1} = \tau_0^{-1} + 2\Gamma d, \quad (2.28)$$

where τ_0 is the electron mean free time in a single grain.

The next step is to consider the diffusion motion of electrons through the granular metal. The diffusion motion inside a single grain is given by the usual ladder diagram that results in the diffusion propagator $D(\omega)$, Eq. (2.20). Tunneling between grains does not change the selection rules for the diagrams. Typical diagrams are shown in Fig. 8(b). The diagrams are generated by connecting the tunneling vertices, and only diagrams without the intersection are to be kept. This is similar to what one has in the standard impurity technique (Abrikosov *et al.*, 1965). In order to derive the total diffusion propagator one should sum up the ladder diagrams shown in Fig. 8(b). For the periodic array of the grains we arrive at the following diffusion propagator $D(\omega, \mathbf{q})$ (Beloborodov *et al.*, 2001):

$$D(\omega, \mathbf{q}) = \tau^{-1} (|\omega| + \Gamma \lambda_{\mathbf{q}})^{-1}, \quad (2.29)$$

where

$$\lambda_q = 2 \sum_{\mathbf{a}} (1 - \cos \mathbf{q} \cdot \mathbf{a}), \quad (2.30)$$

\mathbf{a} are the (super)lattice vectors and \mathbf{q} is the quasimomentum. In Eq. (2.29) only the zero-space harmonics of the diffusion motion in the grain is taken into account. This approximation is valid in the limit

$$\Gamma \ll E_{\text{Th}}, \quad (2.31)$$

where the energies Γ and E_{Th} are given by Eqs. (2.2) and (1.5), respectively. In the limit of small quasimomenta $q \ll a^{-1}$ we have $\lambda_q \rightarrow a^2 q^2$ such that the propagator (2.29) describes the diffusion motion on scales much larger than the size of a single grain a with an effective diffusion coefficient

$$D_{\text{eff}} = a^2 \Gamma. \quad (2.32)$$

The other necessary blocks of the diagrammatic technique can be constructed analogously to the diffusion propagator.

3. Coulomb interaction and gauge transformation

Taking an alternative route, one can eliminate the explicit Coulomb term in the model for granular metals, Eqs. (2.15)–(2.17), (2.23), (2.24), and (2.27), by introducing a new phase field via a gauge transformation.

To introduce this approach it is convenient to adopt the formalism of functional integration, which allows calculations with the Hamiltonian \hat{H} , Eq. (2.15), to be replaced by computation of a functional integral over classical fermion fields $\psi_i(X)$ and their complex conjugate $\psi_i^*(X)$, where $X = (\mathbf{r}, \tau)$. These fields must satisfy the fermionic antiperiodicity condition

$$\psi_i(\tau) = -\psi_i(\tau + \beta), \quad (2.33)$$

where $\beta = 1/T$ is the inverse temperature. We define the field $\psi_i(X)$ such that it is different from zero only in the i th grain.

The Lagrangian $L[\psi]$ entering the functional integral for the partition function Z ,

$$Z = \int \exp\left(-\int_0^\beta L[\psi] d\tau\right) D\psi, \quad (2.34)$$

takes the form

$$L[\psi] = \sum_i L_{0i}[\psi] + L_i[\psi] + L_c[\psi], \quad (2.35)$$

where

$$L_{0i}[\psi] = \int \psi_i^*(X) \left(\frac{\partial}{\partial \tau} - \frac{\nabla^2}{2m} + u(\mathbf{r}) - \mu \right) \psi_i(X) d\mathbf{r}, \quad (2.36)$$

$$L_i[\psi] = \sum_{i,j:p,q} t_{ij;pq} \psi_{pi}^*(\tau) \psi_{qj}(\tau), \quad (2.37)$$

and

$$L_c[\psi] = \frac{e^2}{2} \sum_{ij} n_i(\tau) C_{ij}^{-1} n_j(\tau), \quad (2.38)$$

with $n_i(\tau) = \int \psi_i^*(X) \psi_i(X) d\mathbf{r}$ the density field of the grain i .

The Coulomb interaction $L_c[\psi]$, Eq. (2.38), can be decoupled using a Gaussian integration over the auxiliary field $\bar{V}_i(\tau)$ (Efetov and Tschersich, 2003),

$$\begin{aligned} & \exp\left(-\frac{e^2}{2} \sum_{ij} \int_0^\beta n_i(\tau) C_{ij}^{-1} n_j(\tau) d\tau\right) \\ &= \int \exp\left(i \sum_i \int_0^\beta \bar{V}_i(\tau) \psi_i^\dagger(X) \psi_i(X) dX\right) \\ & \quad \times Z_{\bar{V}}^{-1} \exp[-S(\bar{V})] d\bar{V}_i, \end{aligned} \quad (2.39)$$

where $\bar{V}_i(\tau)$ is the bosonic field obeying the boundary condition $\bar{V}_i(\tau) = \bar{V}_i(\tau + \beta)$ and $Z_{\bar{V}}$ is the partition function,

$$Z_{\bar{V}} = \int \exp[-S(\bar{V})] d\bar{V}_i.$$

The action $S(\bar{V})$ has the following form:

$$S[\bar{V}] = \frac{1}{2e^2} \int_0^\beta d\tau \sum_{ij} \bar{V}_i(\tau) C_{ij} \bar{V}_j(\tau). \quad (2.40)$$

We see from Eqs. (2.32)–(2.39) that the Lagrangian becomes quadratic in fields ψ after the decoupling, Eq. (2.39). Instead of dealing with the Coulomb interaction $L_c[\psi]$, Eq. (2.38), one should consider an effective Lagrangian $L_{0i}^{\text{eff}}[\psi, \bar{V}]$ for the grain i :

$$L_{0i}^{\text{eff}}[\psi, \bar{V}] = L_{0i}[\psi] - i \int_0^\beta \bar{V}_i(\tau) \psi_i^\dagger(\tau) \psi_i(\tau) d\tau. \quad (2.41)$$

The effective action $L_{0i}^{\text{eff}}[\psi, \bar{V}]$ is now expressed in terms of electron motion in granular matter in the presence of the fluctuating potential $\bar{V}_i(\tau)$ of the grains.

We remove the field $\bar{V}_i(\tau)$ from the Lagrangian $L_{0i}^{\text{eff}}[\psi, \bar{V}]$, Eq. (2.41), using a gauge transformation of the fermionic fields

$$\psi_i(\mathbf{r}, \tau) \rightarrow e^{-i\varphi_i(\tau)} \psi_i(\mathbf{r}, \tau), \quad \dot{\varphi}_i(\tau) = \bar{V}_i(\tau), \quad (2.42)$$

where the phases $\varphi_i(\tau)$ depend on imaginary time τ but not on the coordinates inside the grains. This is a consequence of the Coulomb interaction, Eqs. (2.23) and (2.38). Since the action of an isolated grain is gauge invariant, the phases $\varphi_i(\tau)$ enter the Lagrangian of the system only through the tunneling matrix elements

$$t_{ij} \rightarrow t_{ij} e^{i\varphi_{ij}(\tau)}, \quad (2.43)$$

where $\varphi_{ij}(\tau) = \varphi_i(\tau) - \varphi_j(\tau)$ is the phase difference of the i th and j th grains.

At first glance, the transformation Eq. (2.42), has removed completely the potentials $\bar{V}(\tau)$ from the effective Lagrangian $L_{0i}^{\text{eff}}[\psi, \bar{V}]$, Eq. (2.41). In fact, this is not the

case since the gauge transformation as defined in Eq. (2.42) violates the antiperiodicity condition Eq. (2.33), and the resulting effective Lagrangian for the single grain changes. In order to preserve the boundary condition Eq. (2.33), certain constraints should be imposed on the phases $\varphi_i(\tau)$ and potentials $\bar{V}_i(\tau)$; namely, the phases should obey the condition

$$\varphi_i(\tau) = \varphi_i(\tau + \beta) + 2\pi k_i, \quad (2.44)$$

which leads to the following constraint for the potential $\bar{V}_i(\tau)$:

$$\int_0^\beta \bar{V}_i(\tau) d\tau = 2\pi k_i, \quad (2.45)$$

where $k_i = 0, \pm 1, \pm 2, \pm 3, \dots$

The constraint on the phases $\varphi_i(\tau)$, Eq. (2.44), can be reformulated via introducing a function $\phi_i(\tau)$ assuming arbitrary real values from $-\infty$ to ∞ and obeying the periodicity condition

$$\phi(\tau) = \phi(\tau + \beta). \quad (2.46)$$

With the aid of this function the phase $\varphi_i(\tau)$ can be written in the form

$$\varphi_i(\tau) = \phi_i(\tau) + 2\pi T k_i \tau, \quad (2.47)$$

which satisfies Eq. (2.44). The potential $\bar{V}_i(\tau)$, in its turn, is taken in the form

$$\bar{V}_i(\tau) = \rho_i + \tilde{V}_i(\tau), \quad (2.48)$$

where the static variable ρ_i varies in the interval

$$-\pi T < \rho_i < \pi T, \quad (2.49)$$

and the dynamic variable $\tilde{V}_i(\tau)$ satisfies the constraint (2.45). Note that the static part of the potential ρ_i cannot be gauged out, contrary to the dynamic contribution $\tilde{V}_i(\tau)$, and the effective Lagrangian assumes the form $L_{0i}^{\text{eff}}[\psi, \rho]$. In the limit of not very low temperatures

$$T \gg \delta, \quad (2.50)$$

the static potential ρ_i drops out from the fermionic Green's functions and does not influence the system behavior. This can be understood by noticing that at moderately high temperatures (2.50) the discreteness of the levels in the grains is important. Then, in the Green's functions one may replace the variable $\varepsilon_p - \mu \rightarrow \xi$, where ε_p are eigenenergies and ξ is a continuous variable varying from $-\infty$ to ∞ . Integrating over ξ one may shift the contour of the integration into the complex plane and remove ρ_i provided it obeys the inequality (2.49). More details have been presented by [Efetov and Tschersich \(2003\)](#). Note that the variable ρ_i cannot be neglected in the Lagrangian $L_{0i}^{\text{eff}}[\psi, \rho]$ in the limit of very low temperatures.

The integer k_i in Eqs. (2.44), (2.45), and (2.47) represents an extra degree of freedom related to the charge quantization and is usually called the ‘‘winding number.’’

The physical meaning of the winding numbers becomes especially clear in the insulating regime where they represent static classical electron charges.

Thus at not very low temperatures, Eq. (2.50), one can write the partition function Z in the form

$$Z = \int \exp\left(-\int (L_0[\psi] + L_1[\psi, \varphi] + L_2[\varphi]) d\tau\right) \times D\psi D\varphi, \quad (2.51)$$

where

$$L_0[\psi] = \sum_i L_{0i}[\psi], \quad (2.52)$$

with $L_{0i}[\psi]$ from Eq. (2.36). The tunneling term $L_1[\psi, \varphi]$ is

$$L_1[\psi, \varphi] = \sum_{ij} \int_0^\beta d\tau t_{ij;pq} \psi_{ip}^*(\tau) \psi_{jq}(\tau) \exp[i\varphi_{ij}(\tau)], \quad (2.53)$$

and the term $L_2[\varphi]$ describing the charging effects reads

$$L_2[\varphi] = \sum_{ij} \frac{C_{ij}}{2e^2} \frac{d\varphi_i(\tau)}{d\tau} \frac{d\varphi_j(\tau)}{d\tau}. \quad (2.54)$$

One should integrate Eq. (2.51) over the anticommuting variables ψ with the antiperiodicity condition Eq. (2.33). The integration over φ includes integrating over the variable ϕ_i [see Eq. (2.47)] and summation over k_i . Equations (2.51)–(2.54), (2.46), and (2.47) completely specify the model that will be studied in subsequent sections.

4. Ambegaokar-Eckern-Schön functional

The partition function Z , Eqs. (2.51)–(2.54), can be further simplified by integration over the fermion fields ψ . This can hardly be done exactly but one can use a cumulant expansion in the tunneling term $L_1[\psi, \varphi]$, Eq. (2.53). Of course, even in the absence of tunneling the random potential in $L_0[\psi]$, Eqs. (2.52) and (2.36), can make the problem highly nontrivial. Yet, in the limit of not very low temperatures, Eq. (2.50), the problem can possibly be simplified because of neglecting interference effects and considering the disorder within the SCBA, taking the Green's functions from Eq. (2.18). We perform the cumulant expansion in the tunneling term $S_1[\psi, \varphi]$ up to the lowest nonvanishing second order, integrating over fermionic degrees of freedom and averaging over the tunneling matrix elements with the help of Eq. (2.27).

The resulting action, originally derived by [Ambegaokar *et al.* \(1982\)](#) for a system of two weakly coupled superconductors, contains only the phases $\varphi_i(\tau)$ but no fermionic degrees of freedom. For granular metals the partition function Z can be written as

$$Z = \int \exp(-S) D\varphi, \quad S = S_c + S_t, \quad (2.55)$$

where S_c describes the charging energy,

$$S_c = \frac{1}{2e^2} \sum_{ij} \int_0^\beta d\tau C_{ij} \frac{d\varphi_i(\tau)}{d\tau} \frac{d\varphi_j(\tau)}{d\tau}, \quad (2.56)$$

and S_t stands for tunneling between the grains,

$$S_t = \pi g \sum_{\langle ij \rangle} \int_0^\beta d\tau d\tau' \alpha(\tau - \tau') \sin^2 \left(\frac{\varphi_{ij}(\tau) - \varphi_{ij}(\tau')}{2} \right). \quad (2.57)$$

The function $\alpha(\tau - \tau')$ in Eq. (2.57) has the form

$$\alpha(\tau - \tau') = T^2 \text{Re} \{ \sin^{-2} [\pi T (\tau - \tau' + i\eta)] \}, \quad (2.58)$$

where $\eta \rightarrow +0$ and one should take the real part in Eq. (2.58). Despite the fact that the above functional was obtained via an expansion in the tunneling term $S_t[\psi, \varphi]$, its validity is not limited to only the insulating regime $g \ll 1$. The functional can be used in the metallic regime at temperatures $T \gg \Gamma$, where Γ is given by Eq. (2.2).

Of course, the phase action loses some information about the original model, Eqs. (2.34)–(2.38), and its applicability in each particular case has to be carefully analyzed. In general, the functional S , Eqs. (2.55)–(2.58), does not apply in cases where the coherent diffusive motion of an electron on the scale of many grains is important. For example, the weak-localization correction cannot be obtained using this approach.

Moreover, one has to be careful when using this approach, even in the weak-coupling regime $g \ll 1$. For example, the hopping conductivity in the low-temperature elastic regime is also beyond the accuracy of the phase action, Eqs. (2.55)–(2.58), since it requires consideration of the elastic multiple co-tunneling processes which the phase action misses.

Yet the phase functional approach is extremely powerful for many applications. For example, it enables non-perturbative results for the conductivity to be obtained in the metallic regime at temperatures $T \gg \Gamma$.

C. Metallic properties of granular arrays at not very low temperatures

In this section, we derive the logarithmic correction to the conductivity Eq. (2.6) in the temperature regime $T \gg \Gamma$. While this correction has the same origin as the Altshuler-Aronov result derived for homogeneously disordered metals (Altshuler and Aronov, 1985; Lee and Ramakrishnan, 1985), its form is specific to granular metals. In contrast to Eq. (2.6), Altshuler-Aronov corrections are sensitive to the sample dimensionality and exhibit the logarithmic behavior only in two dimensions.

The logarithmic correction Eq. (2.6), as shown below, can be obtained as a result of the renormalization of the tunneling coupling g due to Coulomb correlations. It comes from the short distances, and this explains its insensitivity to the sample dimensionality. At tempera-

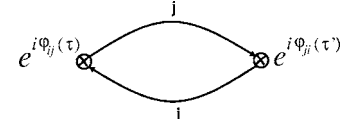


FIG. 9. The diagram representing the conductivity to leading order in $1/g$. The crossed circles represent the tunneling matrix elements $t_{kk'}^{ij} e^{i\varphi_{ij}(\tau)}$ where phase factors appear from the gauge transformation.

tures smaller than Γ , coherent electron motion on the scale of many grains becomes important, and the conductivity correction acquires a form similar to that for homogeneously disordered metals.

For the sake of simplicity we consider a periodic system, assuming that the granular array forms a cubic lattice. This implies that all grain sizes and intergranular conductances are equal to each other. At the end of this section we discuss the applicability of the result (2.6) to systems containing irregularities. We start with perturbation theory in $1/g$ and then generalize our derivation of Eq. (2.6) using the renormalization-group approach.

1. Perturbation theory

In the limit of large tunneling conductances $g \gg 1$ the tunneling term S_t , Eq. (2.57), suppresses large fluctuations of the phase $\varphi(\tau)$. In this regime the tunneling term S_t can be expanded in phases $\varphi_{ij}(\tau)$ because they are small. Charge quantization effects in this regime are not pronounced, allowing neglect of all nonzero winding numbers k_i . At the same time, phase fluctuations can change the classical result considerably, Eq. (2.1).

The part of the action S quadratic in $\varphi_i(\tau)$ in Eqs. (2.55)–(2.57) will serve as the bare action for the perturbation theory. Keeping second-order terms in $\varphi_i(\tau)$ in Eqs. (2.55)–(2.57) and performing the Fourier transformation in both the coordinates of the grains and the imaginary time we reduce the action S in Eq. (2.55) to the form

$$S_0 = T \sum_{\mathbf{q}, n} \varphi_{\mathbf{q}, n} G_{\mathbf{q}, n}^{-1} \varphi_{-\mathbf{q}, -n}, \quad (2.59)$$

where

$$G_{\mathbf{q}, n}^{-1} = \omega_n^2 / 4E(\mathbf{q}) + 2g |\omega_n| \lambda_{\mathbf{q}} \quad (2.60)$$

and $\lambda_{\mathbf{q}}$ is given by Eq. (2.30). Here \mathbf{q} are the quasi-momenta of a periodic array; $E(\mathbf{q})$ is the Fourier transform of the charging energy related to the Fourier transform of the capacitance matrix $C(\mathbf{q})$ as $E(\mathbf{q}) = e^2 / 2C(\mathbf{q})$. The conductivity $\sigma(\omega)$ of the grain arrays can be obtained from the current-current correlation function via the standard Kubo formula. The conductivity to leading order in $1/g$ is shown in Fig. 9. Its analytical expression is given by (Efetov and Tschersich, 2003)

$$\sigma(\omega) = \frac{2\pi e^2 g T^2 i a^{2-d}}{\omega} \int_0^\beta d\tau \frac{1 - e^{i\Omega\tau}}{\sin^2(\pi T\tau)} \exp[-\tilde{G}_a(\tau)], \quad (2.61)$$

where the analytic continuation to the real frequency is assumed as $\Omega \rightarrow -i\omega$, and the function $\tilde{G}_a(\tau)$ is

$$\tilde{G}_a(\tau) = 4Ta^d \sum_{\omega_n > 0} \int \frac{d^d \mathbf{q}}{(2\pi)^d} G_{\mathbf{q}n} \sin^2 \frac{\mathbf{q} \cdot \mathbf{a}}{2} \sin^2 \frac{\omega_n \tau}{2}, \quad (2.62)$$

where d is the dimensionality of the array. The factor $\exp[-\tilde{G}_a(\tau)]$ in Eq. (2.61) is responsible for the interaction effects and appears as a result of averaging the phase exponents $e^{i\phi(\tau)}$ emerging after the gauge transformation Eq. (2.42). One can see from Eqs. (2.60) and (2.62) that the function $\tilde{G}_a(\tau)$ behaves as a logarithm $\ln(gE_c\tau)$ at values of τ of the order $1/T$ that are essential for the calculation. With logarithmic accuracy one can neglect the ω_n^2 term in $G_{\mathbf{q}n}^{-1}$, Eq. (2.60), and reduce Eq. (2.62) to

$$\tilde{G}_a(\tau) = \frac{T}{dg} \sum_{\omega_n > 0} \frac{1 - \cos(\omega_n \tau)}{\omega_n}. \quad (2.63)$$

In Eq. (2.63) one should sum over positive Matsubara frequencies up to the cutoff $\omega_c \sim gE_c$. For larger frequencies the first term in Eq. (2.60) is no longer small and there is no logarithmic contribution from these large frequencies. Equation (2.63) shows a lack of dependence of the result on the structure of the lattice. It is also important that there are no ‘‘infrared’’ divergencies in the integral over \mathbf{q} in any dimensionality including two and one dimensions.

With logarithmic accuracy, one can replace τ by $1/T$ in the function $\tilde{G}_a(\tau)$ and calculate the remaining integral over τ in Eq. (2.61), ignoring the dependence of the function \tilde{G}_a on τ . Taking the limit $\omega \rightarrow 0$ we obtain the result (2.6) in the temperature interval $T \gg \Gamma$:

$$\sigma = \sigma_0 \left(1 - \frac{1}{2\pi dg} \ln \left[\frac{gE_c}{T} \right] \right). \quad (2.64)$$

It was shown by [Efetov and Tschersich \(2003\)](#) that terms of the order $(1/g)^2 \ln^2(gE_c/T)$ are canceled out in the expansion of the conductivity correction, which means that the accuracy of Eq. (2.64) exceeds the accuracy of the first-order correction. Furthermore, this cancellation is not accidental and the result (2.64) turns out to be applicable even at temperatures at which the conductivity correction becomes of the same order as σ_0 itself. This fact is explained in the next section where the temperature dependence of the conductivity is considered within the renormalization-group (RG) scheme.

2. Renormalization group

In order to sum all logarithmic corrections to the conductivity we use the RG scheme suggested for the one-

dimensional XY model long ago ([Kosterlitz, 1976](#)) and used later in a number of works ([Guinea and Schön, 1986](#); [Bulgadaev, 1987a, 1987b, 2006](#); [Falci *et al.*, 1995](#)). As the starting functional we take the tunneling action S_t ,

$$S_t = \pi g \sum_{\langle i,j \rangle} \int_0^\beta \int_0^\beta d\tau d\tau' \alpha(\tau - \tau') \sin^2 \left(\frac{\varphi_{ij}(\tau) - \varphi_{ij}(\tau')}{2} \right). \quad (2.65)$$

The charging part S_c is not important for the renormalization group because it determines only the upper cut-off of integrations over frequencies. In the limit $T \rightarrow 0$ the function $\alpha(\tau - \tau')$ is proportional to $(\tau - \tau')^{-2}$ and the action is dimensionless. We neglect in this section the nonzero winding numbers k_i and replace the phases $\varphi_i(\tau)$ by the variables $\phi_i(\tau)$ [Eq. (2.47)].

Following standard RG arguments we want to determine the change in the form of the action S_t when the cutoff is changed. Generally speaking, it is not guaranteed that after integrating over the phases ϕ in an interval of the frequencies one comes to the same function $\sin^2 \phi$ in the action. The form of the functional may change, which would lead to a functional renormalization group.

In the present case appearance of terms $\sin^2 2\phi$, $\sin^2 4\phi$, etc., is not excluded and they are generated in many-loop approximations of the RG. Fortunately, the one-loop approximation is simpler and the renormalization in this order results in a change of the effective coupling constant g only.

To derive the RG equation we represent the phase ϕ in the form

$$\phi_{ij\omega} = \phi_{ij\omega}^{(0)} + \bar{\phi}_{ij\omega}, \quad (2.66)$$

where the function $\phi_{ij\omega}^{(0)}$ is the slow variable and is not equal to zero in the frequency interval $0 < \omega < \lambda\omega_c$, while the function $\bar{\phi}_{ij\omega}$ is finite in the interval $\lambda\omega_c < \omega < \omega_c$, where λ is in the interval $0 < \lambda < 1$. Substituting Eq. (2.66) into Eq. (2.65), we expand the action S_t up to terms quadratic in $\bar{\phi}_{ij\omega}$. Integrating Eq. (2.65) for the partition function

$$Z = \int \exp(-S_t[\phi]) D\phi$$

over the fast variable $\bar{\phi}_{ij\omega}$ with logarithmic accuracy we come to a new renormalized effective action \tilde{S}_t ,

$$\tilde{S}_t = 2\pi g \sum_{\langle i,j \rangle} \int_0^\beta \int_0^\beta d\tau d\tau' \alpha(\tau - \tau') \times \sin^2 \left(\frac{\phi_{ij}(\tau) - \phi_{ij}(\tau')}{2} \right) \left(1 - \frac{\xi}{2\pi g d} \right), \quad (2.67)$$

where $\xi = -\ln \lambda$. It follows from Eq. (2.67) that the form of the action is reproduced for any dimensionality d of the grain lattice. This allows us to write the following renormalization-group equation:

$$\frac{\partial g(\xi)}{\partial \xi} = -\frac{1}{2\pi d}. \quad (2.68)$$

The solution of Eq. (2.68) is simple. Neglecting the Coulomb interaction in the action S_t , Eq. (2.65), is justified only for energies smaller than gE_c and this gives the upper cutoff. Then the renormalized conductance $g(T)$ takes the form

$$g(T) = g - \frac{1}{2\pi d} \ln\left(\frac{gE_c}{T}\right) \quad (2.69)$$

and using Eq. (2.1) we come to Eq. (2.64) for the conductivity. Both quantities depend on the temperature logarithmically.

Equation (2.69) is obtained in the one-loop approximation and should be valid so long as the effective conductance $g(T)$ remains much larger than unity. This assumes that the perturbation theory result, Eq. (2.64), can be extended to a wider temperature interval and, in fact, it is valid as long as

$$g - (2\pi d)^{-1} \ln(gE_c/T) \gg 1. \quad (2.70)$$

At high temperatures, when the inequality (2.70) is satisfied, one can speak of metallic behavior of the system. At lower temperatures $T < T_c$, where

$$T_c = gE_c \exp(-2\pi gd), \quad (2.71)$$

the system is expected to show insulating properties.

The result for the conductivity correction (2.64) was obtained using a cubic lattice model. It is important to understand how it will change in the more realistic case of an irregular array. First, we note that Eq. (2.64) can be generalized to the case of an arbitrary periodic lattice with the result

$$\sigma = \sigma_0 \left(1 - \frac{1}{\pi z g} \ln \left[\frac{gE_c}{T} \right] \right), \quad (2.72)$$

where z is the coordination number of the arbitrary periodic lattice.

Dispersion of the tunneling conductance was studied by Feigel'man *et al.* (2004) within a 2D model that assumed regular periodic positions and equal sizes of grains but random tunneling conductances. It was shown that the dependence (2.72) holds in a wide temperature range in the case of a moderately strong conductance dispersion. However, the distribution of conductances broadens and this effect becomes important close to the metal-insulator transition; it was suggested to describe the transition in terms of percolation (Feigel'man *et al.*, 2004). One may expect that in 3D samples the conductance dispersion effect on macroscopic transport will be less important than in 2D ones, while on the contrary it will be more dramatic in 1D samples.

Finally, we comment on the validity of Eq. (2.72) for an arbitrary irregular array. In the RG approach capacitance disorder leads to a local renormalization of tunneling conductances. The general irregular system can be viewed as an irregular array of equal-size grains with random tunneling conductances. The main difference

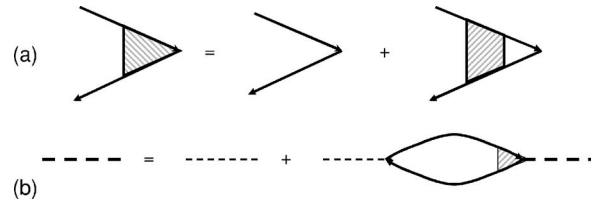


FIG. 10. Diagrams representing (a) the vertex correction and (b) the renormalized Coulomb interaction.

between such a system from that considered by Feigel'man *et al.* (2004) is that the coordination number varies from grain to grain. In this case one expects that the coefficient in front of the second term in Eq. (2.72) will be determined by an effective coordination number in the system, which is expected to be close to the average number of neighbors of a grain.

Following the RG scheme we did not take into account nonzero winding numbers k_i , Eqs. (2.44)–(2.47). This is a natural approximation because the contribution of such configurations should be exponentially small in g [$\sim \exp(-cg)$, where c is of the order of unity]. So long as the effective conductance g is large in the process of the renormalization, the contribution of the nonzero winding numbers k_i can be neglected. They become important when g becomes of the order of unity. This is the region of the transition into the insulating state and apparently the nonzero winding numbers play a crucial role in forming this state. [However, recent publications (Altland *et al.*, 2004, 2006; Meyer *et al.*, 2004) have argued that the nonzero winding numbers might become important in 1D samples at temperatures T^* parametrically exceeding T_c , Eq. (2.71).]

D. Metallic properties of granular arrays at low temperatures

The phase functional technique may not be used for obtaining the conductivity corrections at temperatures $T \leq \Gamma$ since in this regime the coherent electron motion over a large number of grains, which is missed in the functional approach (Ambegaokar *et al.*, 1982), becomes important. In this section we derive the conductivity correction using the diagrammatic perturbation theory described in Sec. II.C.1. Unlike the phase functional approach, this technique does not allow us to obtain nonperturbative results in an easy way but has an advantage of being applicable at arbitrary temperatures. In particular, we show below that it reproduces at $T \gg \Gamma$ the perturbative result Eq. (2.64). The conductivity correction agrees in the low-temperature regime with the one obtained by Altshuler and Aronov (1985), Lee and Ramakrishnan (1985), and Belitz and Kirkpatrick (1994) for homogeneously disordered samples.

In Sec. II.C.1, we described the main building blocks of the diagrammatic technique including, in particular, the diffusion propagator defined by the ladder diagram in Fig. 8. The same ladder diagram describes the dressing of the interaction vertex as shown in Fig. 10(a). The dressed vertex can be used to obtain the polarization

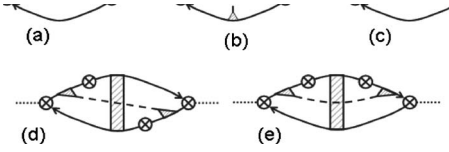


FIG. 11. Diagrams describing the conductivity of granular metals: diagram (a) corresponds to σ_0 in Eq. (2.5) and it is the analog of the Drude conductivity. Diagrams (b)–(e) describe first-order corrections to the conductivity of granular metals due to the electron-electron interaction. The solid lines denote the propagators of electrons and dashed lines describe effective screened electron-electron propagators. The sum of the diagrams (b) and (c) results in the conductivity correction $\delta\sigma_1$ in Eq. (2.5). The other two diagrams, (d) and (e), result in the correction $\delta\sigma_2$. From Beloborodov *et al.*, 2003.

operator that defines the effective dynamically screened Coulomb interaction [Fig. 10(b)]:

$$V(\Omega, \mathbf{q}) = \left[\frac{C(\mathbf{q})}{e^2} + \frac{2\lambda_{\mathbf{q}}}{|\Omega| + \lambda_{\mathbf{q}}\Gamma} \right]^{-1}. \quad (2.73)$$

The conductivity of granular metals is given by the analytical continuation of the Matsubara current-current correlation function. In the absence of the electron-electron interaction the conductivity is represented by diagram (a) in Fig. 11 which results in the high-temperature (Drude) conductivity σ_0 defined in Eq. (2.1). First-order interaction corrections to the conductivity are given by diagrams (b)–(e) in Fig. 11. These diagrams are analogous to those considered by Altshuler and Aronov (1985) for the correction to the conductivity of homogeneous metals.

We consider the contributions from diagrams (b), (c) and (d), (e) separately. The sum of diagrams (b), (c) results in the following correction to the conductivity:

$$\frac{\delta\sigma_1}{\sigma_0} = -\frac{1}{2\pi dg} \text{Im} \sum_{\mathbf{q}} \int d\omega \gamma(\omega) \lambda_{\mathbf{q}} \tilde{V}(\omega, \mathbf{q}), \quad (2.74)$$

where $\gamma(\omega) = (d/d\omega)\omega \coth(\omega/2T)$, and the potential $\tilde{V}(\omega, \mathbf{q})$ is the analytic continuation of the screened Coulomb potential $V(\Omega, \mathbf{q})$ with dressed interaction vertices including those attached at both ends,

$$\tilde{V}(\omega, \mathbf{q}) = \frac{2E_c(\mathbf{q})}{(\lambda_{\mathbf{q}}\Gamma - i\omega)[4\lambda_{\mathbf{q}}E_c(\mathbf{q}) - i\omega]}. \quad (2.75)$$

The expression for the screened Coulomb interaction $\tilde{V}(\omega, \mathbf{q})$, Eq. (2.75), is written in a simplified form using the fact that the charging energy $E_c(\mathbf{q}) = e^2/2C(\mathbf{q})$, expressed in terms of the Fourier transform of the capacitance matrix $C(\mathbf{q})$, is much larger than the escape rate Γ .

Performing the integration over the frequency and summing over the quasimomentum \mathbf{q} in Eq. (2.74) with logarithmic accuracy we obtain the correction to the conductivity, Eq. (2.6). One can see from Eq. (2.74) that the contribution $\delta\sigma_1$ in Eq. (2.6) comes from the large

energy scales, $\varepsilon \geq \Gamma$. At low temperatures $T \leq \Gamma$, the logarithm is cut off by the energy Γ and is no longer temperature dependent.

To obtain the total correction to the conductivity of a granular sample the two other diagrams, (d) and (e) in Fig. 11, should be taken into account. These diagrams result in the following contribution to the conductivity (Beloborodov *et al.*, 2003):

$$\frac{\delta\sigma_2}{\sigma_0} = -\frac{2g\delta}{\pi d} \sum_{\mathbf{q}} \int d\omega \gamma(\omega) \text{Im} \frac{\tilde{V}(\omega, \mathbf{q}) \sum_{\mathbf{a}} \sin^2(\mathbf{q} \cdot \mathbf{a})}{\lambda_{\mathbf{q}}\Gamma - i\omega}. \quad (2.76)$$

In contrast to the contribution from $\delta\sigma_1$, Eq. (2.74), the main contribution to the sum over the quasimomentum \mathbf{q} in Eq. (2.76) comes from low momenta $q \ll 1/a$. In this regime the capacitance matrix $C(\mathbf{q})$ in Eqs. (2.75) and (2.76) has the asymptotic form

$$C^{-1}(\mathbf{q}) = \frac{2}{a^d} \times \begin{cases} \ln(1/qa), & d=1 \\ \pi/q, & d=2 \\ 2\pi/q^2, & d=3. \end{cases} \quad (2.77)$$

Using Eqs. (2.75)–(2.77), we obtain the result for the correction $\delta\sigma_2$ in Eq. (2.7). This correction has a physical meaning similar to that of the Altshuler-Aronov correction (Altshuler and Aronov, 1985) derived for homogeneously disordered metals.

Comparing the results in Eqs. (2.5)–(2.7) with those obtained in the previous section using the Ambegaokar-Eckern-Schön functional one can see that the correction to the conductivity obtained in Sec. II.C is equivalent to the correction $\delta\sigma_1$ in Eq. (2.5), which corresponds in the diagrammatic approach to the sum of diagrams (b) and (c) in Fig. 11. The correction $\delta\sigma_2$ in Eq. (2.5) becomes important only at low temperatures $T \leq \Gamma$ where the Ambegaokar-Eckern-Schön functional is not applicable.

Using the final results of the calculations, Eqs. (2.6) and (2.7), we now make an important statement about the existence of a metal-insulator transition in three dimensions. It follows from Eq. (2.7) that for a 3D granular array there are no essential corrections to the conductivity at low temperatures $T \ll \Gamma$ coming from low energies $\omega \leq \Gamma$, since the correction $\delta\sigma_2$ is always small. This means that the result for the renormalized conductance, Eq. (2.69), for 3D samples can be written within logarithmic accuracy in the form

$$\tilde{g}(T) = g - \frac{1}{6\pi} \ln \left(\frac{gE_C}{\max(\tilde{g}\delta, T)} \right), \quad (2.78)$$

such that it is valid for all temperatures as long as the renormalized conductance is large, $\tilde{g}(T) \gg 1$.

One can see from Eq. (2.78) that for a large bare conductance, $g \gg (1/6\pi)\ln(gE_C/\delta)$, the renormalized conductance \tilde{g} is always large and the system remains metallic down to zero temperatures. In the opposite limit $g < (1/6\pi)\ln(gE_C/\delta)$, on decreasing temperature the system flows to the strong-coupling regime, $\tilde{g} \sim 1$, which in-

indicates the onset of the insulating phase. One can see that with logarithmic accuracy the critical value of the conductance g_c is given by Eq. (2.12), and this value separates the metallic and insulating states (Beloborodov *et al.*, 2003).

One can see from Eq. (2.7) that in 1D and 2D samples the correction to the conductivity, being negative, grows with decreasing temperature and diverges in the limit $T \rightarrow 0$. This behavior is usually attributed to localization in the limit $T \rightarrow 0$.

However, the actual situation is more interesting. Recently (Basko *et al.*, 2005) it was demonstrated that there must be a metal-insulator transition at finite temperature T_k in systems with weak repulsion, provided all one-particle states are localized. This means that the conductivity is strictly zero at $T < T_k$ and becomes finite at $T > T_k$. The 1D and 2D granular systems with Coulomb interaction discussed here should belong to the class of models considered by Basko *et al.* (2005) (all one-particle states should be localized in 1D and 2D systems for any disorder) and one can expect such a transition. Clearly, the results of Eq. (2.7) should hold for $T \gg T_k$.

At the same time, the 3D samples do not fall into the class of models studied by Basko *et al.* (2005) because there exist both localized and extended one-particle states. Therefore for 3D granular systems one can speak of the metal-insulator transition at $T=0$ only. The transition point can be varied by changing, e.g., the tunneling conductance between the grains or their size.

Finally, we note that the low-temperature conductivity correction $\delta\sigma_2$ is less sensitive to a particular model of a granular sample than the high-temperature result, Eq. (2.64). As discussed in the next section, the low-temperature conductivity correction is determined by scales larger than the single-grain size and can be expressed in terms of the effective diffusion coefficient D_{eff} . This assumes that the underlying structure of the model is not important in this regime.

E. Universal description of granular materials

One can see from the previous subsection that at low temperatures $T \ll \Gamma$ the dependence of the correction $\delta\sigma_2$, Eq. (2.7), to the conductivity of granular metals coincides exactly with the corresponding result for the conductivity of homogeneously disordered samples. A question immediately arises: Is it an accidental coincidence that the two different physical systems exhibit in the main approximation identical low-temperature transport behavior, or there is an underlying deep connection between the two? Can one describe both regions $T \leq \Gamma$ and $T \geq \Gamma$ in a unified manner? The main goal of this section is to answer these important questions.

A convenient description of low-temperature behavior of homogeneously disordered metals is based on the so-called σ model. There are several formulations of the σ model based on the replica trick (Wegner, 1979; Efetov *et al.*, 1980), supersymmetry (Efetov, 1983, 1997),

and Keldysh Green's functions (Kamenev and Andreev, 1999). The approach of Efetov *et al.* (1980) has been generalized by Finkelstein (1990) to include interaction effects. It is clear that the σ model of Finkelstein (1990) cannot be used for granular materials because it does not contain the scale Γ .

Fortunately, the approach of Finkelstein (1990) can be extended to include the granularity. This can be done using Eqs. (2.15)–(2.23) and following the usual method (Beloborodov *et al.*, 2001; Andreev and Beloborodov, 2004): (i) we write a generating functional in terms of functional integrals over anticommuting Grassmann variables, (ii) we average over the disorder using a replica trick, (iii) we decouple a ψ^4 effective interaction appearing after the averaging by a Gaussian integration over a Q -matrix field and do the same for the Coulomb interaction term in Eq. (2.23) using auxiliary fields \bar{V} (Efetov *et al.*, 1980; Finkelstein, 1990), (iv) we integrate the exponential of quadratic form thus obtained over the ψ fields, and finally (v) we find a saddle point in the free-energy functional containing the fields Q and \bar{V} only and expand around this saddle point. The final expression for the effective low-energy action reads

$$S[Q, \bar{V}] = -\frac{\pi}{2\delta} \sum_i \text{Tr}[(\hat{\epsilon} + \bar{V}_i)Q_i] - \frac{\pi g}{8} \sum_{(i,j)} \text{Tr}[Q_i Q_j] + \frac{1}{2e^2} \sum_{i,j} C_{ij}(\bar{V}_i \bar{V}_j). \quad (2.79)$$

Here the sums are performed over the grain indices, the symbol $\langle \dots \rangle$ means summation over the nearest neighbors, C_{ij} is the capacitance matrix, $\hat{\epsilon} = i\partial_\tau$, and the symbol Tr means the trace over spin and replica indices and integration over τ . The field \bar{V} in Eq. (2.79) is a time-dependent vector in the replica space and the corresponding scalar product is implied: $(\bar{V}_i \bar{V}_j) = \sum_\alpha \int_0^{1/T} \bar{V}_{i\alpha}(\tau) \bar{V}_{j\alpha}(\tau) d\tau$, where α is the replica index ($0 \leq \alpha \leq N$). The Q matrix in Eq. (2.79) is a matrix in time (it depends on two times τ and τ'), spin, and replica spaces subject to the constraints $Q^2 = 1$, $\text{Tr} Q = 0$. The variable τ enters Q in the same way as the replica and spin ones, which means that $(Q_1 Q_2)_{\tau, \tau'} \equiv \int Q_1(\tau, \tau') Q_2(\tau', \tau) d\tau'$.

For energies smaller than the Thouless energy E_{Th} of one grain, Eq. (1.5), the Q matrices in Eq. (2.79) are coordinate independent within each grain. They can be written in the form

$$Q_i = U_i \Lambda U_i^{-1}, \quad (2.80)$$

where the function Λ is given by

$$\Lambda_{\tau, \tau'} = \frac{iT}{\sin \pi T(\tau - \tau')}, \quad (2.81)$$

and U_i is a unitary matrix. The action $S[Q, \bar{V}]$ in Eq. (2.79) describes the entire region of both low, $T \leq \Gamma$, and not very low, $T \geq \Gamma$, temperatures discussed previously. For $T \gg \Gamma$, an essential contribution comes from $U(\tau, \tau')$

in Eq. (2.80), diagonal in time, spin, and replica spaces. This means that we write this function as

$$U_i(\tau, \tau') = \delta_{\alpha\beta} \delta(\tau - \tau') \exp[i\varphi_{\alpha i}(\tau)], \quad (2.82)$$

where α and β stand for both replica and spin indices.

Substituting Eqs. (2.80)–(2.82) into Eq. (2.79), calculating the integral

$$\int \exp(-S[Q, \bar{V}]) D \bar{V},$$

and taking the limit $N=0$, which is trivial here, we come to the Ambegaokar-Eckern-Schön action Eqs. (2.55) and (2.58).

The σ model of Eq. (2.79) has a well-defined continuum limit. It can be obtained for slow spatial variations of the Q matrix by expanding the second term in Eq. (2.79) to the second order in gradients of Q , and replacing the summation over i by integration over \mathbf{r} . The tunneling term in Eq. (2.79) describes diffusion in the continuum limit and we reduce the action Eq. (2.79) to the form

$$S = -\pi\nu \int \text{Tr} \left((\hat{\varepsilon} + \bar{V}) Q - \frac{D}{4} (\nabla Q)^2 \right) d\mathbf{r} + \int \frac{d\mathbf{r} d\mathbf{r}'}{a^{2d}} \text{Tr} \left(\bar{V}_{\mathbf{r}} \frac{C_{\mathbf{r}\mathbf{r}'}}{2e^2} \bar{V}_{\mathbf{r}'} \right), \quad (2.83)$$

where ν is the density of states. The coefficient D in the second term of Eq. (2.83) is in this approximation the classical diffusion coefficient determined by Eq. (2.3).

However, we can derive Eq. (2.83) more accurately, not by neglecting the contributions of energies exceeding Γ but taking them into account. In calculating the contribution of the energies exceeding Γ we can use Eq. (2.82) for the excitations with such energies. As a result, we come again to Eq. (2.83) but with a renormalized coefficient D that can be written in the form

$$D = g_{\text{eff}} a^2 \delta, \quad (2.84)$$

where g_{eff} is given by [compare with Eq. (2.69)]

$$g_{\text{eff}} = g - \frac{1}{2\pi d} \ln \left(\frac{E_c}{\delta} \right). \quad (2.85)$$

Since the effective model (2.83) operates with matrix fields Q that have only long-range degrees of freedom, it applies after an appropriate high-energy renormalization to any disordered metal including a homogeneously disordered one. Integrating over the potentials \bar{V} one can come to the σ model of Finkelstein (1990) (the limit of a long-range interaction is implied).

Thus all information about the granularity of the sample is hidden in the low-temperature limit in the coefficients of the effective model (2.83). The conductivity of the sample is related to the effective diffusion coefficient through the usual Einstein relation

$$\sigma = 2e^2 D (a^d \delta)^{-1}. \quad (2.86)$$

The effective model Eq. (2.83), together with Eq. (2.69) for the renormalized conductance, naturally explains the results for the low-temperature $T \ll \Gamma$ conductivity described in Sec. II.D. The interaction correction to conductivity consists of two terms. (i) The first contribution is temperature independent and comes from the high-energy renormalization of the diffusion coefficient D , Eqs. (2.86) and (2.87). It can be written in the form [compare with Eq. (2.6)]

$$\delta\sigma_1 = -\sigma_0 \frac{1}{2\pi d g} \ln \left(\frac{E_c}{\delta} \right), \quad (2.87)$$

where σ_0 is the classical Drude conductivity defined in Eq. (2.1). This contribution is specific for granular materials. (ii) The second contribution to the conductivity Eq. (2.7) is temperature dependent and comes from the low-energy renormalization of the diffusion coefficient D in the effective model (2.83). It coincides with the corresponding correction to conductivity obtained for homogeneously disordered metals (Altshuler and Aronov, 1985).

Making use of the effective description of granular metals in terms of the effective σ model Eq. (2.83), applicable at low temperatures, we conclude that all phenomena described in terms of this model, including localization effects, magnetoresistance, Hall conductivity, etc., are universal.

Using the σ model, Eq. (2.83), we also describe quantum interference (weak-localization) corrections to the conductivity (Gorkov *et al.*, 1979). To leading order in the inverse tunneling conductance $1/g$, the interaction and weak-localization corrections can be considered independently. The quantum interference corrections may be obtained from the effective σ model, Eq. (2.83), using directly the corresponding results for homogeneously disordered metals (Efetov *et al.*, 1980) with the proper effective diffusion coefficient $D = ga^2 \delta$. For 2D and 1D samples it is important to take into account dephasing effects since the weak-localization correction diverges. The dephasing time τ_ϕ can also be extracted directly from the results for homogeneously disordered metals (Altshuler *et al.*, 1982) with the proper effective diffusion coefficient D . The final result for the weak-localization corrections is given by Eqs. (2.8) and (2.9).

F. Insulating properties of granular metals: Periodic model

In the previous section we discussed the transport properties of metallic granular arrays with strong intergranular tunneling coupling. Now we turn to the opposite limit of weakly coupled grains $g \ll 1$. We start our consideration with a detailed description of a periodic granular array model. As a reminder, the periodic model assumes periodic arrangements of equal-size grains as well as the absence of disorder in conductances and

grain potentials. At the same time, the electron motion inside the grain is chaotic and this brings disorder into the model.

As discussed in the Introduction, the periodic granular array model predicts insulating conductivity behavior with a hard gap in the electron excitation spectrum and, for this reason, it cannot describe the transport properties of realistic granular systems where the conductivity is governed by the variable-range-hopping mechanism. Nevertheless, it is instructive to consider this model for two reasons: first, it is important to see explicitly that such a model may produce only activation conductivity dependence; second, this model illustrates the general effect of the charge renormalization on the Coulomb energy due to intergranular coupling.

1. Activation conductivity behavior

First, we consider a periodic granular array with a small intergranular coupling $g \ll 1$. The conductivity in this case can be found via the gauge transformation technique described in Sec. II.B.3. The phase action in the lowest order in the tunneling conductance g is given by the Coulomb term S_c , Eq. (2.56). With the help of the Kubo formula the conductivity in the first nonvanishing order in g may be written as (Efetov and Tschersich, 2003)

$$\sigma(\omega) = \frac{2\pi e^2 g T^2 i a^{2-d}}{\omega} \int_0^\beta d\tau \frac{1 - \exp(i\Omega\tau)}{\sin^2(\pi T\tau)} \Pi(\tau). \quad (2.88)$$

Here the analytic continuation to real frequency is assumed as $\Omega \rightarrow -i\omega$ and the function $\Pi(\tau)$ represents the phase correlation function,

$$\Pi(\tau_1 - \tau_2) = \langle \exp\{i[\varphi(\tau_1) - \varphi(\tau_2)]\} \rangle, \quad (2.89)$$

where the averaging is performed with the Coulomb action S_c in Eq. (2.56).

At first glance, calculation of the correlation function $\Pi(\tau_1 - \tau_2)$ with the action S_c reduces to computation of a Gaussian integral. However, this is not the case because at finite temperatures it is necessary to take into account all winding numbers, Eq. (2.47), in order to obtain the correlation function $\Pi(\tau)$ correctly. At low temperature a straightforward calculation results in (Efetov and Tschersich, 2003)

$$\sigma = 2\sigma_0 \exp(-E_c/T), \quad (2.90)$$

where σ_0 is the Drude high-temperature conductivity and E_c is the single-grain charging energy. This result has a clear physical meaning: The conductivity of an insulating granular array is mediated by electrons and holes that are present in the system as real excitations. Their concentration is given by the Gibbs law and the factor 2 appears due to the presence of both electrons and holes. From the result (2.90) we conclude that the activation exponent is determined by the Mott gap—that is, the energy cost to add or remove an electron from the system.

One can extend the calculation of the conductivity to higher orders in g by expanding in the tunneling term S_t , Eq. (2.57). It was shown by Loh *et al.* (2005) that the activation behavior persists at least in the next order in g . Clearly, the activation behavior, Eq. (2.13), is quite universal for periodic arrays and what one should clarify is the dependence of the Mott gap Δ_M on the conductance g . Now we turn to this question.

2. Mott gap at small tunneling conductances

At finite intergranular coupling the Mott gap is reduced due to the process of virtual tunneling of electrons to neighboring grains. This effect can be most easily studied in the limit of low coupling between grains within straightforward perturbation theory in the tunneling conductance. The gap Δ_M can be defined as

$$\Delta_M = E_{N=1} - \mu - E_{N=0}, \quad (2.91)$$

where μ is the chemical potential, $E_{N=0}$ is the ground-state energy of the charge-neutral array, and $E_{N=1}$ is the minimal energy of the system with an extra electron added to the neutral state. The correction to the Mott gap due to electron tunneling on neighboring grains can be found in the second order of perturbation theory,

$$\Delta E = - \sum_k \frac{|V_{k,0}|^2}{E_k - E_0}, \quad (2.92)$$

where the matrix elements of a perturbation V are taken between the ground state 0 and excited states k .

The correction to the energy due to finite intergranular coupling should be included in both terms $E_{N=1}$ and $E_{N=0}$ in Eq. (2.91). We consider in the zero approximation isolated grains and the tunneling Hamiltonian \hat{H}_t , Eq. (2.24), is our small perturbation. Using Eq. (2.92) we calculate matrix elements of tunneling between neighboring grains. As all grains are equivalent, we consider the tunneling between grains 1 and 2 assuming that the charge N on the grain 1 can be 0 or 1, while grain 2 is initially neutral. The contribution of hops between grain 1 and all its other neighbors leads merely to the factor z (coordination number) in the final result. Using Eq. (2.92) we calculate the corrections to the energies $E_{N=0}$ and $E_{N=1}$.

First, we consider the correction to the ground-state energy $E_{N=0}$. In this case the matrix elements $V_{k,0}$ correspond to electron tunneling between initially neutral neighboring grains. The excitation energy of this process is $\varepsilon_{k_1} + \varepsilon_{k_2} + E_{eh}$, where ε_{k_2} is the bare (with no Coulomb energy included) energy of an electron excitation in grain 2, ε_{k_1} is the bare energy of a hole excitation in grain 1, and E_{eh} is the electrostatic energy the electron-hole excitation determined from Eq. (2.23). It is given by $E_{eh} = E_{11}^c + E_{22}^c - 2E_{12}^c$, where E_{ij} can be obtained from Eq. (2.23) by putting $n_i=1$ and $n_j=-1$. For the periodic array of grains under consideration, the energy E_{eh} reduces to

$$E_{eh} = 2E_c - 2E_{12}^c. \quad (2.93)$$

The energy correction corresponding to such a process is

$$-\Delta E_{N=0} = 2 \sum_{k_1, k_2} \frac{|t_{k_1 k_2}|^2}{\varepsilon_{k_1} + \varepsilon_{k_2} + E_{eh}}, \quad (2.94)$$

where the factor 2 takes into account the equivalent process of electron hopping from grain 2 to grain 1.

Analogously, we find the correction to the energy $E_{N=1}$. The excitation energy of the process of electron tunneling from grain 2 to grain 1 is $\varepsilon_{k_1} + \varepsilon_{k_2} + 3E_{11}^c + E_{22}^c - 4E_{12}^c = \varepsilon_{k_1} + \varepsilon_{k_2} + 2E_{eh}$, while the excitation energy of electron tunneling from grain 1 to grain 2 is $\varepsilon_{k_1} + \varepsilon_{k_2} + E_{11}^c - E_{22}^c = \varepsilon_{k_1} + \varepsilon_{k_2}$. The corresponding correction to the energy $E_{N=1}$ reads

$$-\Delta E_{N=1} = \sum_{k_1, k_2} \frac{|t_{k_1 k_2}|^2}{\varepsilon_{k_1} + \varepsilon_{k_2} + 2E_{eh}} + \frac{|t_{k_1 k_2}|^2}{\varepsilon_{k_1} + \varepsilon_{k_2}}. \quad (2.95)$$

One can see that the corrections to the energy levels, Eqs. (2.94) and (2.95), are ultraviolet divergent. However, their difference is finite and gives the correction to the Mott gap Δ_M . Subtracting Eq. (2.94) from Eq. (2.95), replacing the summation over the states by integrals over a continuous variable ε , such that $\varepsilon_{k_1(k_2)} \rightarrow \varepsilon_{1(2)}$, we can calculate the Mott gap Δ_M . Taking into account the spin degeneracy we obtain the following expression for the Mott gap (Beloborodov, Lopatin, and Vinokur, 2005):

$$\Delta_M = E_c - \frac{2z}{\pi} g E_{eh} \ln 2, \quad (2.96)$$

where z is the coordination number of the array of grains and E_{eh} is the energy necessary to create an electron-hole excitation in the system by removing an electron from a given grain and putting it on a neighboring one. In the case of a diagonal Coulomb interaction $E_{ij} = E_c \delta_{ij}$ the energy of an electron-hole excitation E_{eh} is simply twice the Coulomb charging energy E_c .

The derivation of Eq. (2.96) was carried out neglecting the fact that an extra electron added to the neutral system in the presence of a finite intergranular coupling can move diffusively over the sample. Contributions corresponding to such processes are suppressed by an extra small factor $\delta/E_c \ll 1$ and thus can be neglected. More details of the calculations can be found in Beloborodov, Lopatin, and Vinokur (2005).

3. Mott gap at large tunneling conductances

From Eq. (2.96) one can see that the Mott gap Δ_M is significantly reduced at values $gz \sim 1$, where perturbation theory becomes inapplicable. Suppression of the gap Δ_M at large tunneling conductances g can be found with the help of the phase action, Eqs. (2.55)–(2.57). In fact, the renormalization of the charging energy at $gz \gg 1$ can be obtained with the renormalization-group approach described in Sec. II.C.2.

Indeed, the RG equation (2.68) is written assuming that g is a function of the independent variable ξ . We can invert this equation and assume that ξ is a function

of g . The running variable ξ determines the effective charging energy E_c^{eff} as $\xi = \ln E_c^{\text{eff}}$ and we obtain, by solving the latter equation

$$E_c^{\text{eff}} \sim A \exp(-\pi gz), \quad (2.97)$$

where A is a constant.

In order to determine the Mott gap Δ_M we notice that at conductances $gz \sim 1$ the charging energy is of the order of the Mott gap Δ_M , as one can see from Eq. (2.96). Matching Eq. (2.97) with Eq. (2.96) we conclude that the Mott gap Δ_M at large gz is reduced exponentially and can be written as

$$\Delta_M \sim E_c \exp(-\pi gz). \quad (2.98)$$

The RG approach used to obtain Eq. (2.98) is applicable only at energy scales larger than the inverse escape rate from a single grain Γ , which means that Eq. (2.98) is valid as long as the Mott gap Δ_M is larger than Γ . In this region the system should be an insulator. In the opposite limit one can expect that the granular material becomes a metal.

Taking $\Delta_M \sim \Gamma$ and solving Eq. (2.98) with respect to the conductance g we obtain the critical conductance g_c , Eq. (2.12), that marks the boundary between the insulating and metallic phases at low temperature. Thus we concluded that the Mott gap Δ_M remains finite as long as $g < g_c$, which assumes the activation behavior Eq. (2.13). The Arrhenius law Eq. (2.13) is typical for crystalline insulators.

4. Metal-insulator transition in periodic granular arrays

In the previous section we showed that in three-dimensional arrays there is a critical conductance g_c , such that samples with $g < g_c$ are insulators at $T \rightarrow 0$, while those with $g > g_c$ are metals. The analysis was performed from both the metallic and insulating sides and both approaches agree as to the value of the critical conductance g_c , Eq. (2.12). Unfortunately, they are not applicable in the vicinity of the phase transition and do not allow us to find the critical behavior of the Mott gap Δ_M near g_c .

The order of the Mott transition in the 3D periodic granular array is also not known, since one cannot exclude a weakly first-order phase transition. For example, the Mott transition in the Hubbard model with dimensionality $d \geq 3$ is believed to be of first order, and since the physics of the transition is similar, the same can be expected for a periodic granular array. We note, however, that in spite of the similarities between the periodic granular array model and the Hubbard model, there are essential differences between the two; namely, in granular metals, even in the case of periodic samples, the electron motion within a grain as well as on scales exceeding the intergranular distance is diffusive, while in the Hubbard model electrons move through a periodic lattice that allows us to label their states by quasimomenta. The model of granular metals has also an additional physical

parameter δ —the mean energy-level spacing in a single grain, which has no analog in the Hubbard model.

In the case of 1D and 2D granular samples the question of the Mott transition at $T \rightarrow 0$ cannot be formulated since, even in the metallic phase, the conductivity corrections are divergent at low temperatures [see Eqs. (2.6)–(2.9)]. However, the critical conductance g_c still has the meaning of the boundary between the hard-gap insulator behavior at $g < g_c$ and weak insulating behavior at $g > g_c$. We note that the fate of ordinary disordered metals with interaction at low temperature is not quite clear because of difficulties related to the divergence of the conductivity corrections (Finkelstein, 1990). In particular, the metal-to-insulator transition observed in disordered films (Abrahams *et al.*, 2001; Kravchenko and Sarachik, 2004) has not been yet theoretically understood, although some plausible scenarios have been suggested recently [see, e.g., Punnoose and Finkelstein (2005)].

It is clear that understanding the metal-insulator transition in granular materials is one of the most difficult theoretical problems and considerable efforts will be necessary to solve it.

G. Hopping conductivity in granular materials

In the previous section we showed that a strictly periodic granular model predicts and explains only the activation conductivity behavior. The experimentally observed temperature behavior of the conductivity of granular metals and arrays of quantum dots at low temperatures, however, is usually not of the activation type, but resembles the Efros-Shklovskii law Eq. (1.1), (Yakimov *et al.*, 2003; Yu *et al.*, 2004; Liao *et al.*, 2005; Romero and Drndic, 2005; Tran *et al.*, 2005). As already discussed in the Introduction, it is crucial for understanding the hopping transport in granular metals to take into account the electrostatic disorder that appears present in any realistic system. This disorder can be viewed as a random potential V_i applied to each grain that lifts the Coulomb blockade on some of the grains in the sample such that the conductivity is mediated by electron hopping between sites where the Coulomb blockade is almost removed. Below, we consider in more detail two essential ingredients of hopping conductivity—the density of states and the mechanisms of electron tunneling through a dense granular system in different regimes.

1. Density of states

The electrostatic disorder causes fluctuations in the electrostatic energy of granules and can thus lift the Coulomb blockade at some sites of the granular sample. This results, in its turn, in a finite density of states at the Fermi level and makes variable-range hopping the dominant mechanism of conductivity. The bare density of states induced by the random potential can be substantially suppressed due to the presence of long-range Coulomb interaction in the same way as in semiconductors

where the density of states (DOS) $\nu_g(\varepsilon)$ is given by the Efros-Shklovskii expression (Efros and Shklovskii, 1975; Shklovskii and Efros, 1988)

$$\nu_g(\varepsilon) \sim (\tilde{\kappa}/e^2)^d |\varepsilon|^{d-1}, \quad (2.99)$$

with e the electron charge and $\tilde{\kappa}$ the dielectric constant. This result was confirmed by Mullar and Ioffe (2004) and Pankov and Dobrosavljevic (2005) analytically using a locator approximation.

As explained in Sec. II.B, the Coulomb interaction in the granular matter may be considered by writing classical electrostatic formulas for the electron-electron interaction Eq. (2.23). This approach can also be used in the limit of weak coupling between grains, $g \ll 1$. We describe the Coulomb interaction in the presence of electrostatic disorder by writing the following expression for the Hamiltonian H :

$$H = \sum_i V_i n_i + \sum_{ij} n_i E_{ij}^c n_j, \quad (2.100)$$

where V_i is the random external potential, n_i is the number of excess electrons on the grain i , and E_{ij}^c is the Coulomb interaction between grains i and j . Taking into account the asymptotic behavior of the Coulomb interaction matrix $E_{ij}^c \sim e^2/2r_{ij}\tilde{\kappa}$, where r_{ij} is the distance between the grains i and j and $\tilde{\kappa}$ is the effective dielectric constant of the granular sample, we see that the classical model (2.100) for granular materials is essentially equivalent to the one studied by Efros and Shklovskii. Therefore their results have to be applicable to the model of the granular array, Eq. (2.100), as well.

At the same time, one expects that the DOS in an array of metallic granules is larger than that in a semiconductor since each metallic grain has a dense electron spectrum. Indeed, one should be reminded that there are many electron states in a grain that correspond to the same grain charge, while in the model of impurity levels in semiconductors the charge is uniquely (up to the spin) identified with the electron state.

The energy of an unoccupied state ε_i in the model specified by Eq. (2.100) is by definition the energy of an electron placed on this state. In a granular metal, any state with energy larger than ε_i is also available for the electron. Thus in order to translate the Efros-Shklovskii result Eq. (2.99) to the density of the electron spectrum in granular metals one has to integrate the dependence (2.99) over the energy ε and multiply it by the bare DOS in a single grain. As a result, we obtain

$$\nu(\varepsilon) \sim \nu_0 (|\varepsilon| \tilde{\kappa}/e^2)^d, \quad (2.101)$$

where ν_0 is the average DOS in a single grain (defined as the number of states per energy). However, Eq. (2.101) cannot be used in the Mott argument for the hopping conductivity where one needs to estimate the distance to the first available state r within the energy shell ε via the relation

$$r^d \int_0^\varepsilon d\varepsilon' \nu_g(\varepsilon') \sim 1. \quad (2.102)$$

The problem with using Eq. (2.101) for the DOS in Eq. (2.102) is that Eq. (2.101) takes into account the fact that if there is a state available for placement of an electron with a given energy then typically, on the same grain, there will be plenty of other states available for electron placement. However, for application to hopping conductivity we should not count different electron states that belong to the same grain since it is enough to find at least one state to ensure the transport.

Thus when finding the DOS relevant for hopping transport, we should count only the lowest-energy states within each grain. Then we arrive at the conclusion that, although the electron DOS in granular metals is modified according to Eq. (2.101), one has to use the Efros-Shklovskii expression for the DOS in its form (2.99) even in granular metals in order to find the distance to the first available state within a given energy shell via Eq. (2.102).

Similar considerations were presented by Zhang and Shklovskii (2004). Following this work we call the DOS that counts only the lowest excited states in each grain and that is relevant for the hopping conductivity “the density of ground states.” In order to distinguish this quantity from the conventional density of states of Eq. (2.101) we ascribe to it the subscript g , as in Eq. (2.99).

The arguments presented demonstrate that one can obtain a finite density of states in a granular material in the insulating regime. Although this is the necessary ingredient for establishing the mechanism of hopping conductivity, it alone is not sufficient for this type of transport. The problem is that an electron has to hop over several grains, which at first glance does not look probable in the case of a closely packed granular array. For quite a long time this fact did not allow us to apply the Efros-Shklovskii theory for explanation of the behavior Eq. (1.1) in granular materials, and the rather artificial model of Abeles *et al.* (1975) was used.

Only recently has a resolution of this puzzle been suggested independently (Beloborodov, Lopatin, and Vinokur, 2005; Feigel'man and Ioselevich, 2005). These authors demonstrated that the well-known phenomenon of co-tunneling (virtual hops) (Averin and Nazarov, 1990, 1992; Averin and Likharev, 1991) through a grain might be responsible for the long-range hops of electrons [see also Shklovskii (1984)]. One has to distinguish between elastic and inelastic co-tunneling processes. Elastic co-tunneling is the dominant mechanism for the hopping conductivity at low temperatures $T < T_{\text{cross}}$, while at higher temperatures $T > T_{\text{cross}}$ electron transport occurs via inelastic co-tunneling processes. The characteristic temperature T_{cross} of the crossover from the elastic to inelastic tunneling is given by

$$T_{\text{cross}} = \bar{c} \sqrt{E_c \delta}, \quad (2.103)$$

where $\bar{c} \approx 0.1$ is a numerical coefficient. In the next sections we discuss the elastic and inelastic contributions to the variable-range hopping.

2. Hopping via elastic co-tunneling

In considering the probability for an electron to tunnel from the site i_0 to site i_{N+1} it is convenient to put the Coulomb interaction energy at these sites to zero and count the initial ξ_0 and final ξ_{N+1} electron energies from the Fermi level. The presence of the electrostatic disorder on the grains is modeled by the random potential V_i . The energy of the electron (hole) excitation on the site i is

$$E_i^\pm = E_i^c \pm \mu_i, \quad (2.104)$$

where $\mu_i = V_i + 2\sum_j E_c^{ij} n_j$ is the local potential which along with the bare potential V_i includes the potential induced by neighboring grains. The probability P_{el} of a tunneling process via elastic co-tunneling can be found for the case of the diagonal Coulomb interaction $E_{ij}^c = E_i^c \delta_{ij}$. We leave calculational details for Appendix A and use here only the final result of the derivation.

The probability of the elastic co-tunneling through N grains can be written as

$$P_{\text{el}} = w g_0 \left(\frac{\bar{\Gamma}}{\pi \bar{E}} \right)^N \delta(\xi_{N+1} - \xi_0), \quad (2.105)$$

where $w = n(\xi_0)[1 - n(\xi_{N+1})]$ takes into account the occupations $n(\xi_0)$ and $n(\xi_{N+1})$ of the initial and final states, respectively (the initial state is filled and the final one is empty) and g_0 is the tunneling conductance between the 0th and 1st grains. The overbar in Eq. (2.105) denotes the geometrical average of the physical quantity along the tunneling path. For example, the average energy $\bar{\Gamma}$ is defined as

$$\ln \bar{\Gamma} = \frac{1}{N+1} \sum_{k=0}^N \ln \Gamma_k, \quad (2.106)$$

where the summation extends over the tunneling path $\Gamma_k = g_k \delta_k$ and g_k is the tunneling conductance between the k th and $(k+1)$ st grains. (Note that the meaning of Γ_i as an escape rate from a grain does not hold in the insulating regime under consideration.) Yet we use this notation even in the insulating state. The energy \bar{E} is the geometrical average $\ln \bar{E} = \frac{1}{N} \sum_{k=1}^N \ln \tilde{E}_k$, of the following combination of electron and hole excitation energies:

$$\tilde{E}_k = 2(1/E_k^+ + 1/E_k^-)^{-1}. \quad (2.107)$$

The presence of the delta function in Eq. (2.105) reflects the fact that the tunneling process is elastic.

The form of Eq. (2.105) for the tunneling probability P_{el} corresponds to an independent sequential tunneling from grain to grain. This equation means that on average the probability decreases exponentially with increasing distance s along the path:

$$P_{\text{el}} \sim \exp(-2s/\xi_{\text{el}}), \quad (2.108)$$

where the dimensionless localization length ξ_{el} can be written as

$$\xi_{\text{el}} = \frac{2}{\ln(\bar{E}\pi/c\bar{g}\delta)}. \quad (2.109)$$

Both the distance s and the length ξ_{el} in Eqs. (2.108) and (2.109) are measured in units of the grain size a . The numerical constant c in Eq. (2.109) is equal to unity for the model with diagonal Coulomb interaction $E_{ij}^c = E_c \delta_{ij}$. We show in Appendix A that inclusion of the off-diagonal part of the Coulomb interaction results in a renormalization of the constant c to a certain value $0.5 \leq c < 1$.

Applying the conventional Mott-Efros-Shklovskii arguments, i.e., optimizing the full hopping probability, which is proportional to

$$\exp[-(2s/\xi_{\text{el}}) - (e^2/\tilde{\kappa}Tas)], \quad (2.110)$$

one obtains Eq. (2.14) for the hopping conductivity with the characteristic temperature

$$T_0 \sim e^2/a\tilde{\kappa}\xi_{\text{el}}, \quad (2.111)$$

where $\tilde{\kappa}$ is the effective dielectric constant of a granular sample, a is the average grain size, and ξ_{el} is given by Eq. (2.109) [when deriving Eq. (2.111) we considered the tunneling path as nearly straight].

In the presence of a strong electric field \mathcal{E} , a direct application of the results of Shklovskii (1973) gives in the limit of low temperatures

$$\frac{T}{e\xi_{\text{el}}a} \ll \mathcal{E} \ll \frac{\sqrt{E_c}\delta}{ea}$$

the following expression for the nonlinear current dependence:

$$j \sim j_0 \exp[-(\mathcal{E}_0/\mathcal{E})^{1/2}], \quad (2.112)$$

where the characteristic electric field \mathcal{E}_0 is given by

$$\mathcal{E}_0 \sim T_0/ea\xi_{\text{el}}. \quad (2.113)$$

In full analogy with the hopping conductivity in semiconductors (Shklovskii and Efros, 1988), in granular metals also inelastic processes are required to allow an electron to tunnel to a state with higher energy. In granular metals such processes occur due to interaction with phonons as well as due to inelastic collisions with other electrons. It is clear that these processes were not considered when deriving Eq. (2.105). Therefore the results presented in this section are valid as long as the contribution of inelastic co-tunneling to the hopping conductivity can be neglected. This corresponds to the limit of low temperatures and electric fields $T, \mathcal{E}ea \ll T_{\text{cross}}$. Below we present results for the opposite limit when inelastic processes give the main contribution to the hopping conductivity.

3. Hopping via inelastic co-tunneling

Inelastic co-tunneling is the process when the charge is transferred by different electrons on each elementary

hop. During such a process the energy transferred to a grain by the incoming electron differs from the energy taken away by the outgoing one.

As in the case of elastic co-tunneling we assume that the electron tunnels from the grain i_0 with energy ξ_0 to the grain i_{N+1} with energy ξ_{N+1} . For the probability of such a tunneling process through a chain of the grains we find the following expression [see Appendix B and Beloborodov, Lopatin, and Vinokur (2005)]:

$$P_{\text{in}} = \frac{w}{4\pi T} \frac{\bar{g}^{N+1}}{\pi^{N+1}} \left(\frac{4\pi T}{\bar{E}} \right)^{2N} \frac{|\Gamma(N + i\Delta/2\pi T)|^2}{\Gamma(2N)} \times \exp\left(-\frac{\Delta}{2T}\right), \quad (2.114)$$

where $\Gamma(x)$ is the gamma function and $\Delta = \xi_{N+1} - \xi_0$ is the energy difference between the final and initial states. The appearance of the factor $\exp(-\Delta/2T)$ is consistent with the detailed balance principle. Indeed, at finite temperatures an electron can tunnel in two ways: either with an increase or with a decrease of its energy. According to the detailed balance principle the ratio of such probabilities is $\exp(\Delta/T)$, which is indeed the case for the function P_{in} , Eq. (2.114), since apart from the factor $\exp(-\Delta/2T)$ the rest of the equation is even in Δ .

In order to obtain the expression for the hopping conductivity one has to optimize Eq. (2.114) with respect to the hopping distance N under the constraint

$$Na\tilde{\kappa}\Delta/e^2 \sim 1, \quad (2.115)$$

which follows from the Efros-Shklovskii expression for the density of the ground states (2.99). Optimization of Eq. (2.114) is a somewhat more involved procedure than the standard derivation of the Mott-Efros-Shklovskii law based on the Gibbs energy distribution function (see Appendix B). Nevertheless, it leads to essentially the same result, i.e., the Efros-Shklovskii law Eq. (2.14), where the characteristic temperature $T_0(T)$ takes the form

$$T_0(T) \sim e^2/a\tilde{\kappa}\xi_{\text{in}}(T), \quad (2.116)$$

with a dimensionless weakly temperature-dependent localization length $\xi_{\text{in}}(T)$,

$$\xi_{\text{in}}(T) = \frac{2}{\ln(\bar{E}^2/16c\pi T^2\bar{g})}, \quad (2.117)$$

and the coefficient c equals unity for a model with a diagonal Coulomb interaction matrix.

Comparing the characteristic lengths $\xi_{\text{el}}(T)$ and $\xi_{\text{in}}(T)$ for the elastic and inelastic processes, respectively, we see easily that $\xi_{\text{el}}(T) > \xi_{\text{in}}(T)$ at temperatures $T < T_{\text{cross}}$, where the temperature T_{cross} is given by Eq. (2.103). This means that the mechanism of inelastic scattering is more efficient at not very low temperatures exceeding T_{cross} .

As in the case of elastic co-tunneling, the long-range electrostatic interaction results in the reduction of the coefficient to $1/4 \leq c < 1$.

At zero temperature, Eq. (2.114) for the inelastic probability P_{in} can be simplified for $\Delta < 0$ to the form

$$P_{\text{in}}(T=0) = \frac{w 2^{2N} \pi}{(2N-1)!} \frac{|\Delta|^{2N-1}}{\bar{E}^{2N}} \left(\frac{\bar{g}}{\pi} \right)^{N+1}, \quad (2.118)$$

while for $\Delta > 0$, Eq. (2.114) gives zero since electron tunneling with an increase of the electron energy is prohibited at zero temperature.

In order to obtain the hopping conductivity in the regime of a strong electric field \mathcal{E} and low temperature, we use following Shklovskii (1973) the condition (2.115) to define the distance to the first available electron site within the energy shell Δ . We use also

$$e\mathcal{E}r \sim \Delta, \quad (2.119)$$

which relates Δ to the electric field \mathcal{E} , and the fact that the distance between the initial and final tunneling sites is $r \sim Na$. Equations (2.115) and (2.119) allow us to determine the quantities $\Delta \sim \sqrt{\mathcal{E}e^3/\bar{\kappa}}$ and $N \sim \sqrt{e/\bar{\kappa}\mathcal{E}a^2}$. Inserting their values into Eq. (2.118), we come to the following expression for the current:

$$j \sim j_0 \exp[-(\mathcal{E}_0/\mathcal{E})^{1/2}], \quad (2.120)$$

where the characteristic electric field \mathcal{E}_0 is a weak function of the applied field \mathcal{E} ,

$$\mathcal{E}_0(\mathcal{E}) \sim \frac{e}{\bar{\kappa}a^2} \ln^2(\bar{E}^2/e^2\mathcal{E}^2a^2\bar{g}). \quad (2.121)$$

The results obtained in the insulating regime show that the hopping conductivity is the main mechanism of transport in the low-temperature regime. The temperature dependence of the conductivity is determined by the Efros-Shklovskii law Eq. (2.14) and is similar to the one in amorphous semiconductors. The exponential dependence of the current on a strong electric field is given by Eqs. (2.112) and (2.120). Again, this is the same dependence as in amorphous semiconductors. Of course, the characteristic temperature T_0 and electric field \mathcal{E}_0 are model dependent.

The theory for variable-range hopping (VRH) via virtual electron tunneling through many grains is based on the assumption that the hopping length r^* exceeds the size of a single grain a . This hopping length r^* should be found by minimizing the exponent in Eq. (2.110). From this condition we see that the characteristic length $r^*(T)$ is given by

$$r^*(T) = \sqrt{\frac{e^2\xi a}{2T\bar{\kappa}}}, \quad (2.122)$$

where the dimensionless localization length ξ is given by either Eq. (2.109) or Eq. (2.117), and that it decreases with increasing the temperature. At temperatures $\tilde{T} \sim e^2\xi/2a\bar{\kappa}$ the hopping length becomes of the order of the grain size $r^*(\tilde{T}) \sim a$. At such distances the VRH picture no longer works because electrons hop between neighboring grains only. This means that at comparatively high temperatures $\tilde{T} \ll T \ll \Delta_M$ one should use the

Arrhenius law, Eq. (2.13), instead of the Efros-Shklovskii law, Eq. (2.14). Such a crossover has been observed experimentally (Tran *et al.*, 2005).

Thus we have obtained a remarkable result: Even though the array of grains may look very regular, i.e., have a periodic structure and equal size and shape of the grains, it is almost inevitable that at low temperatures the main mechanism of conduction is variable-range electron hopping and the conductivity is determined by Eq. (2.14) as if the system were amorphous. This applies to other formulas also, like Eqs. (2.112) and (2.120).

III. ARRAYS COMPOSED OF SUPERCONDUCTING GRAINS

In this section we consider the properties of granular materials consisting of superconducting particles. As in Sec. II devoted to the study of normal metals we start our presentation with a qualitative discussion of the most interesting effects that occur in these systems. A quantitative analysis of these effects is given subsequently.

A. General properties of granular superconductors

1. Single grain

A granular superconductor, like a granular metal, can be viewed as an array of superconducting granules coupled via electron tunneling. The superconducting properties of an array are in many ways determined by the properties of the granules of which it is formed. For this reason we begin by reviewing the properties of superconductivity in a single small isolated grain.

This question was first addressed by Anderson (1959) who realized that *s*-wave superconductivity is almost insensitive to disorder of a general kind as long as it does not break time-reversal invariance. This includes, in particular, diffusive scattering by grain boundaries which is in many ways similar to the scattering by potential impurities in the bulk. As long as time-reversal invariance is not broken, one can choose a basis of exact eigenfunctions and then apply the Bardeen-Cooper-Schrieffer (BCS) theory in the usual way. The critical temperature can still be expressed via the BCS effective coupling constant and the density of states in the vicinity of the chemical potential. The BCS coupling constant does not change considerably when changing the basis and the average density of states is not sensitive to weak disorder. Thus one concludes (Anderson, 1959) that the critical temperature of a single grain has to be close to the bulk value.

Anderson has also pointed out that these arguments hold even for small grains provided the average distance between the energy levels δ , Eq. (1.3), is still smaller than the superconducting gap Δ in the bulk (Anderson, 1959). As soon as the energy-level spacing δ reaches the superconducting gap, the conventional BCS theory is no longer applicable.

This fact can easily be understood from the BCS equation for the order parameter, which can be written as

$$\Delta = \delta \lambda_0 T \sum_{\omega} \sum_{\xi_k} \frac{\Delta}{\omega^2 + \xi_k^2 + |\Delta|^2}, \quad (3.1)$$

where λ_0 is the standard dimensionless constant describing the attraction between electrons, $\omega = 2\pi T(n+1/2)$ are Matsubara frequencies, and δ is the average mean energy-level spacing in a grain determined by Eq. (1.3). The discrete variable ξ_k is

$$\xi_k = \epsilon_k - \mu, \quad (3.2)$$

where ϵ_k are the energies of electron states in the grains and μ is the chemical potential.

If the grain size is very large, such that the mean level spacing δ is much smaller than the superconducting critical temperature T_{c0} , the sum over the states in Eq. (3.1) can be replaced by the integral

$$\delta \sum_{\xi_k} \rightarrow \int_{-\infty}^{\infty} d\xi, \quad (3.3)$$

and we come to the conventional BCS equation.

At the same time, it is clear from Eq. (3.1) that a finite difference between the energy levels ξ_k plays a similar role as a finite temperature, namely, it reduces the superconducting gap $|\Delta|$. As soon as the mean level spacing δ exceeds T_{c0} [or $\Delta(T=0)$ for the bulk superconductors], the superconducting gap $|\Delta|$ vanishes. To be more precise, it remains finite due to fluctuations but its value is sufficiently reduced and in this regime the grain cannot be considered as a “true” superconductor. Nevertheless, the superconducting pairing is still present and shows, for example, the parity effect (Smith and Ambegaokar, 1996; von Delft *et al.*, 1996; Matveev and Larkin, 1997).

The Anderson theory agrees well with experiments. In particular, the electron spectrum of ultrasmall superconducting Al grains was studied by Ralph *et al.* (1995), Black *et al.* (1996), and Davidović and Tinkham (1999) where a well-defined superconducting gap was shown to survive down to grain sizes ~ 10 nm, while smaller grains ≤ 5 nm did not show any superconducting features in their electron spectrum.

It is worth noting that, while in diffusive or chaotic grains the density of states in the vicinity of the chemical potential indeed agrees well with the corresponding bulk values, this is not necessarily the case for ballistic grains possessing certain geometric symmetries. For example, in a spherical grain one naturally expects that energy levels are strongly degenerate. This may change the density of states at the Fermi level significantly resulting in a considerable change of the transition temperature. The possibility of utilizing the enhanced density of states that may appear from the orbital degeneracy in order to increase the single-grain critical temperature was suggested by Ovchinnikov and Kresin (2005a, 2005b).

Although all these effects are very interesting, here we follow our line of studying models with parameters

that can easily be achieved in existing granular materials. We assume everywhere that the granules are sufficiently large to maintain the local superconductivity within each grain, i.e., that the Anderson criterion is satisfied,

$$\delta \ll \Delta. \quad (3.4)$$

We assume also that the grains are diffusive or do not have an ideal shape like spheres or cubes, which excludes the possibility of a systematic degeneracy of the electron spectrum.

As a final remark in our discussion of superconductivity in a single grain, we point out that the thermodynamics of a single grain is not affected by the presence of the Coulomb interaction as long as the latter can be expressed in a standard way through the operator of the total electron number. The reason is that the number of particles in an isolated grain is conserved and thus the Coulomb term in the Hamiltonian commutes with the rest of the Hamiltonian and does not influence the thermodynamic quantities.

At the same time, phase fluctuations of the order parameter $\Delta(\tau)$,

$$\Delta(\tau) = |\Delta_0| \exp[2i\varphi(\tau)], \quad (3.5)$$

are very sensitive to the presence of the charging term Eq. (2.23). These fluctuations can be conveniently characterized by the correlation function $\Pi_s(\tau)$,

$$\Pi_s(\tau) = \langle \exp\{2i[\varphi(\tau) - \varphi(0)]\} \rangle, \quad (3.6)$$

where the averaging should be performed over the states of the Hamiltonian including the Coulomb interaction, Eq. (2.23).

Actually, the average over the states of the Hamiltonian in Eq. (3.6) reduces to an average with the action S_c , Eq. (2.56), and can be calculated (Efetov, 1980) leading to the result at $T=0$,

$$\Pi_s(\tau) = \exp(-4E_c\tau), \quad (3.7)$$

where $E_c = E_{ii}$ is the Coulomb energy of a single grain and the factor 4 appears because of the doubled Cooper pair charge. Equation (3.7) is written for the imaginary time τ . Changing to real time, $\tau \rightarrow it$, one concludes that the correlation function $\Pi_s(\tau)$ oscillates in time. Although the exponential form of the function $\Pi_s(\tau)$ does not lead to changes in the thermodynamics, it is crucial for the problem of coherence in an array of many grains.

2. Macroscopic superconductivity

Having listed the superconducting properties of a single grain we turn now to discussing the superconductivity in the whole sample. In order to simplify the presentation we first restrict ourselves to the zero-temperature case.

It is clear that an array with sufficiently strongly coupled grains should be able to maintain the superconducting coherence in the whole sample because the coupling reduces the phase fluctuations. In contrast, in the opposite limit of weak coupling, one expects that the

strong Coulomb interaction should lead to the Coulomb blockade of the Cooper pairs in analogy with the Coulomb blockade of electrons in granular metals in the low-coupling regime.

In order to quantify this intuitive statement [Abeles \(1977\)](#), following the earlier idea of [Anderson \(1964\)](#), suggested comparing the energy of the Josephson coupling of neighboring grains with the Coulomb energy. Indeed, the Josephson coupling tends to lock the phases of neighboring grains and to delocalize the Cooper pairs, while the Coulomb interaction tends to localize the Cooper pairs and thus enhance the quantum phase fluctuations.

Comparing the Josephson energy J ,

$$J = \pi g \Delta / 2, \tag{3.8}$$

with the Coulomb energy one comes to the conclusion that samples with $g > g_s \sim E_c / \Delta$ should be superconductors, while those with $g < g_s$ are insulators. This result was later derived with a superconducting granular array model including both Coulomb and Josephson interactions in a number of theoretical works ([McLean and Stephen, 1979](#); [Simánek, 1979](#); [Efetov, 1980](#)) using different methods. We review the main results of these studies in Sec. III.C.

The Anderson-Abeles criterion predicts that the superconductivity may survive even in samples that would be insulators if they were made from normal grains under equivalent conditions. Indeed, for samples with a small ratio $E_c / \Delta \ll 1$, there is a parametrically large interval of conductances $E_c / \Delta \ll g \ll 1$ where superconductivity should exist in spite of the fact that the corresponding normal array would be an insulator.

Qualitatively, this prediction was supported by experiments ([Shapira and Deutscher, 1983](#)) where some superconducting samples were found to show clear insulating behavior above the critical temperature. (We note, however, that although the ratio E_c / Δ in the samples used in this experiment was certainly large, this fact, as shown below, may be explained via renormalization of the Coulomb energy.) The corresponding dependence of the resistance on temperature according to [Shapira and Deutscher \(1983\)](#) is shown in Fig. 12.

However, the Anderson-Abeles criterion was found later to be in conflict with many other experiments. After pioneering work ([Orr *et al.*, 1985, 1986](#); [Jaeger *et al.*, 1986, 1989](#)) it became clear that the boundary between the superconducting and insulating states at $T=0$ is determined by the normal-state conductance of the film rather than the ratio of the Josephson and Coulomb energies.

This fact is illustrated by the experimental temperature dependencies of the resistivity of samples with different thicknesses shown in Fig. 13 for Ga and Pb ultrathin films. One can see that there exists a critical value of the normal-state resistance R_0 close to the value of quantum resistance $h / (2e)^2 \approx 6.4 \text{ k}\Omega$ such that samples with resistance $R < R_0$ eventually become superconducting under temperature decrease, while those with R

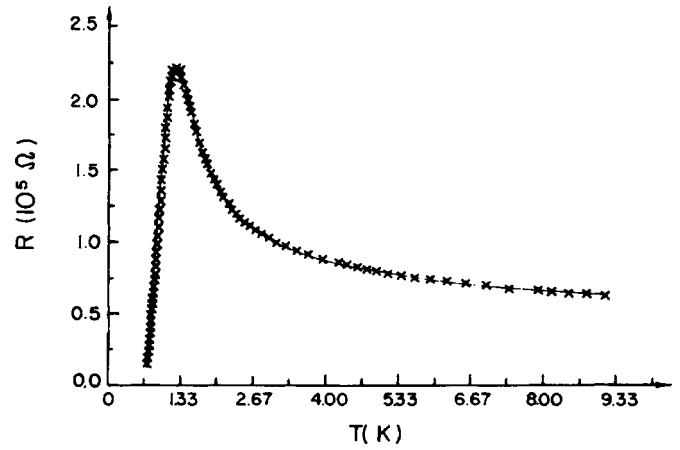


FIG. 12. Resistance as a function of temperature of a granular sample from [Shapira and Deutscher \(1983\)](#). In spite of the fact that the sample exhibits strong insulating behavior in the intermediate temperature range it finally turns to the superconducting state. From [Shapira and Deutscher, 1983](#).

$> R_0$ show a tendency to insulating behavior. This behavior turned out to be generic and was observed in a number of granular [as well as homogeneously disordered ([Liu *et al.*, 1993](#); [Marković *et al.*, 1999](#); [Frydman *et al.*, 2002](#))] films made from different materials.

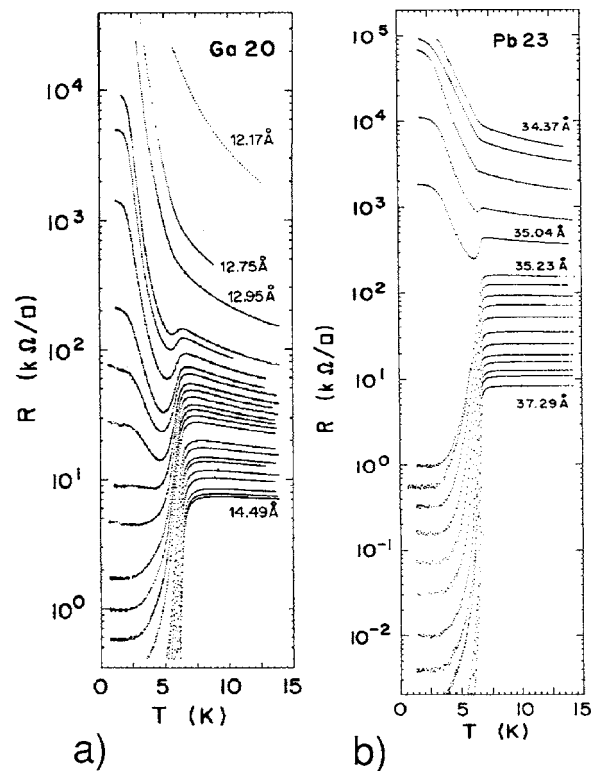


FIG. 13. Temperature dependence of resistivity of granular (a) Ga and (b) Pb ultrathin films according to [Jaeger *et al.* \(1989\)](#). Different curves correspond to films with different normal-state resistance which is tuned by the sample thickness. The low-temperature state is controlled by the film normal-state resistance. From [Jaeger *et al.*, 1989](#).

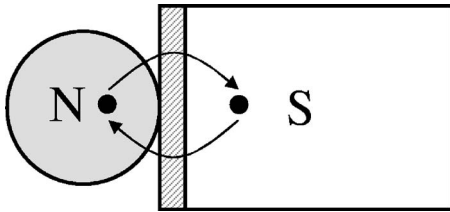


FIG. 14. Illustration of the renormalization of the Coulomb energy of a normal grain placed in contact with bulk superconductor. Due to virtual electron tunneling processes the Coulomb energy of a normal grain E_c is renormalized down to the values $\tilde{E}_c = \Delta/2g$. The conductance of the contact is supposed to be large, $g \gg 1$, and the initial Coulomb energy is assumed to be larger than the superconducting gap Δ .

In this respect, the superconductor-insulator transition in thin granular films resembles the analogous transition in a resistively shunted Josephson junction (Schmid, 1983; Bulgadaev, 1984) where the state of the system is known to be controlled by the value of the shunt resistance only, no matter what the ratio of the Coulomb and Josephson energies [for a review, see Schön and Zaikin (1990)]. The resistive shunt in this approach is included via the Caldeira-Leggett approach (Caldeira and Leggett, 1981, 1983) which allows us to take into account dissipative processes on the quantum-mechanical level. A similar approach based on the inclusion of a phenomenological dissipative term that models the resistive coupling of grains was applied to the granular system in order to resolve the disagreement with experiment (Chakravarty *et al.*, 1986; Fisher, 1986; Simánek and Brown, 1986). It was found that in the limit $E_c/J > 1$, in agreement with experiment, the boundary between the superconducting and insulating states is controlled by the resistance of the shunts only rather than by the ratio E_c/J .

However, the presence of the phenomenological resistive coupling between grains is rather difficult to justify, especially in the limit of low temperatures where all quasiparticles are frozen out. This problem was finally resolved by Chakravarty *et al.* (1987) on the basis of a model that took into account the direct electron tunneling processes between grains in addition to the Josephson couplings. The phase diagram obtained in this approach turned out to be similar to the one obtained within the “dissipative” model. At the same time, the considered model did not rely on any phenomenological assumptions and the virtual intergrain tunneling processes were well described in terms of the original tunneling Hamiltonian.

According to the approach of Chakravarty *et al.* (1987), the originally strong Coulomb interaction is reduced by the electron tunneling to other grains. This renormalization of the Coulomb energy can be well understood using the example of a simplified model of a normal grain placed in contact with a bulk superconductor shown in Fig. 14. It is clear that the Coulomb charging energy is reduced due to the possibility for an electron to be present virtually in the superconductor.

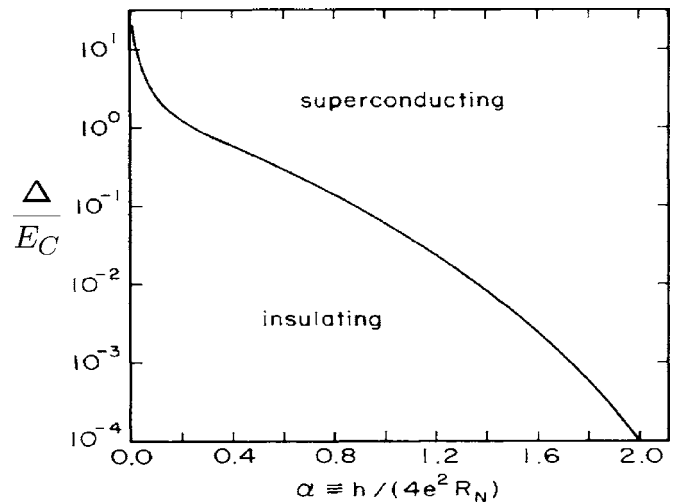


FIG. 15. Zero-temperature phase diagram of the granular superconducting array. The dimensionless parameter α is related to the conductance g as $\alpha = \pi g$. From Chakravarty *et al.*, 1987.

Actually, this renormalization is nothing but the screening of the Coulomb interaction by free charges, which is usual for metals.

The value of the screened charging energy in the case of strong coupling between grains, $g \gg 1$, and strong Coulomb interaction, $E_c \gg \Delta$, turns out to be $\sim \Delta/g$; and, which is remarkable, is independent of the original energy E_c . We see that in the limit $g \gg 1$ the Josephson energy $J \sim g\Delta$ is always larger than the effective Coulomb energy Δ/g , meaning that a sample with $g \gg 1$ should always be a superconductor at sufficiently low temperature (Larkin and Ovchinnikov, 1983; Eckern *et al.*, 1984). Another important conclusion is that the superconductor-insulator transition occurs at $g \sim 1$, which is in agreement with the experiments. The phase diagram obtained by Chakravarty *et al.* (1987) is presented in Fig. 15.

The fact that an array consisting of strongly coupled superconducting grains ($g \gg 1$) has to be in a superconducting state at sufficiently low temperatures can be understood from a somewhat more general consideration. In the strong-coupling regime, the granular system resembles the homogeneously disordered system. According to Anderson (1959), within the accuracy of the mean-field BCS theory the thermodynamics of such a system is essentially the same as that of a pure bulk electron system. This means that the granular sample turns to the superconducting state immediately after the superconducting gap appears locally in each grain.

Thus the insulating state where superconductivity exists locally, while being absent in the whole sample, may be obtained only beyond the BCS approximation. Corrections to the BCS theory may come from the Coulomb interaction and superconducting fluctuations but they are expected to be small in the limit $g \gg 1$. The fact that corrections due to the Coulomb interaction are small in normal metals in the limit $g \gg 1$ has been demonstrated in Sec. II. This result allows us to come to the conclusion

that at $g \gg 1$ the BCS theory is a good starting point to describe the granular system.

This means in particular that the critical temperature of a well-conducting granular sample ($g \gg 1$) is approximately given by the single-grain BCS critical temperature and that corrections to T_c can be studied by means of perturbation theory in $1/g$. In the case of homogeneously disordered films such a perturbative approach to the calculation of T_c is well known (Ovchinnikov, 1973; Maekawa *et al.*, 1983; Finkelstein, 1987). Analogously, one can consider the corrections to the critical temperature in granular systems using perturbation theory in the inverse conductance. We discuss this approach and the results obtained in Sec. III.D.

In the opposite limit $g \ll 1$ the critical temperature can be found from an effective model that includes the Josephson and Coulomb interaction only. As the probability of tunneling from grain to grain is small, the effect of screening due to the electron tunneling can be neglected. In particular, in the simplest case of a very small charging energy, one can estimate the critical temperature T_c by comparing the Josephson energy $J \sim \Delta g$ with the temperature, which leads to the estimate $T_c \sim \Delta g$. We consider this question within a mean-field approximation in more detail in the next section.

3. Granular superconductor in a magnetic field

Now we present new features in the behavior of a granular array that are manifest in an applied magnetic field. It turns out that magnetic properties of granular metals are very different from those of the corresponding bulk systems even in the limit of large tunneling conductances $g \gg 1$. In particular, there appears a new characteristic conductance value

$$g^* \approx 0.16(a\delta)^{-1}\sqrt{\Delta_0 D}, \quad (3.9)$$

where Δ_0 is the superconducting order parameter for a single grain at zero magnetic field and zero temperature and D is the diffusion coefficient in the grain.

The critical magnetic field H_c of samples with $g < g^*$ is close to the critical field H_c^{gr} of a single grain, while for samples with $g > g^*$, it is close to that in homogeneously disordered metals with the diffusion coefficient $D_{\text{eff}} = g\delta a^2$ [cf. Eqs. (2.2) and (2.3)]. The latter is the effective diffusion coefficient of the granular array. We note that the conductance g^* corresponds to well-conducting samples. Indeed, expressing g^* in terms of the Thouless energy $E_{\text{Th}} \sim D/a^2$ we obtain

$$g^* \sim \left(\frac{E_{\text{Th}} \Delta_0}{\delta^2} \right)^{1/2} \gg 1. \quad (3.10)$$

The dependence of the critical magnetic field on the sample conductance and temperature are considered in detail in Sec. III.C. Here we will show only how the new conductance scale (3.9) appears. The critical magnetic field H_c^{gr} destroying the superconductivity in a single grain of a spherical form due to the orbital mechanism is given by (Larkin, 1965)

$$H_c^{\text{gr}} = \frac{c}{e} \sqrt{\frac{5\Delta_0}{2R^2 D}}, \quad (3.11)$$

where the grain radius R is related to the period of the cubic granular array a as $R = a/2$. At sufficiently strong coupling the critical field of the sample, on the contrary, has to be given by the bulk value expressed via the effective diffusion coefficient:

$$H_c^{\text{bulk}} = \frac{\Phi_0}{2\pi D_{\text{eff}}} \frac{\Delta_0}{e}, \quad (3.12)$$

where $\Phi_0 = hc/2e$ is the flux quantum. Comparing Eqs. (3.11) and (3.12) one can see that the two critical magnetic fields H_c^{gr} and H_c^{bulk} become of the same order at tunneling conductances $g \approx g^*$.

The orbital mechanism of destruction of superconductivity leading to Eqs. (3.11) and (3.12) is dominant provided the grains are not very small. However, in the limit of very small sizes of the grain, the Zeeman mechanism of destruction can become more important (Tinkham, 1996; Kee *et al.*, 1998; Beloborodov *et al.*, 2000) (everywhere we consider s -wave singlet pairing).

If the Zeeman mechanism dominates the orbital one, the critical magnetic field H_c^z is given by the Clogston value

$$H_c^z = \Delta_0 / \sqrt{2} \mu_B, \quad (3.13)$$

where $\mu_B = e\hbar/2mc$ is the Bohr magneton (Clogston, 1960). Note that the phase transition between the superconducting and normal states is in this case of first order.

In the opposite limit, when superconductivity is destroyed mainly by the orbital mechanism, the Zeeman splitting has no dramatic effect on the phase diagram. Comparing the orbital and Zeeman critical magnetic fields, Eqs. (3.11) and (3.13), one can see that the latter can be neglected as long as the grain is not too small $a > a_c$ with the critical grain size a_c given by

$$a_c \approx \sqrt{\frac{5}{D\Delta_0 m^2}} \sim \frac{1}{p_0} \sqrt{\frac{E_{\text{Th}}}{\Delta_0}}, \quad (3.14)$$

where p_0 is the Fermi momentum. Throughout we assume that grains are not too small such that the phase transition within a single grain remains of the second order. Of course, we speak about the phase transition within the mean-field approximation. Fluctuations of the order parameter Δ smear the transition in the isolated grain.

4. Transport properties of granular superconductors

The experimentally observed dependencies of the resistivity of granular superconductors on temperature and applied magnetic field are very rich and all details are currently far from being well understood theoretically. Here we discuss only briefly the general transport properties, touching in detail only the latest developments related to the low-temperature magnetoresistance in granular superconductors. A broader discussion of theoretical advances in understanding the transport

properties of granular superconductors (networks of Josephson junctions) can be found in [Fazio and van der Zant \(2001\)](#).

In the absence of a magnetic field, the dependence of the resistivity of a granular superconductor on temperature is typically nonmonotonic. One of the examples is shown in [Fig. 12](#). Decreasing the temperature first leads to a growth of the resistivity, which is due to the enhancement of the Coulomb correlations that suppress the current. However, the resistivity starts decreasing closer to the superconducting transition temperature. In this region the conductivity is enhanced due to the fluctuation contribution of the Cooper pairs ([Aslamazov and Larkin, 1968](#)).

Granular films with the normal-state resistance close to the critical value $R_0 \sim 6.4 \text{ k}\Omega$ exhibit often a more complicated reentrant behavior as seen in [Fig. 13](#). The resistance of such samples increases again after a drop associated with the fluctuating conductivity. This effect might be a consequence of the competition between the conductance increase due to the fluctuating Cooper pairs and the freezing of excitations due to the opening of the superconducting gap in the density of states.

A systematic theoretical description of this phenomenon is not available yet. We note only that the reentrant behavior of the conductivity seems to be a consequence of the granularity. Homogeneous films made from the same material having no (or less pronounced) granular structure do not show such a behavior ([Liu *et al.*, 1993](#)).

A magnetic field applied to a granular system supplies an extra control parameter allowing us to change the resistivity and to tune the state of the granular system. In particular, sufficiently strong magnetic fields can always destroy the superconductivity even at low temperatures.

What is interesting is that the resistance of a granular superconductor has a nonmonotonic dependence on the applied magnetic field at low temperatures. As an example we present results of a measurement on granular Al from [Gerber *et al.* \(1997\)](#), see [Fig. 16](#). The samples used by [Gerber *et al.* \(1997\)](#) were three dimensional and monodisperse with a typical grain diameter of $\approx 120 \text{ \AA}$. A surprising feature of the experimental curves is that there is a region with a negative magnetoresistance and a pronounced peak in the resistivity at the magnetic field of several teslas is seen. Only at extremely strong fields $H > 6 \text{ T}$ is the resistivity almost independent of the field.

The nonmonotonic behavior of the resistivity can be understood in terms of the corrections to the conductivity due to superconducting fluctuations ([Beloborodov and Efetov, 1999](#); [Beloborodov *et al.*, 2000](#)). In the vicinity of the phase transition the resistivity decreases due to the opening of an additional transport channel via fluctuating Cooper pairs. This is what is called the Aslamazov-Larkin conductivity correction ([Aslamazov and Larkin, 1968](#)).

We note that this correction always gives a positive contribution to the conductivity and thus cannot explain the negative magnetoresistance at higher fields. How-

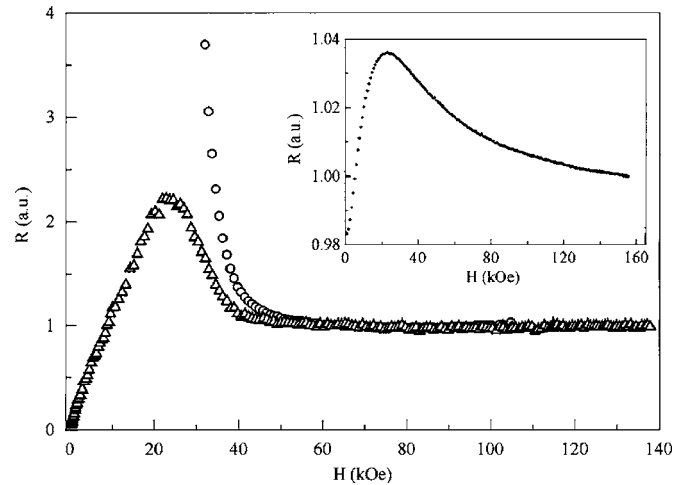


FIG. 16. Low-temperature resistance of 3D Al granular samples as a function of magnetic field at low temperatures $T \ll T_c$. The curves are shown for two samples with different normal-temperature resistance. The inset shows a much less pronounced peak in the resistance at higher temperatures $T - T_c \ll T_c$. From [Gerber *et al.*, 1997](#).

ever, at stronger fields another conductivity correction, appearing as a result of the reduction of the density of states due to fluctuating Cooper pairs, begins to dominate electronic transport ([Beloborodov and Efetov, 1999](#)). As a result, in this regime the conductivity becomes lower than that in the normal metal approaching the latter only in the limit $H \gg H_c$, where all superconducting fluctuations are completely suppressed by the magnetic field. The magnetoresistance of granular superconductors is discussed in more detail in [Sec. III.E](#).

Tuning the magnetic field in the limit $T \rightarrow 0$ one can cross the boundary between the superconducting and metallic or insulating states and investigate transport around the zero-temperature (quantum) phase transition. The corresponding transition point at $T=0$ is referred to as the quantum critical point ([Sondhi *et al.*, 1997](#); [Sachdev, 2001](#)).

Quantum phase transitions are analogous to classical phase transitions with the difference that at $T \rightarrow 0$ the system has to be described not only via the characteristic spatial (coherence length) ξ but also via the characteristic time scale τ . Both τ and ξ , as in the case of classical transitions, are assumed to scale as powers of the parameter δ that controls the closeness of the system to the quantum critical point.

Scaling ideas were applied to the problem of the superconductor-to-insulator transition by [Fisher \(1990\)](#) and [Fisher *et al.* \(1990\)](#) and had a substantial impact on the field. Scaling expressions for the resistivity seem to work well for many samples. However, one of the central predictions by [Fisher \(1990\)](#) and [Fisher *et al.* \(1990\)](#)—the universal conductance at the superconductor-to-insulator transition—is not supported by all experiments ([van der Zant *et al.*, 1992](#); [Goldman and Marković, 1998](#); [Chervenak and Valles, 2000](#)).

Of course, the scaling approach to resistivity behavior is not restricted to granular systems and homogeneously disordered films are much more suitable candidates for experimental study of such phenomena. For this reason we will not examine this question further, referring the reader to [Sondhi *et al.* \(1997\)](#), [Goldman and Marković \(1998\)](#), and [Fazio and van der Zant \(2001\)](#).

B. Phase diagram of granular superconductors

In this section the phase diagram of granular superconductors in the absence of the magnetic field is discussed. We mainly concentrate on the mean-field approach; we will not touch the critical behavior in the very vicinity of the phase transition nor discuss in detail the superconductor-insulator transition. The latter phenomenon relates to a wide class of disordered superconductors and represents the field of research on its own. For reviews on this subject we refer the reader to [Goldman and Marković \(1998\)](#), [Larkin \(1999\)](#), and [Fazio and van der Zant \(2001\)](#).

Arrays of superconducting grains can be conveniently described using a phase functional analogous to the functional $S[\varphi]$ derived in Sec. II for normal granular metals. In the next section we introduce such a functional.

1. Phase functional for granular superconductors

The description of a granular superconductor in terms of the phase action is very similar to that used for normal metals and the derivation can be extended to include the superconducting order parameter. In order to simplify the discussion we consider the limit of low temperatures $T \ll T_{c0}$, where T_{c0} is the critical temperature in the bulk in the BCS approximation. We assume that the superconducting gap is still smaller than the Thouless energy, Eq. (1.5),

$$\Delta \ll E_{\text{Th}}, \quad (3.15)$$

which allows us to consider a single grain as zero dimensional. Another way to write this inequality is

$$\xi_{\text{eff}} \gg a, \quad (3.16)$$

where $\xi_{\text{eff}} = \sqrt{\xi_0 l}$, $\xi_0 = v_F / T_{c0}$, and l is the mean free path.

The derivation of the action $S[\varphi]$ can be carried out in the same way as in Sec. II, decoupling the Coulomb interaction by an auxiliary field V_i and performing the gauge transformation. The phase φ is determined by Eqs. (2.44)–(2.47). Expanding the action in the tunneling amplitude t_{ij} up to the second order we obtain the action $S[\varphi]$ in the form of a sum of three terms,

$$S[\varphi] = S_c[\varphi] + S_{ts}[\varphi] + S_J[\varphi]. \quad (3.17)$$

The first term $S_c[\varphi]$ stands for the charging energy and is given by Eq. (2.56). This means that the charging energy of the superconducting grain is the same as that of the normal one provided the same charge is placed on the grains.

The second term $S_{ts}[\varphi]$ can be written in the form of Eq. (2.57) but with another function $\alpha_s(\tau)$ instead of $\alpha(\tau)$, Eq. (2.58). In the low-temperature limit this function takes the form ([Eckern *et al.*, 1984](#)).

$$\alpha_s(\tau) = \frac{1}{\pi^2} \Delta^2 K_1^2(\Delta|\tau|), \quad (3.18)$$

where $K_1(x)$ is the modified Bessel function. This difference between the functions $\alpha(\tau)$, Eq. (2.58), and $\alpha_s(\tau)$ is very important. The function $\alpha_s(\tau)$, Eq. (3.18), decays exponentially when increasing τ , while the function $\alpha(\tau)$ decays only algebraically at large τ . The good convergence of the kernel (3.18) allows us to expand the term S_{ts} , Eqs. (2.57) and (3.18), in powers of $\tau - \tau'$ and to write the term S_{ts} in a simplified form,

$$S_{ts} = \frac{3\pi g}{64\Delta} \sum_{\langle ij \rangle} \int_0^\beta \varphi_{ij}^2(\tau) d\tau, \quad (3.19)$$

which should be correct for $\tau \gg \Delta^{-1}$. Only the third term S_J in Eq. (3.17) is new as compared with normal metals; it describes the Josephson coupling between grains and in the limit $\tau \gg \Delta^{-1}$ can be written as

$$S_J = -\frac{1}{2} \sum_{\langle ij \rangle} \int_0^\beta J_{ij} \cos\{2[\varphi_i(\tau) - \varphi_j(\tau)]\} d\tau. \quad (3.20)$$

The sum in Eq. (3.20) should be performed over the nearest neighbors i, j , and $J = J_{ij}$ for these values of i, j is determined by Eq. (3.8).

Equations (3.17), (2.56), (2.57), (3.18), (3.20), and (3.8) completely describe granular superconductors in the low-temperature limit. They can easily be extended to higher temperatures by writing proper expressions for the functions $\alpha_s(\tau)$ and J_{ij} . We do not consider these complications here since we are trying to present the physical picture in the simplest way.

The action $S[\varphi]$ contains only the phases φ , whereas fluctuations of the modulus of the order parameter are neglected. This is justified at low temperatures provided the inequality (3.4) is satisfied. A microscopic derivation of the action $S_c + S_J$ was originally done using another approach by [Efetov \(1980\)](#). It was also written phenomenologically by [Simánek \(1979\)](#) assuming, however, that the variable φ varied from $-\infty$ to ∞ . The existence of the term S_{ts} was realized later ([Eckern *et al.*, 1984](#)) and used for a system of Josephson junctions by [Chakravarty *et al.* \(1987\)](#).

Assuming that large times $\tau \gg \Delta^{-1}$ are most important, we use in the subsequent calculations Eq. (3.19) for the term S_{ts} . Then, denoting

$$S_0[\varphi] = S_c[\varphi] + S_{ts}[\varphi], \quad (3.21)$$

we write the quadratic form $S_0[\varphi]$ as

$$S_0[\varphi] = \frac{1}{4} \sum_{ij} \int (\tilde{E}_c^{-1})_{ij} \dot{\varphi}_i(\tau) \dot{\varphi}_j(\tau) d\tau, \quad (3.22)$$

where

$$\tilde{E}_c(\mathbf{q}) = \frac{1}{2}[C(\mathbf{q})/e^2 + (3\pi g/16\Delta)\lambda_{\mathbf{q}}]^{-1} \quad (3.23)$$

and $\lambda_{\mathbf{q}}$ is from Eq. (2.30). The function $E(\mathbf{q})$ is the Fourier transform of the function E_{ij} and \mathbf{q} is the quasimomentum. When integrating over the phases φ , one should remember about the winding numbers. Looking at Eq. (3.23) one can understand that the term S_{IS} , Eqs. (2.57) and (3.18), leads to a screening of the Coulomb interactions.

2. Mean-field approximation

In spite of many simplifications, the action

$$S[\varphi] = S_0[\varphi] + S_J[\varphi] \quad (3.24)$$

is still complicated and it is not possible to describe the system without making approximations. A common way to understand, at least qualitatively, the properties of a model is to develop a mean-field theory. Following this approach one should replace the initial Hamiltonian (action) by a simplified one and determine parameters of the effective model self-consistently.

Now consider the action $S[\varphi]$, Eq. (3.24), in the mean-field approximation. Following Efetov (1980) in the action S_J , Eq. (3.20), we make the following replacement:

$$\sum_{\langle i,j \rangle} J_{ij} \cos[2(\varphi_i - \varphi_j)] \rightarrow Jz \langle \cos 2\varphi \rangle_{\text{MF}} \sum_j \cos 2\varphi_j. \quad (3.25)$$

The average $\langle \cos 2\varphi \rangle_{\text{MF}}$ in Eq. (3.25) should be calculated with the action $S_{\text{eff}}[\varphi]$ that can be obtained from $S[\varphi]$, Eq. (3.24), by making the replacement, Eq. (3.25), in $S_J[\varphi]$, Eq. (3.20). Actually, this average is the order parameter for macroscopic superconductivity.

Assuming that the transition between the superconductor and insulator is of the second order we can find the critical point from the condition that at this point the mean field $\langle \cos 2\varphi \rangle_{\text{MF}}$ vanishes. The corresponding equation determining the boundary of the superconducting state is

$$1 = \frac{zJ}{2} \int_0^\beta \Pi_s(\tau) d\tau, \quad (3.26)$$

where z is the coordination number of the lattice and $\Pi_s(\tau)$ is determined by Eq. (3.6), assuming, however, that the average $\langle \dots \rangle$ in that equation should be calculated with the action $S_0[\varphi]$, Eqs. (3.22) and (3.23).

In order to simplify calculations further we neglect the off-diagonal terms in the matrix E_{ij} , Eq. (3.22), keeping the value $E_0(g) = \tilde{E}_c^{ii}$ only. This value can be written as

$$E_0(g) = a^d \int \tilde{E}_c(\mathbf{q}) \frac{d^d \mathbf{q}}{(2\pi)^d}, \quad (3.27)$$

where $\tilde{E}_c(\mathbf{q})$ is determined by Eq. (3.23). Then for $\Pi_s(\tau)$ instead of Eq. (3.7) we obtain the following expression:

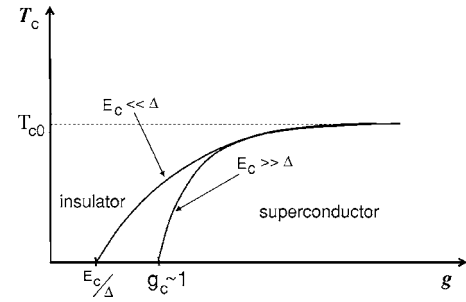


FIG. 17. A phase diagram sketch of a granular superconductor in the coordinates critical temperature vs tunneling conductance for two cases $E_c \ll \Delta_0$ and $E_c \gg \Delta_0$. At large tunneling conductances $g \gg 1$ the Coulomb interaction is screened due to electron intergrain tunneling and the transition temperature is approximately given by the single-grain BCS value. In the opposite case $g \ll 1$ the boundary between the insulating and superconducting states is obtained by comparing the Josephson $E_J = g\Delta$ and Coulomb E_c energies.

$$\Pi_s(\tau) = \exp(-4E_0\tau). \quad (3.28)$$

Solving Eq. (3.26) at $T \rightarrow 0$ one obtains the relation between the Josephson and Coulomb energies at the phase transition

$$zJ = 8E_0(g). \quad (3.29)$$

Equation (3.29) agrees at small $g \ll 1$ (up to a coefficient) with the Anderson-Abeles criterion (Abeles, 1977). In this limit we obtain using Eq. (3.8) the critical value for the conductance in the form

$$g_c^* = 16E_0(0)/\pi z\Delta. \quad (3.30)$$

Samples with tunneling conductances $g < g_c^*$ are insulators, while those with $g > g_c^*$ are superconductors. We note that this result suggests that even samples with weakly coupled granules $g_c^* < g \ll 1$ are still superconductors in spite of the fact that the corresponding array of normal grains with the same Coulomb interaction would be an insulator in this regime.

It is clear from Eq. (3.26) that the zero-temperature result (3.30) holds also at finite temperatures so long as $T \ll E_c$. In the opposite limit $T \gg E_c$ (but still $T \ll T_{c0}$), one obtains $\Pi_s(\tau) = 1$, which leads to the critical temperature

$$T_c = \frac{1}{2}zJ = \frac{1}{4}z\pi g\Delta. \quad (3.31)$$

The results (3.30) and (3.31) correspond to the low-coupling part (small g) of the phase diagram shown in Fig. 17.

As mentioned previously, the Anderson-Abeles criterion fails to produce the correct phase boundary between the insulating and superconducting states for arrays with a stronger coupling $g \geq 1$. According to experiments (Orr *et al.*, 1986; Jaeger *et al.*, 1989) the superconductor-insulator transition is controlled by the resistance of the array only and the critical resistance R_c

(in the case of granular films) is close to the resistance quantum $R_0 \approx 6.4$ k Ω . The Coulomb interaction drops out from the result.

This interesting observation can be understood using Eqs. (3.29), (3.27), (3.23), and (3.8). It is important to notice that the energy $E_0(g)$ depends on the dimensionality. Using Eqs. (3.23) and (3.27) we see that in 3D arrays of grains the function $E_0(g)$ is given by

$$E_0(g) = c\Delta/g, \quad (3.32)$$

where c is a number of the order unity, while in two dimensions we obtain with logarithmic accuracy

$$E_0(g) = \frac{2\Delta}{3\pi^2 g} \ln(gE_c/\Delta). \quad (3.33)$$

One can see from Eqs. (3.32) and (3.33) that the effective charging energy is independent of the originally strong Coulomb interaction in the 3D case and is almost independent of it in the 2D case. Substituting Eqs. (3.32) and (3.33) into Eqs. (3.29), we come to the conclusion that in the limit $E_c \gg \Delta$ the superconductor-insulator transition occurs at $g_c \sim 1$, which is in agreement with experiments.

The considerations presented in the original work of Chakravarty *et al.* (1987) lead to results qualitatively similar to those presented here. In particular, the phase boundary at $T \rightarrow 0$ in the two-dimensional case was found to be

$$\alpha_c^2 = \frac{4}{3\pi} \ln\left(1 + \frac{3\pi}{16} \alpha_c \frac{E_c}{\Delta}\right), \quad (3.34)$$

where α_c is the critical value of the dimensionless conductance related to our conductance g as $\alpha = \pi g$. The phase boundary following from the calculations of Chakravarty *et al.* (1987) is represented in Fig. 15.

Summarizing our discussion, we present in Fig. 17 the phase diagram for a granular superconductor in the temperature vs conductance coordinates for two cases of $E_c \ll \Delta$ and $E_c \gg \Delta$.

The strong-coupling regime $g > 1$ can also be analyzed using the diagrammatic technique. This approach is advantageous in many respects since it allows one to find corrections to the critical temperature in a straightforward and rigorous way, not relying on the mean-field approximation used in the treatment of the effective functional. This approach is considered in detail in Sec. III.D.

We note that, while the mean-field theory gives qualitatively correct results, it certainly cannot be viewed as a complete description of the model Eq. (3.17), because fluctuations near the mean-field solutions can be important. In particular, Eq. (3.26) assumes that the system is not affected by Josephson couplings so long as the mean value of φ is zero. However, the Josephson coupling is known to be important even in the insulating state. In the simplest case of the insulating state with low Josephson coupling the effect of the later can be included via

perturbation theory. As a result, the charging energy is reduced, $E_c \rightarrow \tilde{E}_c = E_c + \delta E_c$, with the correction δE_c given by (Sachdev, 2001)

$$\delta E_c = -zJ/2. \quad (3.35)$$

Closer to the superconductor-insulator transition the charging energy is renormalized even more strongly and in the vicinity of the transition it is expected to have the scaling form (Sachdev, 2001)

$$E_0(g) \sim |g_c^* - g|^\gamma, \quad (3.36)$$

where $\gamma > 0$ is a critical index. One may interpret the energy $E_0(g)$ as the increase of charging energy when a Cooper pair is added to a neutral grain. Exactly at the phase transition this energy vanishes according to Eq. (3.36) and this ensures the continuity of the Coulomb gap at the phase transition, since in the superconducting state this gap has to be zero.

The Coulomb gap is an important characteristic of the insulating state. In particular, it controls the low-temperature conductivity, which has an activation form

$$\sigma \sim e^{-4E_0(g)/T}. \quad (3.37)$$

The experimentally measured conductivity of granular samples is, however, usually more complicated than that given by Eq. (3.37) and typically has a variable-range-hopping type of behavior. Such behavior can be obtained by taking into account the electrostatic disorder neglected in the model, Eq. (3.17).

C. Upper critical field of a granular superconductor

As already mentioned, granular superconductors have rather unusual magnetic properties. In particular, at low temperatures, depending on the tunneling conductance g , the critical magnetic field is determined either by the bulk formula (3.12) at $g > g^*$ or by the critical magnetic field of a single grain (3.11) at $g < g^*$, where the characteristic conductance g^* is given in Eq. (3.9). In this section we discuss in detail the dependence of the upper critical field H_{c2} of granular superconductors on the tunneling conductance g at arbitrary temperatures. We consider granular samples that are relatively good metals in their normal state, such that $g \gg 1$. This allows us to neglect the effect of the suppression of the critical temperature by the Coulomb interaction and fluctuations.

1. Critical field of a single grain

We begin with a discussion of the critical magnetic field of a single grain. This problem was first considered by Larkin (1965) by means of averaging the Gor'kov equations over disorder. Another way to consider this problem is based on using a later technique, namely, the semiclassical Usadel equation (Usadel, 1970). This is more convenient for our purposes since it can easily be generalized to the case of a granular array. Assuming that the transition between the superconducting and

normal states is of the second order, we define the critical field as the field at which the self-consistency equation (Abrikosov *et al.*, 1965)

$$\Delta(\mathbf{r}) = \lambda_0 \pi T \sum_{\omega} f_{\omega}(\mathbf{r}), \quad (3.38)$$

where $\omega = \pi T(2n+1)$, acquires a nontrivial solution under decrease of the magnetic field. The function $f_{\omega}(\mathbf{r})$ is a quasiclassical Green function that can be obtained from the anomalous Gor'kov Green's function F by integration over ξ , Eqs. (3.2) and (3.3). The Green's function $f_{\omega}(\mathbf{r})$ can be determined from the Usadel equation, which can be linearized close to the phase transition [see, e.g., Kopnin (2001)],

$$[|\omega| + D(-i\nabla - 2e\mathbf{A}/c)^2/2]f_{\omega}(\mathbf{r}) = \Delta(\mathbf{r}), \quad (3.39)$$

where D is the classical diffusion coefficient in the superconducting grain and \mathbf{A} is the vector potential. We choose the vector potential corresponding to a homogeneous magnetic field \mathbf{H} in the form $\mathbf{A}(\mathbf{r}) = [\mathbf{H} \times \mathbf{r}]/2$, which allows us to reduce Eq. (3.39) to

$$[|\omega| - D\nabla^2/2 + 2D(e\mathbf{A}/c)^2/2]f_{\omega}(\mathbf{r}) = \Delta(\mathbf{r}). \quad (3.40)$$

Equation (3.40) can be solved via perturbative expansion in \mathbf{A}^2 . In the limit determined by Eq. (3.16), one can neglect the dependence of the functions $f_{\omega}(\mathbf{r})$ and $\Delta(\mathbf{r})$ on the coordinates. In the main approximation we can simply replace the term with $\mathbf{A}^2(\mathbf{r})$ in Eq. (3.40) by its average over the volume of the grain. Thus we obtain a simple algebraic equation relating the constant components of f and Δ ,

$$f_{\omega}(|\omega| + \alpha) = \Delta, \quad (3.41)$$

where the depairing parameter α in the case of a spherical grain with the radius R is

$$\alpha = R^2 D(eH/c)^2/5. \quad (3.42)$$

Substituting the solution of Eq. (3.41) into Eq. (3.38) we come to the standard equation (Abrikosov and Gor'kov, 1961) relating the critical temperature T_c to the depairing parameter α , Eq. (3.42),

$$\ln(T_c/T_{c0}) = \psi(1/2) - \psi(1/2 + \alpha/2\pi T_c). \quad (3.43)$$

Here $\psi(x)$ is the digamma function and $T_{c0} \equiv T_c(H=0)$ is the single-grain superconducting critical temperature in the absence of a magnetic field. One can see that at zero temperature the superconductivity is destroyed at

$$\alpha_{c0} = \Delta_0/2, \quad (3.44)$$

where Δ_0 is the superconducting order parameter at $T, H=0$, which is related to the critical temperature T_{c0} in the absence of the magnetic field as $\Delta_0 = \pi T_{c0}/\gamma$ with $\ln \gamma \approx 0.577$ being the Euler constant. For a single grain of spherical shape we obtain Eq. (3.11) for the critical field H_c^{gr} at zero temperature.

The above approach can be easily generalized to take into account the Zeeman splitting by making the shift $|\omega| \rightarrow |\omega| + h \text{sgn } \omega$, where h is the Zeeman energy $h = \mu_B H$. Then Eq. (3.45) is modified to

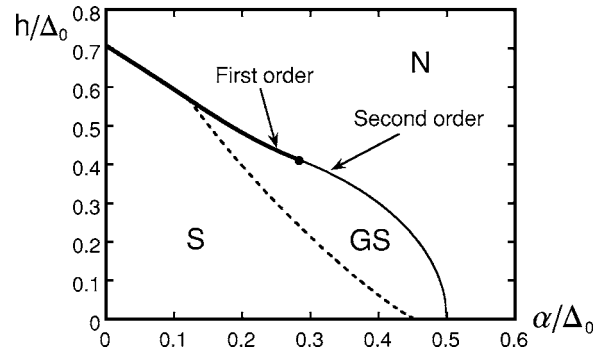


FIG. 18. Phase diagram of a superconducting grain at $T=0$ in coordinates of the Zeeman energy h vs pair-breaking parameter α . The dashed line separates the gapless (GS) and gapped (S) superconducting states. First- and second-order phase transition lines are shown by thick and thin solid lines, respectively. From Beloborodov *et al.*, 2006.

$$\ln(T_c/T_{c0}) = \psi(1/2) - \text{Re}\{\psi[1/2 + (\alpha + ih)/2\pi T_c]\}. \quad (3.45)$$

We note that Eq. (3.45) is valid as long as the phase transition is of the second order. However, in the limit where the Zeeman effect dominates the orbital one (Clogston, 1960) the phase transition is known to be of first order. Analysis of the first-order phase transition at finite temperatures is rather involved and here we present only the corresponding phase diagram at zero temperature (Fig. 18) that illustrates how the second-order phase transition turns into a first-order one (Beloborodov *et al.*, 2006). To simplify the discussion we assume that the Clogston limit is not reached and Eq. (3.45) describing the second-order phase transition is applicable.

At zero temperature, Eq. (3.45) reduces to (Beloborodov *et al.*, 2000)

$$\alpha^2 + h^2 = \Delta_0^2/4, \quad (3.46)$$

such that Eq. (3.11) for the critical field H_c^{gr} in the presence of the Zeeman coupling can simply be generalized via the substitution

$$\Delta_0 \rightarrow \tilde{\Delta}_0 \equiv \sqrt{\Delta_0^2 - (2h)^2}. \quad (3.47)$$

2. Critical magnetic field of a granular sample

According to Sec. III.C.1 the effect of the magnetic field on a single grain reduces to the renormalization of the Matsubara frequency

$$\omega \rightarrow \tilde{\omega} = \omega + ih + \alpha. \quad (3.48)$$

By considering the critical temperature of the whole granular sample, one can take into account the local single-grain effects via the frequency renormalization (3.48). The critical temperature of the granular array can be found again from the linearized Usadel equation which can be written for the granular sample in the Fourier representation as

$$[|\omega| + (g\delta/2)\lambda(\mathbf{q} - 2e\mathbf{A}/c)]f(\mathbf{q}) = \Delta(\mathbf{q}), \quad (3.49)$$

where $\lambda(\mathbf{q} - 2e\mathbf{A}/c) = 2\sum_{\mathbf{a}}\{1 - \cos[(\mathbf{q} - 2e\mathbf{A}/c)\mathbf{a}]\}$ and \mathbf{q} is the quasimomentum of the periodic lattice. In the regime under consideration, Eq. (3.16), the magnetic flux per unit cell of the lattice is always small. This allows us to find the lowest eigenvalue of the operator $\lambda(\mathbf{q} - 2e\mathbf{A}/c)$ as the lowest Landau level of the operator for the corresponding continuous system $a^2(\hat{\mathbf{q}} - 2e\mathbf{A}/c)^2$, which gives $2eH a^2/c$.

Thus evaluation of the orbital effect that originates from flux accumulation on scales involving many grains is very similar to the analogous effect in homogeneously disordered samples, which is a direct consequence of the smallness of the magnetic flux per unit cell. Now one can see that the orbital effect coming from large distances simply gives an additional contribution $g\delta a^2 eH/c$ to the depairing parameter α . Using Eq. (2.3) for the effective diffusive coefficient D_{eff} we obtain the total depairing parameter including both single-grain and bulk orbital effects of the magnetic field

$$\alpha = R^2 D(eH/c)^2/5 + D_{\text{eff}} eH/c. \quad (3.50)$$

We note that, although Eq. (3.50) has been obtained within the periodic cubic lattice array model, it is in fact more general. Indeed, the first term on the right-hand side of Eq. (3.50) represents the single-grain effect and is sensitive to the grain size only. The second term, expressed in terms of the effective diffusive coefficient D_{eff} , is not sensitive to the structure of the array at all.

Comparing the two contributions to the depairing parameter α in Eq. (3.50), we obtain the value H^* characterizing the crossover from the single-grain to the bulk orbital effects,

$$H^* = \frac{5\phi_0 D_{\text{eff}}}{\pi R^2 D}. \quad (3.51)$$

Equations (3.50) and (3.45) determine the superconducting transition line in the T vs H plane.

In the limit of zero temperature $T \rightarrow 0$, Eq. (3.45) reduces to Eq. (3.46), which allows us to find a simple expression for the critical field at $T=0$ resolving Eq. (3.50) with respect to H :

$$H_c(T=0) = \frac{5\phi_0}{2D\pi R^2} \left(\sqrt{D_{\text{eff}}^2 + \frac{2\tilde{\Delta}_0 R^2 D}{5}} - D_{\text{eff}} \right), \quad (3.52)$$

where $\tilde{\Delta}_0$ given by Eq. (3.47) takes into account the Zeeman effect.

D. Suppression of the superconducting critical temperature

The BCS theory gives a very accurate description of superconductors in bulk well-conducting metals. However, in strongly disordered or granular metals there can be considerable deviations from this theory. This concerns, in particular, the superconducting transition temperature.

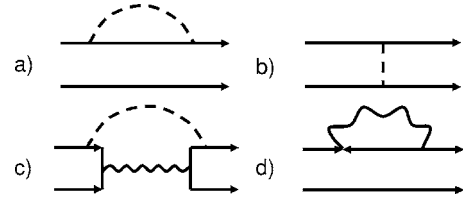


FIG. 19. Schematic representation of two mechanisms for the suppression of superconductivity. Diagrams (a)–(c) describe the correction to the superconducting transition temperature due to Coulomb repulsion. Diagram (d) describes the correction to the transition temperature due to superconducting fluctuations. All diagrams are shown before averaging over the impurities. The solid lines denote the electron propagators, the dashed lines describe screened Coulomb interaction, and the wavy lines describe the propagator of superconducting fluctuations. From Beloborodov, Efetov, *et al.*, 2005.

In this section we consider suppression of superconductivity in granular metals at large tunneling conductances between grains, $g \gg 1$. In this limit, all properties of the system should be close to those following from BCS theory. The mean-field transition temperature T_c of the granular superconductors has to be close to that of the corresponding disordered bulk superconductor. Any difference between the granular and disordered bulk superconductors may appear only in corrections to the BCS theory. These corrections will be discussed here.

The main mechanisms for the suppression of superconductivity are the Coulomb repulsion and fluctuations of the superconducting order parameter (see Fig. 19). For example, disorder significantly shifts the superconducting transition temperature in 2D thin films (Ovchinnikov, 1973; Maekawa and Fukuyama, 1982; Maekawa *et al.*, 1983; Finkelstein, 1987, 1994; Ishida and Ikeda, 1998; Larkin, 1999). The physical reason for the suppression of the critical temperature is that in thin films the interaction amplitude in the superconducting channel decreases due to peculiar disorder-induced interference effects that enhance the effective Coulomb interaction. We refer to this mechanism of superconductivity suppression as the *fermionic* mechanism.

The superconducting transition temperature can also be reduced by fluctuations of the order parameter, the effect being especially strong in low dimensions. The corresponding mechanism of superconductivity suppression is called the *bosonic* mechanism. In particular, the bosonic mechanism can lead to the appearance of an insulating state at zero temperature (Efetov, 1980; Fisher, 1990; Simánek, 1994).

We discuss here the suppression of the superconductivity in terms of perturbation theory. Although this method is restrictive and cannot be used to study the superconductor-insulator transition, it is useful in the sense that both relevant mechanisms of reducing the critical temperature can be included systematically within the same framework. The usefulness of perturbative calculations has been demonstrated when studying the properties of normal granular metals in Sec. II.D where the energy scale Γ , Eq. (2.2), was introduced. In

view of these findings one may expect that the correction to the superconducting transition temperature can be different depending on whether the temperature is larger or smaller than the energy scale Γ .

We start with the following Hamiltonian \hat{H}_s describing the granular system:

$$\hat{H}_s = \hat{H} + \hat{H}_{e\text{-ph}}, \quad (3.53)$$

where the Hamiltonian \hat{H} for the normal granular metals is given by Eq. (2.15) and $\hat{H}_{e\text{-ph}}$ is an additional electron-phonon interaction on each grain,

$$\hat{H}_{e\text{-ph}} = -\lambda \sum_{i,k,k'} a_{i,k}^\dagger a_{i,-k}^\dagger a_{i,-k'} a_{i,k'}, \quad (3.54)$$

where i labels the grains, $k \equiv (\mathbf{k}, \uparrow)$, $-k \equiv (-\mathbf{k}, \downarrow)$; $\lambda > 0$ is the interaction constant; $a_{i,k}^\dagger$ ($a_{i,k}$) are the creation (annihilation) operators for an electron in the state k of the i th grain.

The superconducting transition temperature can be found by considering the anomalous Green's function F in the presence of an infinitesimal source of pairs Δ (Ovchinnikov, 1973). Neglecting fluctuations and interaction effects, the anomalous Green's function F is given by (Abrikosov *et al.*, 1965)

$$F(\xi, \omega) = \Delta / (\omega^2 + \xi^2), \quad (3.55)$$

where $\xi = \mathbf{p}^2 / 2m - \mu$, and $\omega = 2\pi T(n + 1/2)$ is the fermionic Matsubara frequency. The suppression of the transition temperature T_c is determined by the correction to the function $F(\xi, \omega)$,

$$\frac{\Delta T_c}{T_c} = \frac{T}{\Delta} \int d\xi \sum_{\omega} \delta F(\xi, \omega), \quad (3.56)$$

where $\delta F(\xi, \omega)$ represents the leading-order corrections to the anomalous Green's function $F(\xi, \omega)$ due to fluctuations of the order parameter and Coulomb interaction. All diagrams (before impurity averaging) contributing to the suppression of the transition temperature in Eq. (3.56) are shown in Fig. 19. One can see that there exist two qualitatively different classes of diagrams. First, the diagrams (a)–(c) describe corrections to the transition temperature due to Coulomb repulsion and correspond to the so-called fermionic mechanism of the suppression of superconductivity. The second type, diagram (d), describes a correction to the transition temperature due to the superconducting fluctuations and represents the bosonic mechanism. Details of the calculations are presented by Beloborodov, Efetov, *et al.* (2005). They are rather straightforward and therefore we discuss below only the final results for the suppression of T_c .

It is convenient to separate corrections due to the bosonic and fermionic mechanisms and write the result for the suppression ΔT_c of the superconductor transition temperature as

$$\frac{\Delta T_c}{T_c} = \left(\frac{\Delta T_c}{T_c} \right)_b + \left(\frac{\Delta T_c}{T_c} \right)_f, \quad (3.57)$$

where the two terms on the right-hand side correspond to the bosonic and fermionic mechanisms, respectively. The critical temperature T_c in Eq. (3.57) is the BCS critical temperature.

It has been shown by Beloborodov, Efetov, *et al.* (2005) that at high transition temperatures $T_c > \Gamma$ the fermionic correction to the superconducting transition temperature does not depend on the dimensionality of the sample and takes the form

$$\left(\frac{\Delta T_c}{T_c} \right)_f = -c_1 \frac{\delta}{T_c}, \quad d = 2, 3, \quad (3.58)$$

where $c_1 = 7\zeta(3)/2\pi^2 - (\ln 2)/4$ is a numerical coefficient and d is the dimensionality of the array of the grains.

In contrast, in the low-temperature regime $T_c < \Gamma$ the fermionic mechanism correction to the superconducting transition temperature depends on the dimensionality of the sample and is given by (Beloborodov, Efetov, *et al.*, 2005)

$$\left(\frac{\Delta T_c}{T_c} \right)_f = - \begin{cases} \frac{A}{2\pi g} \ln^2 \frac{\Gamma}{T_c}, & d = 3 \\ \frac{1}{24\pi^2 g} \ln^3 \frac{\Gamma}{T_c}, & d = 2, \end{cases} \quad (3.59)$$

where $A = a^3 \int d^3 q / (2\pi)^3 \lambda_{\mathbf{q}}^{-1} \approx 0.253$ is the dimensionless constant, a is the size of the grain, and $\lambda_{\mathbf{q}}$ is given by Eq. (2.30). Note that in the low-temperature regime $T_c < \Gamma$ the correction to the critical temperature in two dimensions agrees with the one obtained for homogeneously disordered superconducting films provided the substitution $\Gamma \rightarrow \tau^{-1}$ is made.

The correction to the transition temperature due to the bosonic mechanism in Eq. (3.57) is qualitatively different from the fermionic one. It remains the same in both regimes $T < \Gamma$ and $T > \Gamma$ and is given by (Beloborodov, Efetov, *et al.*, 2005)

$$\left(\frac{\Delta T_c}{T_c} \right)_b = - \begin{cases} \frac{14A\zeta(3)}{\pi^3} \frac{1}{g}, & d = 3 \\ \frac{7\zeta(3)}{2\pi^4 g} \ln \left(\frac{g^2 \delta}{T_c} \right), & d = 2, \end{cases} \quad (3.60)$$

where $\zeta(x)$ is the zeta function and the dimensionless constant A is given below Eq. (3.59).

Note that the energy scale Γ does not appear in this bosonic part of the suppression of superconducting temperature in Eq. (3.60). This stems from the fact that the characteristic length scale for the bosonic mechanism is the coherence length ξ_{eff} that is assumed to be much larger than the size of the single grain. The result for the two-dimensional case in Eq. (3.60) is written with logarithmic accuracy assuming that $\ln(g^2 \delta / T_c) \gg 1$.

We see from Eqs. (3.59) and (3.60) that suppression of the superconducting transition temperature becomes stronger with diminishing coupling g between the grains.

Of course, the calculations may be justified only when the correction to the transition temperature is much smaller than the temperature itself.

The above expression for the correction to the transition temperature due to the bosonic mechanism was obtained in the lowest order in the propagator of superconducting fluctuations and holds therefore as long as the value for the critical temperature shift given by Eq. (3.60) is larger than the Ginzburg region $(\Delta T)_G$,

$$(\Delta T)_G \sim \begin{cases} \frac{1}{g^2} \frac{T_c^2}{g\delta}, & d=3 \\ \frac{T_c}{g}, & d=2. \end{cases} \quad (3.61)$$

Comparing the correction to the transition temperature T_c given by Eq. (3.60) with the width of the Ginzburg region Eq. (3.61), one concludes that for 3D granular metals the perturbative result (3.60) holds if

$$T_c \ll g^2 \delta. \quad (3.62)$$

In two dimensions the correction to the transition temperature in Eq. (3.60) is only logarithmically larger than $(\Delta T)_G$ in Eq. (3.61). The two-dimensional result (3.60) holds with the logarithmic accuracy in the same temperature interval (3.62) as for the three-dimensional samples.

Note that inside the Ginzburg region higher-order fluctuation corrections become important. Moreover, the nonperturbative contributions that appear, in particular, due to superconducting vortices should be taken into account as well. These effects destroy the superconducting long-range order and lead to the Berezinskii-Kosterlitz-Thouless transition in 2D systems. The suppression of the transition temperature in the limit $T > g^2 \delta$ in three dimensions should be studied considering strong critical fluctuations within the Ginzburg-Landau free-energy functional.

It follows from Eq. (3.58) that in the limit $T \gg \Gamma$ the fermionic mechanism of suppression of the superconductivity is no longer efficient. This can be seen in another way using the phase approach presented in Sec. II.B.4. After the decoupling of the Coulomb term (2.39) by integration over the auxiliary field \bar{V} and gauge transformation (2.42) the phase enters the tunneling term Eq. (2.53) only. However, this term is not important in the limit $T \gg \Gamma$ and we conclude that the long-range part of the Coulomb interaction leading to charging of the grains is completely removed in this limit. Therefore the effect of the Coulomb interaction on the superconducting transition temperature must be small and this is seen from Eq. (3.58). This conclusion matches well the fact that the upper limit in the logarithms in Eq. (3.59) is Γ and, at temperatures exceeding this energy, the logarithms should disappear.

At lower temperatures $T < \Gamma$ the phase description is not applicable and, as a consequence, we obtain a non-trivial result, Eq. (3.59). This result is of pure quantum origin, and interference effects are important for its deri-

vation (one should consider the contribution of diffusion modes). In the high-temperature limit $T \gg \Gamma$ interference effects are suppressed and this is the reason why the fermionic mechanism of the suppression of superconductivity is no longer efficient.

The results obtained, Eqs. (3.58)–(3.62), suggest an experimental method of extracting information about the morphology of the samples from the T_c data. Indeed, one can study the dependence of the superconducting transition temperature T_c of the granular metals as a function of the tunneling conductance g by comparing several granular samples with different tunneling conductances (different oxidation coating). The experimental curves for the suppression of T_c should have different slopes at high $T_c > \Gamma$ and low $T_c < \Gamma$ critical temperatures due to the fact that the suppression of superconductivity is given by two different mechanisms. Information on the morphology of the sample, i.e., whether the samples are homogeneously disordered or granular, is then obtained from the dependencies of the critical temperatures on the tunneling conductance $T_c(g)$. (We remind the reader that the scale Γ exists in granular samples only.)

Another consequence of Eqs. (3.58)–(3.62) is the following: Since at low critical temperatures $T_c \ll \Gamma$ the suppression of the superconductivity in granular metals is provided by the fermionic mechanism and coincides, upon the substitution $\Gamma \rightarrow \tau^{-1}$, with the proper result for homogeneously disordered samples (Ovchinnikov, 1973) one can generalize the renormalization-group result by Finkelstein (1987) for the T_c suppression. The latter result obtained for homogeneously disordered films can be directly applied to granular superconductors by making the proper substitution for the diffusion coefficient $D = \Gamma a^2$, where a is the size of a single grain.

E. Magnetoresistance of granular superconductors

In this section we discuss the magnetoresistance of a granular superconductor in a strong magnetic field. We start with a discussion of the experiment (Gerber *et al.*, 1997) where the transport properties of a system of Al superconducting grains in a strong magnetic field were studied. The samples were three dimensional and quite homogeneous with a typical grain diameter 120 ± 20 Å. Bulk superconductivity could be destroyed by application of a strong magnetic field leading to the appearance of a finite resistivity. A magnetic field above 17 T was enough to destroy even the superconducting gap within each grain.

The dependence of the resistivity on the magnetic field observed by Gerber *et al.* (1997) was not simple. Although at extremely strong fields the resistivity was almost independent of the field, it increased on decreasing the magnetic field. Only at sufficiently weak magnetic fields did the resistivity start to decrease, and finally the samples displayed superconducting properties. Similar behavior has been reported in a number of pub-

lications (Gantmakher *et al.*, 1996; Parthasarathy *et al.*, 2004).

A negative magnetoresistance due to weak localization effects is not unusual in disordered metals (Altshuler *et al.*, 1980; Lee and Ramakrishnan, 1985). However, the characteristic magnetic field in the experiments (Gerber *et al.*, 1997) was several teslas, such that all weak-localization effects had to be strongly suppressed.

We present an explanation for this unusual behavior based on consideration of superconducting fluctuations. At first glance this idea looks counterintuitive, because naively superconducting fluctuations are expected to increase the conductivity. Nevertheless, it turns out that the magnetoresistance of a good granulated metal ($g \gg 1$) in a strong magnetic field $H > H_c$ and at low temperature $T \ll T_c$ is negative. In our model, the superconducting gap in each granule is assumed to be suppressed by the strong magnetic field. All interesting behavior considered below originates from superconducting fluctuations, which lead to a suppression of the density of states (DOS) and decrease the conductivity.

The theory of superconducting fluctuations near the transition into the superconducting state was developed long ago (Aslamazov and Larkin, 1968; Maki, 1968a, 1968b; Abrahams *et al.*, 1970; Thompson, 1970) [for a review, see Larkin and Varlamov (2005)]. Above the transition temperature T_c , nonequilibrium Cooper pairs are formed and a new channel of charge transfer opens (the Aslamazov-Larkin contribution) (Aslamazov and Larkin, 1968). This correction always gives a positive contribution to the conductivity. Another fluctuation contribution comes from coherent scattering of electrons forming a Cooper pair on impurities (the Maki-Thompson contribution) (Maki, 1968a, 1968b; Thompson, 1970). This correction also results in a positive contribution to conductivity, though, in principle, the sign of it is not prescribed.

Formation of nonequilibrium Cooper pairs results also in a fluctuational gap in the one-electron spectrum (Abrahams *et al.*, 1970) but in conventional (nongranular) superconductors the first two mechanisms are more important near T_c and the conductivity increases when approaching the transition.

The total conductivity for a bulk sample above the transition temperature T_c can be written in the following form:

$$\sigma = \sigma_{\text{Drude}} + \delta\sigma, \quad (3.63)$$

where $\sigma_{\text{Drude}} = (e^2 \tau n) / m$ is the conductivity of a normal metal without electron-electron interaction, τ is the elastic mean free time, and m and n are the effective mass and the density of electrons, respectively. In Eq. (3.63), $\delta\sigma$ is a correction to the conductivity due to Cooper pair fluctuations,

$$\delta\sigma = \delta\sigma_{\text{DOS}} + \delta\sigma_{\text{AL}} + \delta\sigma_{\text{MT}}, \quad (3.64)$$

where $\delta\sigma_{\text{DOS}}$ is the correction to the conductivity due to the reduction of the DOS and $\delta\sigma_{\text{AL}}$ and $\delta\sigma_{\text{MT}}$ stand for the Aslamazov-Larkin (AL) and Maki-Thompson (MT)

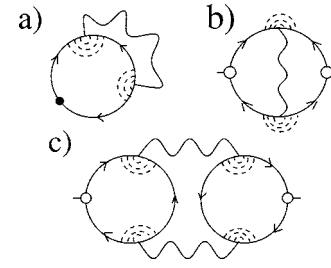


FIG. 20. Corrections to the classical conductivity and density of states (DOS). Diagram (a) describes the correction to the DOS; diagrams (b) and (c) describe corrections to the conductivity due to superconducting fluctuations. The wavy lines denote the propagators of the fluctuations; the dashed lines stand for the impurity scattering. From Beloborodov and Efetov, 1999.

contributions to the conductivity. Close to the critical temperature T_c the AL correction is more important than both the MT and DOS corrections and its contribution can be written as follows (Aslamazov and Larkin, 1968):

$$\frac{\delta\sigma_{\text{AL}}}{\sigma_{\text{Drude}}} = \gamma \left(\frac{T_c}{T - T_c} \right)^\beta, \quad (3.65)$$

where γ is a small dimensionless positive parameter, $\gamma \ll 1$, depending on dimensionality, and $\beta = 1/2$ for the three-dimensional case, 1 for two dimensions, and $3/2$ for quasi-one-dimensions. Equation (3.65) is valid for $\delta\sigma_{\text{AL}} / \sigma_{\text{Drude}} \ll 1$.

For quite a long time superconducting fluctuations have been studied near the critical temperature T_c in a zero or a weak magnetic field. Only recently was the limit of very low temperature $T \ll T_c$ and a strong magnetic field $H > H_c$ considered (Beloborodov and Efetov, 1999; Beloborodov *et al.*, 2000) and some qualitatively new effects were predicted. In this section we concentrate on this limit.

As in conventional bulk superconductors, we can write corrections to the classical conductivity σ_0 , Eq. (2.1), as a sum of corrections to the DOS, Aslamazov-Larkin, σ_{AL} , and Maki-Thompson, σ_{MT} , corrections. Diagrams describing these contributions are represented in Fig. 20. They have the conventional form but the wavy lines standing for superconducting fluctuations should be written taking into account the granular structure. It turns out that in the regime $T \ll T_c$ and $H > H_c$ the DOS corrections play a very important role: This correction reaches its maximum at $H \rightarrow H_c$, where H_c is the field destroying the superconducting gap in a single grain. At zero temperature and close to the critical field H_c such that $\Gamma / \Delta_0 \gg h$, where $h = (H - H_c) / H_c$, the maximum value of $\delta\sigma_{\text{DOS}}$ for 3D granular superconductors is (Beloborodov *et al.*, 2000)

$$\frac{\delta\sigma_{\text{DOS}}}{\sigma_0} = -\frac{1}{3g} \frac{\Gamma}{\Delta_0} \ln\left(\frac{\Delta_0}{\Gamma}\right). \quad (3.66)$$

We see from Eq. (3.66) that the correction to the conductivity $\delta\sigma_{\text{DOS}}$ (i) is negative and its absolute value decreases when the magnetic field increases; (ii) is smaller than σ_0 and becomes comparable with σ_0 when the tunneling conductance $g \sim 1$. However, such values of g mean that we would be in this case not far from the metal-insulator transition. Then we need to take into account all localization effects, which is not done here.

Even in the limit of strong magnetic fields $H \gg H_c$ the correction to σ_0 might still be noticeable (Beloborodov *et al.*, 2000),

$$\frac{\delta\sigma_{\text{DOS}}}{\sigma_0} = -\frac{1}{3g} \frac{\Gamma}{E_0(H)} \ln^{-1}\left(\frac{E_0(H)}{\Delta_0}\right), \quad (3.67)$$

where, for a spherical grain, $E_0(H) = \frac{2}{5} \left(\frac{eHR}{c}\right)^2 D$ with D the diffusion coefficient in a single grain. Equation (3.67) shows that in the region $H \gg H_c$ the correction to the conductivity behaves essentially as $\delta\sigma_{\text{DOS}} \sim H^{-2}$, which is a rather slow decay.

We emphasize that the correction to the conductivity coming from the DOS, Eqs. (3.66) and (3.67), remains finite in the limit $T \rightarrow 0$, thus indicating the existence of virtual Cooper pairs even at $T=0$.

In order to calculate the entire conductivity we investigate the AL and MT contributions [Figs. 20(c) and 20(b)]. Near T_c these contributions are most important, leading to an increase of the conductivity. At low temperatures $T \ll T_c$ and strong magnetic fields $H > H_c$ the situation is completely different. It turns out that both the AL and MT contributions vanish in the limit $T \rightarrow 0$ at all $H > H_c$ and thus the correction to the conductivity comes from the DOS only.

So, at low temperatures, estimating the total correction to the classical conductivity σ_0 , Eq. (2.42), one may use the formulas (3.66) and (3.67). We present the final result for AL correction shown in Fig. 20(c) at $T \ll T_c$ and $h \ll \Gamma/\Delta_0$ for 3D granular superconductors (Beloborodov *et al.*, 2000),

$$\frac{\delta\sigma_{\text{AL}}}{\sigma_0} \sim \frac{1}{g} \frac{T^2}{\Delta_0^{3/2} \Gamma^{1/2}} \left(\frac{H_c}{H - H_c}\right)^{3/2}. \quad (3.68)$$

It follows from Eq. (3.68) that at low temperatures the AL correction to the conductivity is proportional to the square of the temperature, $\delta\sigma_{\text{AL}} \sim T^2$, and vanishes in the limit $T \rightarrow 0$.

For MT corrections shown in Fig. 20(b) one obtains in the limit $T \ll T_c$ and $h \ll \Gamma/\Delta_0$ for 3D granular superconductors (Beloborodov *et al.*, 2000)

$$\frac{\sigma_{\text{MT}}}{\sigma_0} \sim \frac{1}{g} \frac{\Gamma}{\Delta_0 \Delta_0^2}. \quad (3.69)$$

The temperature and magnetic-field dependence of $\delta\sigma_{\text{AL}}$ and $\delta\sigma_{\text{MT}}$ is rather complicated but definitely positive. The competition between these corrections and σ_{DOS} determines the sign of the magnetoresistance. One

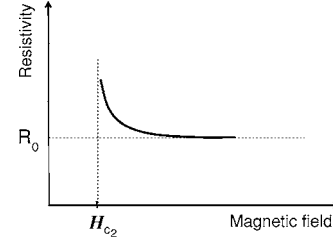


FIG. 21. Schematic picture for resistivity behavior of granular superconductors as a function of the magnetic field at low temperatures $T \ll T_c$. The resistivity at low temperatures grows monotonically on decreasing the magnetic field. It reaches asymptotically the value of the classical resistivity R_0 only at extremely strong magnetic fields. The transition into the superconducting state occurs at a field H_{c2} . From Beloborodov *et al.*, 2000.

can see from Eqs. (3.68) and (3.69) that both the AL and MT contributions are proportional at low temperatures to T^2 . Therefore the σ_{DOS} in this limit is larger and the magnetoresistance is negative for all H_c . In contrast, at $T \sim T_c$ and close to H_c , the AL and MT corrections can become larger than σ_{DOS} , resulting in a positive magnetoresistance in this region. Far from H_c the magnetoresistance is negative again.

In the above considerations we did not take into account the interaction between the magnetic field and the spins of electrons. This approximation is justified if the size of the grains is not very small. Then, the orbital magnetic critical field H_c^{or} destroying the superconducting gap is smaller than the paramagnetic limit $\mu H_c^Z \approx \Delta_0$ and the orbital mechanism dominates the magnetic-field effect on superconductivity. However, the Zeeman splitting leading to the destruction of superconducting pairs can become important if one further decreases the size of the grains. The results for conductivity corrections including the Zeeman splitting can be found in Beloborodov *et al.* (2000).

The results presented in this section show that, even if the superconducting gap in each granule is destroyed by the magnetic field, virtual Cooper pairs can persist up to extremely strong magnetic fields. However, the contribution of Cooper pairs to transport is proportional at low temperatures to T^2 and vanishes in the limit $T \rightarrow 0$. In contrast, they reduce the one-particle density of states in the grains even at $T=0$, thus diminishing the macroscopic conductivity. The conductivity can reach its classical value only in extremely strong magnetic fields when all virtual Cooper pairs no longer exist. This leads to the negative magnetoresistance.

Qualitatively, the results for the resistivity behavior of granular superconductors at low temperatures $T \ll T_c$ and strong magnetic fields $H > H_c$ are summarized in Fig. 21. The resistivity R at low temperatures grows monotonically on decreasing the magnetic field, and it reaches asymptotically the value of the classical resistivity R_0 only at extremely strong magnetic fields. The transition into the superconducting state occurs at a field H_{c2} that may be lower than H_c .

IV. DISCUSSION OF THE RESULTS

A. Quantitative comparison with experiments

The models of the normal and superconducting granular electronic systems considered in this review are relevant to many experiments on different materials and we have presented quite a few of them. This is not accidental because we selected for the presentation such theoretical results as could be relevant for existing experiments.

On the one hand, the review is not as complete as it could be because we did not include many theoretical works where such physical quantities as the tunneling density of states (Beloborodov, Lopatin, Schwiete, *et al.*, 2004), thermal conductivity (Beloborodov, Lopatin, Hekking, *et al.*, 2005; Biagini, Ferone, *et al.*, 2005; Tripathi and Loh, 2006), etc., were considered. The only reason for this omission is that at present we are not aware of clear measurements of these quantities in granular materials.

On the other hand, this gave us the opportunity to concentrate on experimentally well-studied phenomena. Some of them, like the logarithmic temperature dependence of the conductivity of well-conducting granular metals or the hoppinglike temperature dependence of very regular insulating granular systems, remained unexplained for several decades. As we have seen, these dependencies and many interesting features of the experiments can be explained using rather simple models of metallic grains. The simplicity of the models and the small number of parameters characterizing the system suggest that there should be not only a good qualitative but also a quantitative agreement between the theory and experiment.

We now present a quantitative comparison of several theoretical results with experimental data. Of course, we cannot discuss here all existing measurements and therefore only three different experiments are considered.

1. Logarithmic temperature dependence of the conductivity

In this section we compare the logarithmic temperature dependence of the conductivity, Eq. (2.72), with experiments. This formula should be applicable at not very low temperature which simplifies the experimental check. Specially prepared granular metals like those considered by Abeles *et al.* (1975), Simon *et al.* (1987), and Gerber *et al.* (1997) should be the first objects in applying the theory developed.

As an example, we compare Eq. (2.72) with the experimental results of Gerber *et al.* (1997) on films made of Al grains embedded in an amorphous Ge matrix. At low temperatures, superconductivity in the Al grains was destroyed by a strong magnetic field. Depending on the coupling between grains (extracted from the conductivity at room temperatures) the samples of the experiment (Gerber *et al.*, 1997) were macroscopically either in an insulating state with the temperature dependence of the resistivity $R \sim \exp(a/T^{1/2})$ or in a “metallic” one.

However, the resistivity of the metallic state depended on temperature and the authors suggested a power law $R \sim T^\alpha$, with an exponent $\alpha \ll 1$. As the exponent α for the metallic sample was small we can argue that Eq. (2.72) should not be worse for fitting the experimental data. Then we estimate the exponent α without using fitting parameters.

The sample of the experiment (Gerber *et al.*, 1997) had a room-temperature resistivity of $R_0 = 7.3 \times 10^3 \Omega \text{ cm}$. The diameter of the grains was $120 \pm 20 \text{ \AA}$, which allows us, using the value $\hbar/e^2 = 4.1 \times 10^{-3} \Omega$ and the relation between the conductivity and conductance for 3D samples $\sigma = 2e^2g/\hbar a$, to estimate the dimensionless tunneling conductance as $g = 0.34$. Taking $d = 3$ and ($z = 6$) in Eq. (2.72) we obtain $\alpha = 0.15$, which agrees fairly well with the experimental value $\alpha = 0.117$. Keeping in mind that the theoretical dependence (2.72) was obtained for a periodic cubic array while in realistic samples the coordination number can be only approximately close to 6, one can hardly hope for a better agreement.

A logarithmic dependence of the resistivity on temperature has been observed in other granular materials. Simon *et al.* (1987) studied a granular Cermet consisting of Nb grains in a boron nitride insulating matrix. Again, at small coupling between grains the temperature dependence of the resistivity $\exp(a/T^{1/2})$ was observed in a very broad interval of temperatures. The resistivity of samples with a strong coupling between grains was very well described by the law

$$R = R_0 \ln(T_0/T), \quad (4.1)$$

which is close to Eq. (2.72) provided the temperature interval is not very large, such that the variation of the resistivity is small. However, Eq. (4.1) gave a good description for the temperature dependence of the resistivity in a very broad region and the change of resistivity was not small. The reason for the applicability of Eq. (4.1) in so broad an interval of temperatures is not clear because according to the results of the renormalization-group analysis of Sec. II.C not the resistivity but the conductivity should obey Eq. (4.1). A more careful experimental study might clarify this question.

The unusual logarithmic behavior of the type Eq. (4.1) has been observed not only in standard granular systems but also in high- T_c cuprates at very strong magnetic fields. The first observation of this dependence was made on underdoped $\text{La}_{2-x}\text{Sr}_x\text{CuO}_4$ (LSCO) crystals (Ando *et al.*, 1995). The superconductivity in this experiment was suppressed with pulsed magnetic fields of 61 T. It was found that both the in-plane resistivity ρ_{ab} and out-of-plane resistivity ρ_c diverged logarithmically with decreasing temperature. This means that a 3D effect was observed in a very strong magnetic field, and traditional explanations for a logarithmic behavior, like weak localization or the Kondo effect, could not clarify the situation.

In a subsequent publication (Boebinger *et al.*, 1996) a metal-insulator crossover was observed in the same ma-

terial at a Sr concentration near optimum doping ($x \approx 0.16$). In underdoped samples both ρ_{ab} and ρ_c showed no evidence of saturation at low temperatures and diverged as the logarithm of the temperature. The authors called this state an “insulator” in contrast to the state at high doping where the resistivity did not have a pronounced dependence on the temperature. It was conjectured by Boebinger *et al.* (1996) that the logarithmic behavior they observed might be related to that seen in the experiment (Simon *et al.*, 1987) on granular Nb. This would demand a phase segregation throughout the underdoped regime of LSCO.

We hope that our results for the model of granular materials may be applicable to the experiments on $\text{La}_{2-x}\text{Sr}_x\text{CuO}_4$ crystals (Ando *et al.*, 1995; Boebinger *et al.*, 1996), which would mean that underdoped crystals have a granular structure and the logarithmic behavior is due to the Coulomb interaction. The transition to the metallic state noted by Ando *et al.* (1995) and Boebinger *et al.* (1996) would mean that at higher doping the granularity disappears. A quantitative comparison of Eq. (2.72) with the data of Ando *et al.* (1995) and Boebinger *et al.* (1996) was made by Beloborodov *et al.* (2003) and good agreement was found.

What is interesting is that a microscopic granularity was directly experimentally observed in the superconducting state of $\text{Bi}_2\text{Sr}_2\text{CaCu}_2\text{O}_{8+\delta}$ using a scanning tunneling microscope (STM) probe (Lang *et al.*, 2002). As this cuprate is rather similar in its structure to those studied by Ando *et al.* (1995) and Boebinger *et al.* (1996) the assumption that the materials studied there were granular does not look groundless.

Logarithmic dependence of the resistivity on temperature has also been observed in many other experiments. For example, Gerber (1990) observed this dependence in granular Pb films. It was also observed in phase compounds of $\text{Nd}_{2-x}\text{Ce}_x\text{CuO}_{4-y}$ (Radhakrishnan *et al.*, 1990).

2. Hopping conductivity

As mentioned in the previous section, logarithmic temperature dependence is usually seen in samples with a good coupling between grains. If the coupling is weak, one observes usually the Efros-Shklovskii law, Eq. (2.14).

According to the theory developed in Sec. II.G the characteristic temperature T_0 entering Eq. (2.14) is determined by Eqs. (2.111) and (2.116) for elastic and inelastic co-tunneling, respectively.

Now we compare our results for the VRH conductivity of granular metals obtained in Sec. II.G with the most recent experimental data. Tran *et al.* (2005) studied the zero-bias conductivity for bilayers, trilayers, tetralayers, and thick films of Au nanoparticles with particle diameters around 5.5 nm and dispersion less than 5%.

Figure 6 demonstrates that the zero-bias conductivity follows $\sigma(T) \sim \exp[-(T_0/T)^{1/2}]$ over the range 30–90 K for multilayers and 30–150 K for thick films. The fits indicated by the lines give $T_0 = (4.00 \pm 0.02) \times 10^3$ and

$(3.00 \pm 0.01) \times 10^3$ K for the multilayers and thick films, respectively.

At temperatures slightly exceeding 100 K, the conductivity for the multilayers starts deviating from the low-temperature behavior (dashed lines) and crosses over to Arrhenius behavior $\sigma(T) \sim \exp[-U/k_B T]$ (Fig. 6, inset) with the activation energy $U/k_B \approx 320 \pm 8$ K.

Associating this high-temperature behavior with nearest-neighbor tunneling between particles we can use $U \approx 0.2E_c$, in analogy with the monolayers (Parthasarathy *et al.*, 2004). This gives us an estimate of $E_c \approx 1600$ K, where $E_c = e^2/\tilde{\kappa}a$ is the Coulomb charging energy of an individual grain, expressed in terms of the grain radius a , the electron charge e , and the dielectric constant of the surrounding medium $\tilde{\kappa}$. The charging energy $E_c \approx 1600$ K for this system leads to $\tilde{\kappa} \approx 4$.

The energy scale T_0 is related to the localization length ξ by Eqs. (2.111) and (2.116). Using the above values for $\tilde{\kappa}$ and T_0 , we find $3 < \xi < 4$ nm for both multilayers and thick films, which corresponds to localization within one grain. This is an important check because larger values would imply strongly coupled clusters of grains.

The typical hopping distance $r^*(T)$ is given by Eq. (2.122). The number of grains N^* involved in a typical hop is $N^* = r^*/d_0$, with a center-to-center distance $d_0 \approx 8$ nm between neighboring grains. At $T = 10$ K this leads to $N^* = 4$ for multilayers and $N^* = 4-5$ for thick films.

As the temperature increases, N^* decreases down to $N^* \sim 1$ and this is the point of the crossover to a standard activation transport, Eq. (2.13). For the multilayers, this happens at $T \approx 90-95$ K but for the thick films only above $T \approx 130$ K. Both estimates are in excellent agreement with the data in Fig. 6.

3. Negative magnetoresistance

We compare the theoretical predictions for the negative magnetoresistance presented in Sec. III.E with the available experimental results of Gerber *et al.* (1997). In that work three samples were studied. We concentrate our attention on sample 2, Fig. 4, of Gerber *et al.* (1997) which has a metallic conductivity behavior above the critical temperature.

We analyze the case of low temperatures $T \ll T_c$ and magnetic fields $H > H_c$, where $T_c \approx 1.6$ K is the critical temperature for Al grains studied in the experiment and H_c is the critical magnetic field that suppresses the superconductivity in a single grain; $E_0(H_c) = \Delta_0$, where $E_0(H)$ was defined below Eq. (3.67). At temperatures $T \approx 0.3$ K and magnetic fields $H \approx 4$ T this sample shows a large negative magnetoresistance. The resistivity has a maximum at $H = 2.5$ T and the value of this peak is more than twice as large as the resistivity in the normal state (that is, at $H \gg H_c$, when all superconducting fluctuations are completely suppressed). A negative magnetoresistance due to weak localization (WL) is typical for disordered metals and, in order to describe the experi-

mental data, its value should be estimated along with the effects of superconducting fluctuations discussed in the previous section.

The total conductivity of the granular metal under consideration including effects of WL and superconducting fluctuations can be written in the form

$$\sigma = \sigma_0 + \delta\sigma_{\text{DOS}} + \delta\sigma_{\text{AL}} + \delta\sigma_{\text{MT}} + \delta\sigma_{\text{WL}}. \quad (4.2)$$

At low temperatures $T \ll T_c$ the contribution $\delta\sigma_{\text{DOS}}$ originating from the reduction of the DOS due to the formation of virtual Cooper pairs is larger than the contributions $\delta\sigma_{\text{AL}}$ and $\delta\sigma_{\text{MT}}$ since the latter vanish in the limit $T \rightarrow 0$. We concentrate on estimating the contributions $\delta\sigma_{\text{DOS}}$ and $\delta\sigma_{\text{WL}}$.

It is not difficult to show that in the case under consideration the weak-localization corrections originating from the contribution of Cooperons are strongly suppressed by the magnetic field. Using approximations developed by Beloborodov and Efetov (1999) one can obtain the following expression for a 3D cubic lattice of metallic grains at tunneling conductances $g \ll E_0(H)/\delta$:

$$\frac{\delta\sigma_{\text{WL}}}{\sigma_0} \sim -\frac{1}{g} \left(\frac{\Gamma}{E_0(H)} \right)^2. \quad (4.3)$$

Equation (4.3) shows that the weak-localization correction in the strong magnetic fields $H > H_c$ considered here is always small. Comparing Eq. (4.3) with Eq. (3.66) for the DOS correction one can see that in the limit $g \ll \Delta_0/\delta$ the contribution from the weak-localization correction can be neglected.

Now, we estimate the corrections $\delta\sigma_{\text{DOS}}$ and $\delta\sigma_{\text{WL}}$ using the parameters of the experiment (Gerber *et al.*, 1997). For the typical diameter $120 \pm 20 \text{ \AA}$ of Al grains studied by Gerber *et al.* (1997), the mean level spacing δ is approximately $\delta \approx 1 \text{ K}$. Using the critical temperature $T_c \approx 1.6 \text{ K}$ for Al we obtain for the BCS gap in a single grain the following result: $\Delta_0 \approx 1.8T_c \approx 3 \text{ K}$. Substituting the extracted values of the parameters into Eq. (3.66) we estimate the maximal increase of the resistivity. As a result, we obtain $(\delta\rho/\rho_0)_{\text{max}} \approx 0.4$, which is somewhat smaller than but not far from the value $(\delta\rho/\rho)_{\text{expt}} \approx 1$ observed experimentally.

Although Eq. (3.66) gives smaller values of $(\delta\rho/\rho_0)_{\text{max}}$ than the experimental ones, the discrepancy cannot be attributed to weak-localization effects. Using the experimental values of the conductance g , mean level spacing δ , and superconducting gap Δ_0 we find from Eq. (4.3) that $\delta\sigma_{\text{WL}}$ is ten times smaller than $\delta\sigma_{\text{DOS}}$. The value of the correction $\delta\sigma_{\text{WL}}/\sigma_0$, Eq. (4.3), near H_c equals 2.8×10^{-2} .

At the same time, we should not take this disagreement too seriously because all results were obtained under the assumption of a large conductance $g \gg 1$, while experimentally this parameter is not large. As the experimental value of $\delta\sigma/\sigma_0$ is not small, we come again to the conclusion that the parameters of the system are such that Eq. (3.66) is no longer applicable and one should develop a more sophisticated theory to describe this region more accurately.

B. Outlook

We discussed in this review a rather simple general model that allows us to understand many properties of granular materials. This is a model of disordered or chaotic grains coupled to each other by electron tunneling. A very important ingredient of the model is the long-range part of the Coulomb interaction, taken in the form of the charging energy of grains. For the description of the superconducting grains we included the superconducting BCS gap in the consideration.

We considered the limit of temperatures T exceeding the mean level spacing δ in the grains and neglected quantum size effects. For the superconducting grains we assumed that the superconducting gap Δ was larger than δ . These regimes are most easily achieved experimentally and this was the main reason for choosing them.

In spite of its simplicity, a variety of interesting phenomena has been derived from the model involved. Such phenomena as the logarithmic dependence of the conductivity on temperature or the Efros-Shklovskii law for a regular system of grains with an almost perfect shape remained unexplained for several decades and have been clarified within the model only recently. Another interesting effect concerns the negative magnetoresistance due to superconducting fluctuations. For these effects we have obtained not only a qualitative but a good quantitative description.

Granularity is a rather general phenomenon and it may be encountered rather unexpectedly. Thin metallic films are often rather granular than homogeneously disordered (Gantmakher *et al.*, 1996; Goldman and Marković, 1998). Another unexpected conclusion about the granularity of some underdoped high- T_c cuprates has been reached at using the STM technique (Lang *et al.*, 2002).

Studying granular systems may help us to understand some properties of homogeneously disordered metals and superconductors. As all scales involved in the model we studied are much larger than the electron wavelength, this might in some cases simplify explicit calculations, in particular, for study of the regime of $g \sim 1$. We presented arguments that a metal-insulator transition is possible at least in three dimensions. A superconductor-insulator transition is also possible. Studying these transitions is the most challenging extension of the present study, but this may be simpler than investigation of homogeneous strongly disordered systems with interaction.

From the experimental side, an evident extension of the work presented here is fabrication grains made of ferromagnets and studying properties of such systems. One can couple these grains directly or put them into normal metals or superconductors. One can make superconducting grains and embed them in normal metals or not very strong ferromagnets, etc. All these systems promise very unusual properties.

One example of unexpected behavior in a system of ferromagnetic grains embedded in a superconductor is the induction of a magnetic moment in the superconductor over large distances of the order of the size of

Cooper pairs. The direction of this magnetic moment is opposite to that of the ferromagnet and one comes to the phenomenon of “spin screening” (Bergeret *et al.*, 2004, 2005). Different directions of the magnetic moments of the grains may lead to the phenomenon of “odd-triplet” superconductivity (Bergeret *et al.*, 2001, 2005).

The list of new theoretical and experimental possibilities that are anticipated in granular systems can be continued. Taking into account the growing number of existing and potential industrial applications of granular materials, we are confident that all this is only the beginning of an exciting development.

ACKNOWLEDGMENTS

The authors thank Igor Aleiner, Anton Andreev, Mikhail Feigel'man, Alexander Finkel'stein, Andreas Glatz, Frank Hekking, Alexei Koshelev, and Peter Wölfle for useful discussions. They are especially grateful to Anatoly Ivanovich Larkin for invaluable discussions. They also thank Philippe Guyot-Sionnest, Heinrich Jaeger, Xiao-Min, and Thu Tran for continued communication of relevant experimental data and stimulating discussions. K.B.E. thanks SFB Transregio 12 of DFG and DIP for financial support. The work of V.M.V. was partially supported by the Alexander von Humboldt Foundation. This work was supported by the U.S. Department of Energy under Contract No. DE-AC0-06CH11357.

APPENDIX A: CALCULATION OF THE TUNNELING PROBABILITY P_{el} IN THE ELASTIC REGIME, EQ. (2.105)

In this appendix we derive the probability of elastic electron tunneling P_{el} between two distant grains through a chain of other grains, Eq. (2.105). This probability can be found comparatively easily only for a model with diagonal Coulomb interaction $E_{ij}^c = E_i \delta_{ij}$. For this reason we consider first such a simplified model and then discuss the generalization of the results obtained for the case of realistic capacitance matrices E_{ij}^c with nonzero off-diagonal elements.

In the model with diagonal Coulomb interaction, the electron-hole excitation energies E_i^\pm that will enter the final results for the hopping probability are given by

$$E_i^\pm = E_c^i - V_i, \quad (A1)$$

where V_i is the local potential that models the presence of the electrostatic disorder. These energies have to be strictly positive and larger than the energies of the initial and final states, otherwise the tunneling path can be cut into two or more independent parts. This allows us to assume that the temperature is less than all E_i^\pm . For this reason we consider the probability of the elastic process in the limit $T \rightarrow 0$.

The tunneling probability P between sites i_0 and i_{N+1} is proportional to the square of the absolute value of the amplitude $A_{i_0, i_{N+1}}$ of the corresponding tunneling process

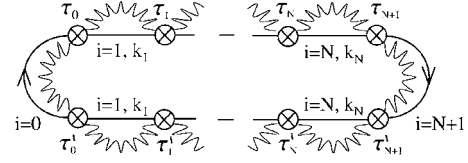


FIG. 22. Diagram representing the tunneling probability via elastic co-tunneling processes. The crossed circles represent the tunneling matrix elements $t_{k,k'}^{ij} e^{i\phi_i(\tau)} e^{-i\phi_j(\tau)}$ where the phase factors appear from the gauge transformation. The wavy lines represent the average of the phase factors $\langle e^{i\phi(\tau_1)} e^{-i\phi(\tau_2)} \rangle$ with respect to the Coulomb action.

$$A_{i_0, i_{N+1}} = \langle 0 | \hat{c}_{i_{N+1}} \hat{S} \hat{c}_{i_0}^\dagger | 0 \rangle. \quad (A2)$$

Here \hat{S} is the evolution operator written in the interaction representation, which takes into account only the tunneling part of the Hamiltonian Eq. (2.15). The conjugate amplitude A^* can be written as the probability of the inverse process of tunneling between the i_{N+1} st and i_0 th grains,

$$A_{i_0, i_{N+1}}^* = A_{i_{N+1}, i_0} = \langle 0 | \hat{c}_{i_0} \hat{S} \hat{c}_{i_{N+1}}^\dagger | 0 \rangle. \quad (A3)$$

The probability of the tunneling process $P = A^* A$ can be found by perturbative expansion of the amplitude in the tunneling matrix elements t_{ij} and further averaging over the realizations of t_{ij} . At the same time the Coulomb interaction cannot be considered perturbatively and should be taken into account exactly. In order to construct a proper perturbative expansion we use the gauge transformation described in Sec. II.B.3, which allows us to transfer the strong Coulomb interaction into the phase factors that accompany the tunneling matrix elements [see Eqs. (2.42) and (2.43)].

Fluctuations of the phases $\varphi_i(\tau)$ are governed by the Coulomb action (2.56) and we obtain the following expression for the correlation function $\Pi(\tau)$, which plays a very important role for a description of the insulating state [cf. Eq. (3.7)]:

$$\begin{aligned} \Pi(\tau_1 - \tau_2) &\equiv \langle \exp[i\phi_i(\tau_1) - i\phi_i(\tau_2)] \rangle \\ &= \exp[-E_c^i |\tau_1 - \tau_2| - V_i(\tau_1 - \tau_2)]. \end{aligned} \quad (A4)$$

Since we are interested in the optimal tunneling path, we consider only trajectories with no return points (no loops). This simplifies the consideration substantially because the phases on different sites are not correlated for the diagonal model under consideration.

The gauge transformation approach allows us to represent the tunneling probability P by the diagram shown in Fig. 22. In order to simplify the derivation we work now using the basis of the exact eigenstates of the single-particle Green's functions which automatically takes into account the presence of the disorder within each grain. An alternative procedure based on the momentum representation leading to the same results would require averaging over disorder in each grain and inclusion of diffusion propagators. The Green's function lines on the initial i_0 and final i_{N+1} grains describe the processes for a

particle located on these sites, while the intermediate Green's function lines represent the tunneling amplitudes A (upper part) and A^* (lower part). The wavy lines denote the correlation function Eq. (A4) that takes into account Coulomb correlations. It may seem surprising that the two wavy lines that belong to the same i th site are considered independently, i.e., that the four-exponent correlation function is factorized in a certain way into two second-order ones. One can check, however, that this factorization is indeed justified as long as the time intervals (τ_{i-1}, τ_i) and (τ'_{i-1}, τ'_i) do not overlap.

This factorization can most easily be understood by presenting the correlation function of N phase exponents as the exponent of the interaction energy of N charges interacting via a linear one-dimensional Coulomb potential. Two nearby charges with opposite signs create an “electric field” only in the region between the two. Thus the energy of the dipoles can be considered independently as long as these dipoles do not overlap geometrically. For a detailed discussion of the Coulomb analogy we refer the reader to the work of [Beloborodov, Lopatin, and Vinokur \(2005\)](#).

It follows from this discussion that all electron Green's functions in Fig. 22 are accompanied by the correlation function $\Pi(\tau)$. For this reason, it is convenient to introduce a modified Green's function $\tilde{G}(\tau)$ in the following way:

$$\tilde{G}(\tau) = G(\tau)\Pi(\tau). \quad (\text{A5})$$

The Green's function $\tilde{G}(\tau)$ has a very simple form in the time representation. For positive arguments the Green's function describes the electron excitation ([Abrikosov *et al.*, 1965](#))

$$\tilde{G}_{\xi_i}(\tau > 0) = [n(\xi_i) - 1]e^{-\xi_i\tau - E_i^+\tau}, \quad (\text{A6})$$

where ξ_i is the bare single-particle electron energy counted with respect to the Fermi energy, Eq. (3.2), and $n(\xi_i)$ is the Fermi distribution function. One can see that the Coulomb part of the electron excitation energy E_i^+ appears naturally in addition to the single-particle energy ξ_i . For negative time arguments the Green's function \tilde{G} describes the hole excitation and is given by

$$\tilde{G}_{\xi_i}(\tau < 0) = n(\xi_i)e^{-\xi_i\tau + E_i^-\tau}, \quad (\text{A7})$$

where $\xi_i < 0$ is the bare electron energy counted with respect to the Fermi energy and E_i^- is the Coulomb part of the hole excitation energy.

Calculating the diagram in Fig. 22, we note that the intermediate time intervals are of the order of the inverse Coulomb energy: $|\tau_{i+1} - \tau_i|, |\tau'_{i+1} - \tau'_i| \sim E_c^{-1}$. In the limit of strong Coulomb interaction ($E_c \gg \delta$) considered here, we integrate over the intermediate times independently. Each intermediate block gives rise to the factor

$$P_k = \frac{\Gamma_k}{2\pi} \int_{-\infty}^{\infty} d\xi \int d\tau_1 d\tau_2 \tilde{G}_{\xi}(\tau_1) \tilde{G}_{\xi}(\tau_2) = \frac{\Gamma_k}{\pi \tilde{E}_k}, \quad (\text{A8})$$

where the energy \tilde{E}_k is the combination of the energies E_k^+ and E_k^- defined by Eq. (2.107) and $\Gamma_k = g_k \delta_k$, with g_k being the conductance between the k th and $(k+1)$ st grains. We note that in the insulating system under consideration the energy scale Γ cannot any longer be interpreted as the escape rate; nevertheless, its introduction is convenient even in this regime.

In order to determine the time dependence of the tunneling process we notice that the time intervals $\tau'_0 - \tau_0$ and $\tau'_{N+1} - \tau_{N+1}$ coincide within the accuracy of the inverse charging energy. In the limit of strong Coulomb interaction one can take both intervals to be equal to the “instanton” time τ that the electron spends out of its original place at $i=0$. Thus the time dependence of the tunneling process is given by

$$e^{-(\varepsilon_{N+1} - \varepsilon_0)\tau}, \quad (\text{A9})$$

where ε_{N+1} and ε_0 are the electron and hole excitation energies on the sites $(N+1)$ st and 0th, respectively. Making an analytical continuation to real times $\tau = it$ and taking the last integral over t we obtain the delta function

$$2\pi\delta(\varepsilon_{N+1} - \varepsilon_0), \quad (\text{A10})$$

which shows that the process is elastic, i.e., electrons can tunnel only to a state with exactly the same energy.

Finally, we obtain for the tunneling probability of the elastic process

$$P_{\text{el}} = w\delta(\varepsilon_{N+1} - \varepsilon_0)g_0 \prod_{k=1}^N P_k, \quad (\text{A11})$$

where $w = n(\xi_0)[1 - n(\xi_{N+1})]$ takes into account the occupation numbers of the initial and final states.

We see that the total probability P_{el} contains the product of the ratios Γ_i/\tilde{E}_i . For this reason it is convenient to introduce the geometrical averages of these quantities along the tunneling path that were introduced in Sec. II.G.2. Writing the total probability P_{el} in terms of the quantities $\bar{\Gamma}, \bar{E}$ we obtain the result in Eq. (2.105).

The factorization of the probability P_{el} , Eq. (A11), into the product of the probabilities P_k means that hops from grain to grain are independent of each other, which is a consequence of the diagonal form of the Coulomb interaction.

If the Coulomb interaction is so long ranged that it involves many granules, the situation is more complicated since integrals over the time variables cannot be taken on each site independently. Nevertheless, one can generalize the results obtained to the case of the long-range Coulomb interaction as follows. The most important effect of the off-diagonal part of the interaction E_c^{ij} is the renormalization of the excitation energies. Since the final result contains the single-particle excitations only, this effect may be included by the proper definition of the electron-hole excitation energies

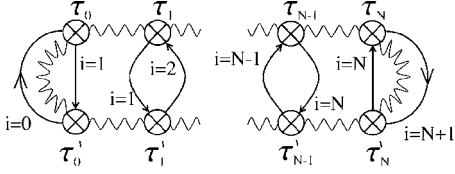


FIG. 23. Diagram representing the tunneling probability via inelastic co-tunneling processes. The crossed circles represent the tunneling matrix elements $t_{k,k'}^{ij} e^{i\phi_j(\tau)} e^{-i\phi_k(\tau)}$ where the phase factors appear from the gauge transformation. The wavy lines represent the average of the phase factors $\langle e^{i\phi(\tau)} e^{-i\phi(\tau_2)} \rangle$ with respect to the Coulomb action.

$$E_i^\pm = E_{ii} - \mu_i, \quad (\text{A12})$$

where μ_i represents the local potential formed by both the external potential V_i and all charges surrounding the grain i . This procedure, however, does not include all the effects of the presence of the off-diagonal part of E_c^{ij} . The problem is that the virtual process represented by Fig. 22 does not correspond to a causal classical process. For this reason the virtual field created by an electron i at time t_i affects in general the same electron when it is present on the other site at a different time.

However, such an interaction decays at least as $1/r^2$ with the distance. This assumes that the long-range effects of the Coulomb interaction are not important, since the corresponding integral along the chain converges. Thus all the effects that are not taken into account by the substitution Eq. (A12) are short ranged and may lead only to the change of a constant under the logarithm of the effective localization length Eq. (2.109). Using the analogy with the classical Coulomb problem (Beloborodov, Lopatin, and Vinokur, 2005) one can estimate the boundaries for the factor under the logarithm as $0.5 \lesssim c < 1.0$.

APPENDIX B: CALCULATION OF THE TUNNELING PROBABILITY P_{in} IN THE INELASTIC REGIME, EQ. (2.114)

In this appendix we derive the probability of the inelastic co-tunneling P_{in} through a chain of grains. As in the case of the elastic processes considered in the previous section, the probability of inelastic processes can easily be found for a model with diagonal Coulomb interaction. For this model, we follow the previous steps, making the gauge transformation described in Sec. II.B.3 and expanding the tunneling probability in the tunneling matrix elements.

The diagram describing the inelastic process is shown in Fig. 23. We see that it consists only of short electron loops, which means that the charge on each step is transferred by different electrons, as it should be in the inelastic process.

All intermediate Green's functions with the grain index $i=0, \dots, N$ enter the diagram in Fig. 23 and are integrated over the internal states of the grain, such that each Green's function is

$$G(\tau) \equiv \sum_k G_k(\tau) = \frac{\pi T}{\sin(\pi T \tau)}. \quad (\text{B1})$$

The processes for electrons located on the initial and final sites (i_0 and i_N) are given by Green's functions that are accompanied by the phase correlations $\Pi(\tau)$ exactly in the same way as in the case of the elastic co-tunneling and thus can be described in terms of the Green's functions \tilde{G} .

The intervals $\tau_0 - \tau'_0$ and $\tau_N - \tau'_N$ coincide with each other within the accuracy of the inverse Coulomb energy and we just put $\tau_0 - \tau'_0 \approx \tau_N - \tau'_N \equiv \tau$. In the same limit, the integrals over the intermediate times intervals $\Delta\tau_k = \tau_k - \tau_{k-1}$ (and over $\tau'_k - \tau'_{k-1}$) can be calculated independently resulting in the contribution

$$\int_{-\infty}^{\infty} d(\Delta\tau_k) e^{-E_k^c |\Delta\tau_k| + \mu_k \Delta\tau_k} = 2/\tilde{E}_k, \quad (\text{B2})$$

where the energy \tilde{E}_k is defined in Eq. (2.107). Collecting all terms for the probability P_{in} one obtains

$$P_{\text{in}}(\tau) = \frac{\bar{g}^{N+1}}{2\pi^{N+1}} \left(\frac{2\pi T}{\bar{E} \sin(\pi T \tau)} \right)^{2N} e^{-\tau \Delta\epsilon}, \quad (\text{B3})$$

where $\Delta\epsilon = \epsilon_{N+1} - \epsilon_0$ is the difference between the energies of the initial and final states and \bar{E} and \bar{g} are geometrical averages along the tunneling path [see Eq. (2.106)].

Finally, in order to find the tunneling probability P_{in} for the inelastic co-tunneling one has to make the analytical continuation in Eq. (B3) to the real times $\tau_w = it_w$ and integrate over t_w arriving at

$$P_{\text{in}} = \frac{w\bar{g}^{N+1}}{2\pi^{N+1}} \int_{-\infty}^{+\infty} dt \left(\frac{2\pi i T}{\bar{E} \sinh(\pi T t)} \right)^{2N} e^{-it\Delta\epsilon}. \quad (\text{B4})$$

Here the singularity of the function $\sinh^{-2N}(\pi T t)$ is assumed to be in the upper half of the complex plane. At zero temperature one can easily calculate the integral over the variable t in Eq. (B4) by shifting the contour of integration in the complex plane either to $-i\infty$ for positive $\Delta\epsilon$ or to $+i\infty$ for negative $\Delta\epsilon$.

In the first case we obtain $P_{\text{in}}=0$. This reflects the fact that the real tunneling process with an increase of the energy of the electron is forbidden at $T=0$. In the latter case, $\Delta\epsilon < 0$, the zero-temperature probability is determined by the pole of the function $\sinh^{-2N}(\pi T t)$ which results in Eq. (2.118).

At finite temperatures the integral in Eq. (B4) can be expressed in terms of the Euler gamma functions, which lead to the general expression Eq. (2.114).

Generalization of the result to include the long-range interaction consists, as in the case of the elastic co-tunneling, of a proper redefinition (A12) of the electron on hole excitation energies. Considerations analogous to those presented in Appendix A allow us to conclude that inclusion of the off-diagonal terms in the capacitance matrix results only in the appearance of the coef-

ficient under the logarithm (Beloborodov, Lopatin, and Vinokur, 2005) in the expression for the localization length Eq. (2.117).

REFERENCES

- Abeles, B., 1977, Phys. Rev. B **15**, 2828.
- Abeles, B., P. Sheng, M. Coutts, and Y. Arie, 1975, Adv. Phys. **24**, 407.
- Abrahams, E., P. Anderson, D. Licciardello, and T. Ramakrishnan, 1979, Phys. Rev. Lett. **42**, 673.
- Abrahams, E., S. V. Kravchenko, and M. P. Sarachik, 2001, Rev. Mod. Phys. **73**, 251.
- Abrahams, E., M. Redi, and J. Woo, 1970, Phys. Rev. B **1**, 208.
- Abrikosov, A., 1988, *Fundamentals of the Theory of Metals* (North-Holland, Amsterdam).
- Abrikosov, A. A., and L. P. Gor'kov, 1961, Sov. Phys. JETP **12**, 1243.
- Abrikosov, A. A., L. P. Gor'kov, and I. E. Dzyaloshinski, 1965, *Methods of Quantum Field Theory in Statistical Physics* (Dover, New York).
- Aleiner, I. I., P. W. Brouwer, and L. I. Glazman, 2002, Phys. Rep. **358**, 309.
- Alhassid, Y., 2000, Rev. Mod. Phys. **72**, 895.
- Altland, A., L. Glazman, and A. Kamenev, 2004, Phys. Rev. Lett. **92**, 026801.
- Altland, A., L. I. Glazman, A. Kamenev, and J. S. Meyer, 2006, Ann. Phys. (N.Y.) **321**, 2566.
- Altshuler, B., and A. Aronov, 1985, *Electron-Electron Interaction in Disordered Conductors* (North-Holland, Amsterdam), Vol. 10, p. 1.
- Altshuler, B. L., A. G. Aronov, and D. E. Khmel'nitskii, 1982, J. Phys. C **15**, 7367.
- Altshuler, B. L., D. E. Khmel'nitskii, A. I. Larkin, and P. A. Lee, 1980, Phys. Rev. B **22**, 5142.
- Ambegaokar, V., and A. Baratoff, 1963, Phys. Rev. Lett. **10**, 486.
- Ambegaokar, V., U. Eckern, and G. Schön, 1982, Phys. Rev. Lett. **48**, 1745.
- Anderson, P. W., 1958, Phys. Rev. **109**, 1492.
- Anderson, P. W., 1959, J. Phys. Chem. Solids **1**, 26.
- Anderson, P. W., 1964, *Lectures on the Many-Body Problems* (Academic, New York), Vol. 2.
- Ando, Y., G. Boebinger, A. Passner, T. Kimura, and K. Kishio, 1995, Phys. Rev. Lett. **75**, 4662.
- Andreev, A. V., and I. S. Beloborodov, 2004, Phys. Rev. B **69**, 081406(R).
- Aslamazov, L. G., and A. I. Larkin, 1968, Fiz. Tverd. Tela (Leningrad), **10** 1104 [Sov. Phys. Solid State **10**, 875 (1968)].
- Averin, D., and Y. Nazarov, 1992, *Single Charge Tunneling* (Plenum, New York), Vol. 294.
- Averin, D. A., and Y. V. Nazarov, 1990, Phys. Rev. Lett. **65**, 2446.
- Averin, D. V., and K. K. Likharev, 1991, *Mesoscopic Phenomena in Solids* (Elsevier, North-Holland, Amsterdam), p. 173.
- Basko, D., I. Aleiner, and B. Altshuler, 2005, Ann. Phys. (N.Y.) **321**, 1126.
- Beenakker, C. W. J., 1997, Rev. Mod. Phys. **69**, 731.
- Belitz, D., and T. R. Kirkpatrick, 1994, Rev. Mod. Phys. **66**, 261.
- Beloborodov, I. S., and K. B. Efetov, 1999, Phys. Rev. Lett. **82**, 3332.
- Beloborodov, I. S., K. B. Efetov, A. Altland, and F. W. J. Hekking, 2001, Phys. Rev. B **63**, 115109.
- Beloborodov, I. S., K. B. Efetov, and A. I. Larkin, 2000, Phys. Rev. B **61**, 9145.
- Beloborodov, I. S., K. B. Efetov, A. V. Lopatin, and V. M. Vinokur, 2003, Phys. Rev. Lett. **91**, 246801.
- Beloborodov, I. S., K. B. Efetov, A. V. Lopatin, and V. M. Vinokur, 2005, Phys. Rev. B **71**, 184501.
- Beloborodov, I. S., Y. Fominov, A. V. Lopatin, and V. M. Vinokur, 2006, Phys. Rev. B **74**, 014502.
- Beloborodov, I. S., A. V. Lopatin, F. J. W. Hekking, R. Fazio, and V. M. Vinokur, 2005, Europhys. Lett. **69**, 435.
- Beloborodov, I. S., A. V. Lopatin, G. Schwiete, and V. M. Vinokur, 2004, Phys. Rev. B **70**, 073404.
- Beloborodov, I. S., A. V. Lopatin, and V. M. Vinokur, 2004a, Phys. Rev. B **70**, 205120.
- Beloborodov, I. S., A. V. Lopatin, and V. M. Vinokur, 2004b, Phys. Rev. Lett. **92**, 207002.
- Beloborodov, I. S., A. V. Lopatin, and V. M. Vinokur, 2005, Phys. Rev. B **72**, 125121.
- Bergeret, F. S., A. F. Volkov, and K. B. Efetov, 2001, Phys. Rev. Lett. **86**, 4096.
- Bergeret, F. S., A. F. Volkov, and K. B. Efetov, 2004, Europhys. Lett. **66**, 111.
- Bergeret, F. S., A. F. Volkov, and K. B. Efetov, 2005, Rev. Mod. Phys. **77**, 1321.
- Biagini, C., T. Caneva, V. Tognetti, and A. A. Varlamov, 2005, Phys. Rev. B **72**, 041102(R).
- Biagini, C., R. Feron, R. Fazio, F. W. J. Hekking, and V. Tognetti, 2005, Phys. Rev. B **72**, 134510.
- Black, C. T., D. C. Ralph, and M. Tinkham, 1996, Phys. Rev. Lett. **76**, 688.
- Boebinger, G. S., Y. Ando, A. Passner, T. Kimura, M. Okuya, J. Shimoyama, K. Kishio, K. Tamasaku, N. Ichikawa, and S. Uchida, 1996, Phys. Rev. Lett. **77**, 5417.
- Bulgadaev, S., 1984, Pis'ma Zh. Eksp. Teor. Fiz. **39**, 264 [JETP Lett., **39**, 314 (1985)].
- Bulgadaev, S., 1987a, Pis'ma Zh. Eksp. Teor. Fiz. **45**, 486 [JETP Lett. **45**, 622 (1987)].
- Bulgadaev, S., 1987b, Phys. Lett. A **125**, 299.
- Bulgadaev, S., 2006, Pis'ma Zh. Eksp. Teor. Fiz. **83**, 659 [JETP Lett. **83**, 563 (2006)].
- Caldeira, A. O., and A. J. Leggett, 1981, Phys. Rev. Lett. **46**, 211.
- Caldeira, A. O., and A. J. Leggett, 1983, Ann. Phys. (N.Y.) **149**, 374.
- Chakravarty, S., G. L. Ingold, S. Kivelson, and A. Luther, 1986, Phys. Rev. Lett. **56**, 2303.
- Chakravarty, S., S. Kivelson, G. T. Zimanyi, and B. I. Halperin, 1987, Phys. Rev. B **35**, 7256.
- Chervenak, J. A., and J. M. Valles, 2000, Phys. Rev. B **61**, R9245.
- Clogston, A. M., 1960, Phys. Rev. Lett. **5**, 464.
- Cohen, M., L. Falicov, and J. Phillips, 1962, Phys. Rev. Lett. **8**, 316.
- Collier, C., T. Vossmeier, and J. Heath, 1998, Annu. Rev. Phys. Chem. **49**, 371.
- Collier, C. P., R. J. Saykally, J. J. Shiang, S. E. Henrichs, and J. R. Heath, 1997, Science **277**, 1978.
- Davidović, D., and M. Tinkham, 1999, Phys. Rev. Lett. **83**, 1644.
- Du, H., C. L. Chen, R. Krishnan, T. D. Krauss, J. M. Harbold, F. W. Wise, M. G. Thomas, and J. Silcox, 2002, Nano Lett. **2**, 1321.

- Eckern, U., G. Schön, and V. Ambegaokar, 1984, *Phys. Rev. B* **30**, 6419.
- Efetov, K., 1983, *Adv. Phys.* **32**, 53.
- Efetov, K. B., 1980, *Zh. Eksp. Teor. Fiz.* **78**, 2017 [*Sov. Phys. JETP* **52**, 568 (1980)].
- Efetov, K. B., 1997, *Supersymmetry in Disorder and Chaos* (Cambridge University Press, New York).
- Efetov, K. B., A. I. Larkin, and D. E. Khmel'nitskii, 1980, *Zh. Eksp. Teor. Fiz.* **79**, 1120 [*Sov. Phys. JETP* **52**, 568 (1980)].
- Efetov, K. B., and A. Tschersich, 2002, *Europhys. Lett.* **59**, 114.
- Efetov, K. B., and A. Tschersich, 2003, *Phys. Rev. B* **67**, 174205.
- Efros, A. L., and B. I. Shklovskii, 1975, *J. Phys. C* **8**, L49.
- Falci, G., G. Schön, and G. T. Zimanyi, 1995, *Phys. Rev. Lett.* **74**, 3257.
- Fazio, R., and H. van der Zant, 2001, *Phys. Rep.* **355**.
- Feigel'man, M. V., and A. S. Ioselevich, 2005, *Pis'ma Zh. Eksp. Teor. Fiz.* **81**, 341 [*JETP Lett.* **81**, 227 (2005)].
- Feigel'man, M. V., A. S. Ioselevich, and M. A. Skvortsov, 2004, *Phys. Rev. Lett.* **93**, 136403.
- Finkelstein, A. M., 1987, *Pis'ma Zh. Eksp. Teor. Fiz.* **45**, 37 [*JETP Lett.* **45**, 46 (1987)].
- Finkelstein, A. M., 1990, *Electron Liquid in Disordered Conductors* (Soviet Scientific Reviews, Harwood, London), Vol. 14.
- Finkelstein, A. M., 1994, *Physica B* **197**, 636.
- Fisher, M. P. A., 1986, *Phys. Rev. Lett.* **57**, 885.
- Fisher, M. P. A., 1990, *Phys. Rev. Lett.* **65**, 923.
- Fisher, M. P. A., G. Grinstein, and S. M. Girvin, 1990, *Phys. Rev. Lett.* **64**, 587.
- Frydman, A., O. Naaman, and R. C. Dynes, 2002, *Phys. Rev. B* **66**, 052509.
- Fujimori, H., S. Mitani, S. Ohnuma, T. Ikeda, T. Shima, and T. Matsumoto, 1994, *Mater. Sci. Eng., A* **181**, 897.
- Gantmakher, V. F., M. Golubkov, J. G. S. Lok, and A. Geim, 1996, *Zh. Eksp. Teor. Fiz.* **82**, 958 [*JETP* **82**, 951 (1996)].
- Gaponenko, S., 1998, *Optical Properties of Semiconductor Nanocrystals* (Cambridge University Press, Cambridge, England).
- Gerber, A., 1990, *J. Phys.: Condens. Matter* **2**, 8161.
- Gerber, A., A. Milner, G. Deutscher, M. Karpovsky, and A. Gladkikh, 1997, *Phys. Rev. Lett.* **78**, 4277.
- Goldman, A. M., and N. Marković, 1998, *Phys. Today* **51** (11), 39.
- Gordon, R., 2000, *MRS Bull.* **25**, 52.
- Gorkov, L. P., A. L. Larkin, and D. E. Khmel'nitskii, 1979, *Pis'ma Zh. Eksp. Teor. Fiz.* **30**, 248 [*JETP Lett.* **30**, 228 (1979)].
- Guinea, F., and G. Schön, 1986, *Europhys. Lett.* **1**, 585.
- Hadacek, N., M. Sanquer, and J. C. Villégier, 2004, *Phys. Rev. B* **69**, 024505.
- Halperin, W. P., 1986, *Rev. Mod. Phys.* **58**, 533.
- Ishida, H., and R. Ikeda, 1998, *J. Phys. Soc. Jpn.* **67**, 983.
- Jaeger, H. M., D. B. Haviland, A. M. Goldman, and B. G. Orr, 1986, *Phys. Rev. B* **34**, 4920.
- Jaeger, H. M., D. B. Haviland, B. G. Orr, and A. M. Goldman, 1989, *Phys. Rev. B* **40**, 182.
- Jha, S., and A. A. Middleton, 2005, e-print cond-mat/0511094.
- Kamenev, A., and A. Andreev, 1999, *Phys. Rev. B* **60**, 2218.
- Kee, H. Y., I. L. Aleiner, and B. L. Altshuler, 1998, *Phys. Rev. B* **58**, 5757.
- Kim, J. S., M. Granström, R. Friend, N. Johansson, W. Salaneck, R. Daik, W. Feast, and F. Cacialli, 1998, *J. Appl. Phys.* **84**, 6859.
- Kopnin, N. B., 2001, *Theory of Nonequilibrium Superconductivity* (Oxford University Press, Oxford).
- Kosterlitz, J., 1976, *Phys. Rev. Lett.* **37**, 1577.
- Kravchenko, S. V., and M. P. Sarachik, 2004, *Rep. Prog. Phys.* **67**, 1.
- Lang, K. M., V. K. M. Lang, V. Madhavan, E. W. H. J. E. Hoffman, H. Eisaki, S. Uchida, and J. C. Davis, 2002, *Nature (London)* **415**, 412.
- Larkin, A. I., 1965, *Zh. Eksp. Teor. Fiz.* **48**, 232 [*Sov. Phys. JETP* **21**, 153 (1965)].
- Larkin, A. I., 1999, *Ann. Phys. (N.Y.)* **8**, 785.
- Larkin, A. I., and Y. N. Ovchinnikov, 1983, *Phys. Rev. B* **28**, 6281.
- Larkin, A. I., and A. Varlamov, 2005, *Theory of Fluctuations in Superconductors* (Oxford University Press, New York).
- Lee, P. A., and T. V. Ramakrishnan, 1985, *Rev. Mod. Phys.* **57**, 287.
- Liao, Z. M., J. Xun, and D. P. Yu, 2005, *Phys. Lett. A* **345**, 386.
- Lin, X., H. M. Jaeger, C. Sorensen, and K. Klabunde, 2001, *J. Phys. Chem. B* **105**, 3353.
- Liu, Y., D. B. Haviland, B. Nease, and A. M. Goldman, 1993, *Phys. Rev. B* **47**, 5931.
- Loh, Y. L., V. Tripathi, and M. Turlakov, 2005, *Phys. Rev. B* **72**, 233404.
- Lukyanov, S., and A. Zamolodchikov, 2004, *J. Stat. Mech.: Theory Exp.* 2004, P05003.
- Maekawa, S., H. Ebisawa, and H. Fukuyama, 1983, *J. Phys. Soc. Jpn.* **52**, 1352.
- Maekawa, S., and H. Fukuyama, 1982, *J. Phys. Soc. Jpn.* **51**, 1380.
- Maki, K., 1968a, *Prog. Theor. Phys.* **39**, 897.
- Maki, K., 1968b, *Prog. Theor. Phys.* **40**, 193.
- Marković, N., C. Christiansen, A. M. Mack, W. H. Huber, and A. M. Goldman, 1999, *Phys. Rev. B* **60**, 4320.
- Matveev, K. A., and A. I. Larkin, 1997, *Phys. Rev. Lett.* **78**, 3749.
- McLean, W., and M. Stephen, 1979, *Phys. Rev. B* **19**, 5925.
- Mehta, M., 1991, *Random Matrices* (Academic, San Diego).
- Meyer, J. S., A. Kamenev, and L. I. Glazman, 2004, *Phys. Rev. B* **70**, 045310.
- Middleton, A. A., and N. S. Wingreen, 1993, *Phys. Rev. Lett.* **71**, 3198.
- Mowbray, D. J., and M. S. Skolnick, 2005, *J. Phys. D* **38**, 2059.
- Muller, M., and L. B. Ioffe, 2004, *Phys. Rev. Lett.* **93**, 256403.
- Murray, C., C. Kagan, and M. Bawendi, 2000, *Annu. Rev. Mater. Sci.* **30**, 545.
- Murray, C. B., D. J. Norris, and M. G. Bawendi, 1993, *J. Am. Chem. Soc.* **115**, 8706.
- Nagaev, E., 1992, *Phys. Rep.* **222**, 199.
- Narayanan, S., J. Wang, and X. M. Lin, 2004, *Phys. Rev. Lett.* **93**, 135503.
- Orr, B. G., H. M. Jaeger, and A. M. Goldman, 1985, *Phys. Rev. B* **32**, 7586.
- Orr, B. G., H. M. Jaeger, A. M. Goldman, and C. G. Kuper, 1986, *Phys. Rev. Lett.* **56**, 378.
- Ovchinnikov, Y. N., 1973, *Zh. Eksp. Teor. Fiz.* **64**, 719 [*Sov. Phys. JETP* **37**, 366 (1973)].
- Ovchinnikov, Y. N., and V. Z. Kresin, 2005a, *Eur. Phys. J. B* **45**, 5.
- Ovchinnikov, Y. N., and V. Z. Kresin, 2005b, *Eur. Phys. J. B* **47**, 333.
- Pankov, S., and V. Dobrosavljevic, 2005, *Phys. Rev. Lett.* **94**, 046402.

- Parthasarathy, R., X.-M. Lin, K. Elteto, T. F. Rosenbaum, and H. M. Jaeger, 2004, *Phys. Rev. Lett.* **92**, 076801.
- Parthasarathy, R., X.-M. Lin, and H. M. Jaeger, 2001, *Phys. Rev. Lett.* **87**, 186807.
- Pollak, M., and C. J. Adkins, 1992, *Philos. Mag. B* **65**, 855.
- Punnoose, A., and A. M. Finkelstein, 2005, *Science* **310**, 289.
- Radhakrishnan, V., C. K. Subramaniam, S. Sankaranarayanan, G. V. S. Rao, and R. Srinivasan, 1990, *Physica C* **167**, 53.
- Ralph, D. C., C. T. Black, and M. Tinkham, 1995, *Phys. Rev. Lett.* **74**, 3241.
- Romero, H. E., and M. Drndic, 2005, *Phys. Rev. Lett.* **95**, 156801.
- Rotkina, L., S. Oh, J. N. Eckstein, and S. V. Rotkin, 2005, *Phys. Rev. B* **72**, 233407.
- Sachdev, S., 2001, *Quantum Phase Transitions* (Cambridge University Press, Cambridge, England).
- Schmid, A., 1983, *Phys. Rev. Lett.* **51**, 1506.
- Schön, G., and A. Zaikin, 1990, *Phys. Rep.* **198**, 237.
- Shapira, Y., and G. Deutscher, 1983, *Phys. Rev. B* **27**, 4463.
- Shklovskii, B. I., 1973, *Sov. Phys. Semicond.* **6**, 1964.
- Shklovskii, B. I., 1984, *Sov. Phys. Solid State* **26**, 353.
- Shklovskii, B. I., and A. L. Efros, 1988, *Electronic Properties of Doped Semiconductors* (Springer-Verlag, New York).
- Simánek, E., 1979, *Solid State Commun.* **31**, 419.
- Simánek, E., 1994, *Nonhomogeneous Superconductors* (Oxford University Press, Oxford).
- Simánek, E., and R. Brown, 1986, *Phys. Rev. B* **34**, 3495.
- Simon, R. W., B. J. Dalrymple, D. Van Vechten, W. W. Fuller, and S. A. Wolf, 1987, *Phys. Rev. B* **36**, 1962.
- Smith, R. A., and V. Ambegaokar, 1996, *Phys. Rev. Lett.* **77**, 4962.
- Sondhi, S., S. Girvin, J. Carini, and D. Shahar, 1997, *Rev. Mod. Phys.* **69**, 315.
- Thompson, R. S., 1970, *Phys. Rev. B* **1**, 327.
- Tinkham, M., 1996, *Introduction to Superconductivity* (McGraw-Hill, New York).
- Tran, T. B., I. Beloborodov, X. M. Lin, T. P. Bigioni, V. M. Vinokur, and H. M. Jaeger, 2005, *Phys. Rev. Lett.* **95**, 076806.
- Tran, T. B., I. Beloborodov, X. M. Lin, T. P. Bigioni, V. M. Vinokur, and H. M. Jaeger, 2005, *Phys. Rev. Lett.* **95**, 076806.
- Tripathi, V., and Y. L. Loh, 2006, *Phys. Rev. Lett.* **96**, 046805.
- Usadel, K. D., 1970, *Phys. Rev. Lett.* **25**, 507.
- van der Zant, H. S. J., F. C. Fritschy, W. J. Elion, L. J. Geerlins, and J. E. Mooij, 1992, *Phys. Rev. Lett.* **69**, 2971.
- von Delft, J., A. D. Zaikin, D. S. Golubev, and W. Tichy, 1996, *Phys. Rev. Lett.* **77**, 3189.
- Wegner, F., 1979, *Z. Phys. B* **35**, 207.
- Wehrenberg, B. L., C. Wang, and P. J. Guyot-Sionnest, 2002, *J. Phys. Chem. B* **106**, 10634.
- Yakimov, A. I., A. V. Dvurechenskii, A. I. Nikiforov, and A. A. Bloshkin, 2003, *Pis'ma Zh. Eksp. Teor. Fiz.* **77**, 445 [*JETP Lett.* **77**, 376 (2003)].
- Yu, D., C. Wang, B. L. Wehrenberg, and P. Guyot-Sionnest, 2004, *Phys. Rev. Lett.* **92**, 216802.
- Yu, X., P. M. Duxbury, G. Jeffers, and M. A. Dubson, 1991, *Phys. Rev. B* **44**, 13163.
- Zhang, J., and B. I. Shklovskii, 2004, *Phys. Rev. B* **70**, 115317.
- Zhu, F., K. Zhang, E. Guenter, and C. Jin, 2000, *Thin Solid Films* **363**, 314.